université PARIS-SACLAY | ÉCOLE DOCTORALE Sciences et technologies de l'information et de la communication (STIC)

THESE DE DOCTORAT
DE L'UNIVERSITE PARIS-SACLAY,
PRÉPARÉE À L'ONERA

ÉCOLE DOCTORALE n°580: Sciences et technologies
de l'information et de la communication (STIC)

Spécialité de doctorat: Robotique

Par Mr Arthur Kahn

Reconfigurable cooperative control for extremum seeking

Commande coopérative reconfigurable pour la recherche d'extremum

Soutenu publiquement le 14 décembre 2015 à l'ONERA Palaiseau

Jury:

Dominique Meizel	Professeur des Universités, XLim	Président
Philippe Bonnifait	Professeur des Universités, UTC	Rapporteur
Hichem Snoussi	Professeur des Universités, UTT	Rapporteur
Raja Chatila	Directeur de Recherches, ISIR	Examinateur
Hélène Piet-Lahanier	Conseiller scientifique, ONERA DCPS	Directeur de thèse
Michel Kieffer	Professeur des Universités, Université Paris Saclay	Co-directeur de thèse
Julien Marzat	Ingénieur de Recherches, ONERA DCPS	Encadrant
Véronique Serfaty	Docteur DGA / MRIS	Invitée

NNT : 2015SACLS269

ONERA
THE FRENCH AEROSPACE LAB

DGA

Remerciement

Cette thèse n'aurait pas pu voir le jour sans l'appui et la confiance de mes encadrants, Hélène Piet-Lahanier, Michel Kieffer et Julien Marzat qui m'ont guidé pendant mes premiers pas dans la recherche académique. Ils ont su m'apprendre dès mes débuts la méthodologie et la rigueur nécessaire. Tout au long de mon travail, ils ont toujours su m'aiguiller et m'apporter la connaissance scientifique nécessaire et jusqu'à la fin, ils m'ont apporté leur soutient et leurs conseils.

Cette thèse doit aussi beaucoup aux réflexions et aux échanges que j'ai pu avoir avec mes collègues doctorants, Loïc, Evrard, Ariane, Christelle, Pawit, Damien et Rata entre autres. Je leur dois surtout la bonne ambiance et l'animation au bureau et en dehors. Des gâteaux du jeudi, aux soirées jeux de société chez Evrard, où Loïc râlait, en passant par les repas que Pawit nous préparait des jours à l'avance.

Parmi les compagnons de l'ombre qui m'ont également soutenu tout au long de cette thèse, je remercie Audrey pour ses nombreuses relectures et corrections en anglais bien qu'elle ne soit pas spécialiste des domaines scientifiques abordés. Enfin avec mon père et bien d'autres, amis du lycée ou d'école, compagnons de voyages ou nouvelles connaissances, ils font partie des soutiens extérieure au monde académique qui ont été là pendant ces trois années et ont donc quelque part, aussi contribué à cette thèse.

Arthur

Contents

List of Figures

Acronyms

MAS	Multi-Agent System
FDI	Fault Detection and Isolation
WSN	Wireless Sensor Network
MPC	Model Predictive Control
UAV	Unmanned Aerial Vehicle
UGV	Unmanned Ground Vehicle
EI	Expected Improvement
EGO	Efficient Global Optimisation
ROC	Receiver Operating Characteristic

Notation

Common notation:

N	Number of agents
n	Space dimension
D	Area of the mission in $\mathbb{R}^n$
t	Continuous time instant
t_k	Discrete time instant
T	Sampling period
ϕ	Unknown scalar spatial field defined over D
ν	Bias of faulty sensor
$\hat{\phi}_{i,k}$	Estimate of the field ϕ of agent i at time t_k
$\mathbf{x}$	Position vector in $\mathbb{R}^n$
$\mathbf{x}_i(t)$	Position vector in $\mathbb{R}^n$ of agent i at time t
$\dot{\mathbf{x}}_i(t) = \frac{\partial \mathbf{x}_i(t)}{\partial t}$	Velocity vector in $\mathbb{R}^n$ of agent i at time t
$\ddot{\mathbf{x}}_i(t) = \frac{\partial^2 \mathbf{x}_i(t)}{\partial t^2}$	Acceleration vector in $\mathbb{R}^n$ of agent i at time t
$y_i(t)$	Field measurement by agent i at time t
$\mathbf{x}_M$	Position of the global maximum of ϕ
$\mathcal{G}$	Communication graph
M	Mass of one agent
$C(\mathbf{x}_i, \dot{\mathbf{x}}_i)(t)$	Dynamic coefficient of agent i at time t
R	Communication range between agents
R_{safety}	Collision avoidance radius
$\mathbf{u}_i(t)$	Control input of agent i at time t
$\eta_i(t_k)$	Status of the sensor of agent i at time t_k (0,1)

p_{01}	Sensor status transition probability from healthy (0) to faulty (1) status
p_{10}	Sensor status transition probability from faulty (1) to healthy (0) status
$n_i(\eta_i(t_k),(t_k))$	Measurement noise of agent i a time t_k
$\sigma^2_{\eta_i(t_k)}$	Variance of the measurement noise $n_i(\eta_i(t_k)),(t_k)$
$\mathcal{N}_i(t_k)$	Set of neighbours of agent i at time t_k
$\mathcal{M}(t_k)$	Set of agents performing a measurement at time t_k
$S_i(t_k)$	Data available for agent i at t_k with measurements and related positions
k_1	Control law gain for velocity matching
k_2	Control law gain for collision avoidance
$k_3(\eta_i)$	Control law gain for position matching
q	Control law parameter for the repulsion between agents

Part 1: Local search

$\widehat{\mathbf{x}}_i^k$	Estimate of $\mathbf{x}_M$ by agent i at time t_k
$\boldsymbol{\chi}_i$	Point where the Hessian of ϕ is computed for agent i
$\boldsymbol{\alpha}_i^k$	Parameter vector of the model of agent i
$\widehat{\boldsymbol{\alpha}}_i^k$	Estimate of the model parameters of agent i
$\bar{\phi}_i$	Linear approximation of the field ϕ by agent i
e_i	Model error from the linear approximation of ϕ by agent i
$\mathbf{x}_i^d(t)$	Desired position vector of agent i at time t
$\mathbf{y}_{i,k}$	Measurement vector of agent i and its neighbours at time t_k
$\bar{\mathbf{R}}_{i,k}$	Regression matrix of agent i at time t_k
$\mathbf{n}_{i,k}$	Measurement noise vector of agent i and its neighbours at time t_k
$\mathbf{e}_{i,k}$	Model error vector of agent i and its neighbours at time t_k
$\boldsymbol{\Sigma}_{i,t_k}$	Diagonal covariance matrix of agent i at time t_k
$J_0(\boldsymbol{\alpha}_i^k)$	Least-square criterion
$\mathbf{W}_{i,k}$	Weight matrix for the least-square estimation of agent i

k_w	Weight parameter
$\hat{\mathbf{\Sigma}}_{\boldsymbol{\alpha}_i^{k+1}}$	Approximation of the estimated covariance of $\widehat{\boldsymbol{\alpha}}_i^{k+1}$
$\mu_{i,j}$	Lagrange multiplier
$\tilde{\mathbf{e}}_i$	Estimate of the model error vector of agent i and its neighbours
K	Lipschitz constant of $\nabla\phi$
μ_K	Mean of the second order Hessian model
σ_K^2	Variance of the second order Hessian model
r_i	Residual of agent i for fault detection and isolation
d_i	Additive fault on agent i measurement
λ_i^k	Gradient step size
V	Lyapunov function for control law stability analysis
τ_i	Orientation of robot i
v_i	Velocity of robot i
$\Delta\omega_{max}$	Maximum angular velocity
L	Half-axis lenght of the robot
r_{wheel}	Wheel radius of the robot
$\gamma^i(\eta_i)$	Criterion for $k_3(\eta_i)$ gain selection

Part 2: Global search

f	Spatial function
Y	Model of function f
$\mathbf{r}$	Regression vector
$\boldsymbol{\beta}$	Model parameter vector
σ_z^2	Nominal variance of the function modelled
ξ	Covariance function
$\mathbf{Y}$	Measurement vector used for the Kriging model
$\mathbf{R}$	Regression matrix used for the Kriging model
$\mathbf{Z}$	Gaussian process vector used for the Kriging model
$\mathbf{k}_p$	Covariance vector used for the Kriging model
$\mathbf{K}$	Covariance matrix used for the Kriging model

$\hat{Y}$	Estimate of Y by Kriging
$\boldsymbol{\lambda}$	Lagrange multiplier
$\mu(\mathbf{x})$	Mean value at position $\mathbf{x}$
$\sigma^2(\mathbf{x})$	Variance value at position $\mathbf{x}$
$\tilde{\mathbf{K}}$	Covariance matrix with measurement noise used for the Kriging model
θ	Parameter of the covariance function
$\mu_i^k(\mathbf{x})$	Mean of the Kriging model of agent i at $\mathbf{x}$ at time t_k
$\sigma_i^k(\mathbf{x})$	Uncertainty of the Kriging model of agent i at position $\mathbf{x}$ at time t_k
$\mathbf{Y}_i^k$	Set of measurements used for the Kriging model by agent i at time t_k
$\mathbf{P}_i^k$	Set of positions used for the Kriging model by agent i at time t_k
$\mathcal{C}_{\text{Kushner}}$	Kushner criterion for sampling
ϵ	Tuning parameter of the Kushner criterion
$f_{\min}$	Minimum value of f on the sampling points
$\hat{f}$	Estimate of f by Kriging
$\mathcal{C}_{\text{EI}}$	Expected Improvement criterion for sampling
$\mathcal{C}_{\text{lcb}}$	Lower confidence bounding criterion
b_{lcb}	Lower confidence bounding parameter
$\mathcal{C}_{\text{Xu}}$	Xu criterion for sampling
$\mathcal{J}$	Set of predefined target points
$f_{\max}^i(t_k)$	Maximum value of the estimate model in $S_i(t_k)$
$\mathbf{x}_i^d(t_k)$	Desired position for the next sampling of agent i
$J_i(t_k)$	Proposed sampling criterion
α	Tuning parameter for spreading agents
b	Tuning parameter for exploration
ε	Tuning parameter to avoid close sampling
ϕ_{upper}	Upper bound of the modelled field
$r_i^{(2)}$	Residual for FDI with Kriging model
m	Tuning parameter for FDI threshold
τ_{Xu}	Sampling period for Xu's criterion

Résumé en français

Les systèmes robotiques multi-agents sont de plus en plus utilisés pour des types de missions variées. Ils représentent un grand intérêt pour les missions dangereuses (dans un environnement hostile pour l'homme comme une zone radioactive ou polluée) et les missions répétitives de type surveillance (surveillance d'une grande zone comme pour la détection de feu de forêt) ou recherche (fuite de produits chimiques, maximum d'un champ inconnu). Dans cette thèse nous avons considéré la mission de localisation du maximum d'un champ spatial inconnu dans une zone par un groupe de véhicules autonomes munis de capteurs. Pour cela, nous avons développé deux approches, l'une basée sur une recherche locale et la seconde sur une recherche globale de maximum.

Pour répondre à la mission donnée, dans un premier temps nous avons considéré une approche locale pour la recherche du maximum. Cette approche est basée sur une estimation du gradient du champ inconnu suivi du déplacement des agents vers le maximum. Pour parvenir à ce résultat, une estimation coopérative du champ et de son gradient est effectuée par les agents à partir de leurs mesures. Les capteurs faisant les mesures sont embarqués sur les agents mobiles, nous nous sommes donc aussi intéressés au placement optimal des capteurs. Plusieurs critères ont été proposés pour ce placement optimal. Une méthode de détection d'erreurs est aussi présentée pour détecter quand un capteur de la flotte devient défaillant et fournit des données aberrantes.

Un autre élément important consiste à développer la loi de guidage afin de déplacer les agents. Les objectifs de cette loi de guidage sont multiples, il lui faut placer les agents en respectant le résultat de l'analyse du placement optimal, il lui faut aussi déplacer l'ensemble de la flotte vers le maximum suivant le gradient local et enfin, il lui faut reconfigurer la flotte lorsqu'une erreur est détectée.

Dans un deuxième temps, après avoir présenté une stratégie de recherche locale

du maximum et présenté ses inconvénients, nous avons proposé une méthode de recherche globale. Cette méthode est basée sur la modélisation du champ par krigeage. Un nouveau critère d'échantillonnage a été développé pour trouver les positions où effectuer des mesures du champ pour converger vers la position du maximum.

Les résultats de ces différentes parties sont résumés dans les sections suivantes.

0.1 État de l'art

Avant de présenter les travaux effectués, nous allons tout d'abord procéder à une présentation des méthodes existantes concernant les différent sujets qui seront abordés dans cette thèse.

0.1.1 Système multi-agents

Depuis maintenant plusieurs années, les systèmes multi-agents ont été utilisés pour des missions de surveillance comme dans (Merino et al., 2005) où une flotte de drones est utilisée pour détecter les incendies ou encore dans (Sirigineedi et al., 2010) où de la surveillance de zones portuaires est effectuée grâce à plusieurs drones. Un des intérêts des systèmes multi-agents est de permettre une coopération entre les agents afin qu'ils puissent remplir leur mission de façon plus efficace que s'ils ne s'entraidaient pas. Par exemple, dans (Parker, 1999) des robots sont utilisés pour déplacer des objets. Lorsqu'un robot ne parvient pas à déplacer un objet seul, un autre le détecte et vient l'aider.

Un des autres intérêts des systèmes multi-agents est la robustesse aux défaillances. Même si un agent rencontre un problème, les autres agents ont la possibilité de continuer leur mission. Dans (Chamseddine et al., 2012), plusieurs agents ont une mission de rendez-vous. Si l'un des agents rencontre un problème qui modifie sa dynamique, les trajectoires des autres agents sont modifiées au besoin pour poursuivre la mission avec l'agent défaillant ou pour l'exclure de la mission et poursuivre sans lui.

Pour agir ensemble, la mission initiale des agents doit être découpée en sous tâches qu'ils vont se répartir. Différentes architectures peuvent être utilisées pour de tels systèmes. L'architecture centralisée délègue à une seule entité les calculs et

la transmission d'information. Cette architecture est facile à implémenter (problèmes de communication mise à part) car toutes les actions sont gérées au même endroit du système. Une telle architecture est utilisée dans (Zhang et al., 2010a) pour analyser les mesures de tout le système et détecter les erreurs. L'architecture distribuée est une alternative plus compliquée à mettre en œuvre mais qui peut s'avérer plus robuste aux erreurs. Chaque agent du système traite lui-même les informations et fait ses propres calculs à partir d'information obtenues par lui-même. Une telle architecture est utilisée dans (Julian et al., 2011) pour que chaque agent calcule sa propre loi de guidage pour déplacer l'ensemble de la flotte. L'architecture hybride se situe entre les deux solutions. Une partie des problèmes est décentralisée alors qu'une autre partie reste centralisée. Dans (Wang et al., 2007), les deux architectures sont mises en commun et chaque agent passe de l'une à l'autre. La partie centralisée guide les agents vers la position désirée alors que la partie décentralisée est là pour éviter les collisions entre agents.

0.1.2 Commande de formation

Il existe différentes méthodes de commande pour les systèmes multi-agents, la plupart des méthodes peuvent être classées parmi les trois grandes classes que sont le suivi de leader, la commande par structure virtuelle et la commande par règles comportementales.

La méthode de commande par suivi de leader consiste à donner plus d'importance à un agent nommé le leader. Les autres agents seront les suiveurs et chercheront à chaque instant à suivre la trajectoire du leader. Les auteurs de (Bošković and Mehra, 2002) proposent une méthode où les suiveurs cherchent à faire correspondre leur orientation et leur vitesse avec celles du leader. Dans (Liu and Liu, 2010), les délais de transmission entre leader et suiveurs sont étudiés afin de garantir la stabilité de la commande. Ce type de commande est utile quand le système n'est pas composé d'agents identiques. Dans (Bıyık and Arcak, 2008), seul le leader est équipé d'un capteur. L'ensemble de la flotte doit effectuer une montée de gradient pour rejoindre le maximum, le leader doit donc faire des déplacements afin d'estimer le gradient alors que les suiveurs ne doivent que suivre la trajectoire globale du leader.

La deuxième méthode de commande, dite par structure virtuelle, ne donne

pas plus d'importance à un agent en particulier. Ce sont des liens virtuels qui donnent forme à la formation. Des leaders virtuels peuvent être employés comme dans (Ögren et al., 2004), ou des champs de potentiels peuvent être utilisés pour attirer et repousser les agents afin d'obtenir la formation désirée comme dans (Leonard and Fiorelli, 2001). D'autres travaux utilisent des formes géométriques et font converger les agents dans des formations de formes voulues. Dans (Tan and Lewis, 1996) le système multi-agents est traité comme un corps rigide de géométrie donnée. Dans (Cheah et al., 2009) des zones d'inclusion et d'exclusion sont utilisées pour créer les formations de géométrie désirée.

La dernière méthode de commande est basée sur des règles comportementales. Chaque agent obéit à un ensemble de règles qui dépendent de son environnement pour décider de sa commande. Une sous-partie des règles comportementales, qui se rapproche de la commande par structure virtuelle est la commande par essaim définie par les trois règles de base de Reynolds dans (Reynolds, 1987). La commande de chaque agent est la somme d'un terme de répulsion inter-agents pour éviter les collisions, un terme de consensus en vitesse pour que tous les agents se dirigent dans la même direction à la même vitesse, et un terme d'attraction pour que l'ensemble des agents se regroupent dans une seule formation. Ces travaux ont été étendus, notamment dans (Olfati-Saber, 2006) qui propose de donner des formes géométriques désirées aux essaims. D'autres règles comportementales permettent aux agents d'agir en fonction de l'état et des besoins des autres agents comme dans (Parker, 1998, Zhang and Parker, 2010) où les agents détectent quand l'un d'entre eux est défaillant, et poursuivent la mission malgré cela.

0.1.3 Détection et isolation de défauts

Comme nous l'avons vu précédemment, les systèmes multi-agents permettent une plus grande robustesse aux erreurs touchant les agents par leur capacité à se reconfigurer. Cela implique d'être capable de détecter quand une erreur survient et quel agent est affecté. Différents types de défauts peuvent toucher les systèmes. Il peut s'agir de défauts sur les actionneurs perturbant la dynamique des agents comme détaillé dans (Marzat et al., 2012), ou de défauts sur les capteurs perturbant les mesures faites par un agent. Dans cette thèse, nous nous sommes focalisés sur le deuxième type de défaut, plus précisément la détection de mesures aberrantes.

Une mesure aberrante est une mesure dont la valeur ne peut pas s'expliquer par le bruit de mesure nominal du capteur. Le système multi-agents utilisé dans notre étude peut être assimilé à un réseau de capteurs répartis spatialement. Une description des différentes méthodes existantes pour la détection de mesures aberrantes peut être consultée dans (Zhang and Parker, 2010). Les méthodes les plus courantes de détection de mesures aberrantes sont la comparaison aux voisins et l'analyse par classifieur. La première méthode s'appuie sur une comparaison des mesures des agents avec leurs voisins. Cela implique des hypothèses de covariance spatiale ou temporelle du champ mesuré. Une telle méthode de détection est présentée dans (Angiulli et al., 2006). La deuxième méthode s'appuie sur les outils de reconnaissance des formes pour construire un classifieur pour les mesures. Chaque nouvelle mesure sera soumise au classifieur qui décidera s'il s'agit d'une mesure normale ou aberrante. Des exemples de détection d'erreurs par classifieur peuvent être trouvés dans (Poonam and Dutta, 2012, Alam et al., 2010).

0.1.4 Estimation et placement de capteur

Les mesures des agents sont utilisées pour estimer un modèle du champ inconnu et de ses caractéristiques dans l'optique de trouver son maximum. Une méthode d'estimation couramment utilisée est l'estimation par moindres carrés (cf. (Panigrahi et al., 2011)) ou sa version pondérée utilisant la corrélation spatiale du champ (Cortés, 2009). Une autre méthode couramment utilisée s'appuie sur le filtre de Kalman pour estimer le champ (Olfati-Saber, 2005, 2007, Zheng et al., 2010).

D'autres méthodes d'estimation utilisent des méthodes d'interpolation de points. Ces méthodes utilisent l'interpolation linéaire, quadratique, par courbe de Bézier ou encore le krigeage. Le krigeage est le meilleur estimateur linéaire non biaisé. Il a été décrit dans (Matheron, 1971). Cette méthode utilise la covariance spatiale du champ pour construire un modèle et une zone de confiance comme on peut le voir en Figure 1. Il a déjà été utilisé dans le cas de systèmes multi-agents notamment dans (Cortés, 2009, Graham and Cortés, 2010, Choi et al., 2008).

Quelle que soit la méthode d'estimation choisie, le modèle est construit à partir des mesures faites par les agents. Le choix de la position à mesurer est un problème à part entière. Différentes méthodes existent pour le placement optimal de capteurs, on peut par exemple chercher les positions qui maximisent l'information

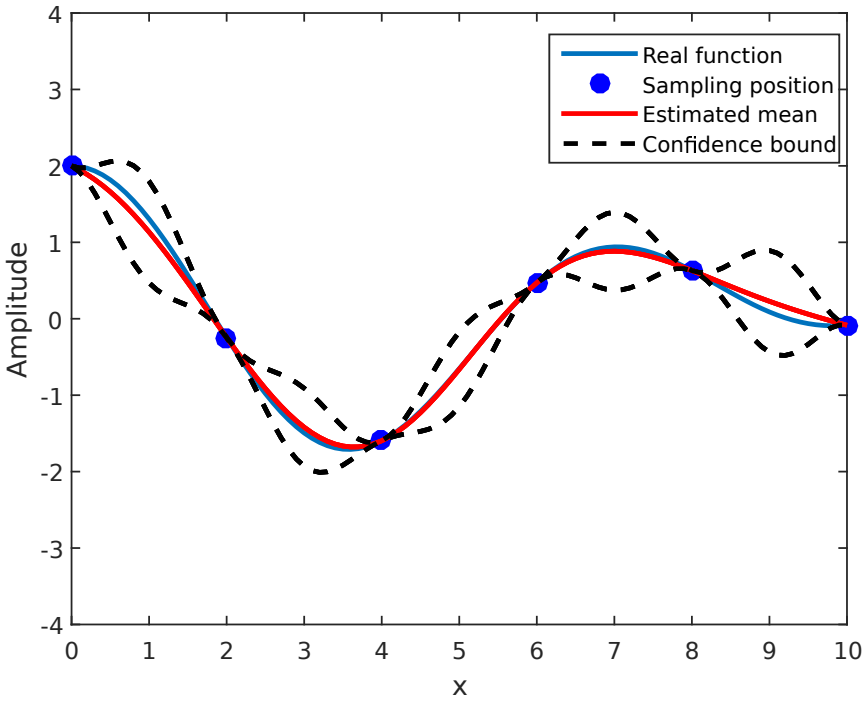

Figure 1: Illustration du modèle de krigeage

pour l'estimation via la matrice d'information de Fisher comme cela a été proposé dans (Pronzato and Walter, 1988). D'autres travaux se sont intéressés au cas de capteurs mobiles pour l'estimation du gradient (cf. (Ögren et al., 2004, Leonard et al., 2007, Zhang and Parker, 2010)).

0.1.5 Recherche locale et globale de maximum

La recherche d'extremum peut se faire de deux façons, soit par recherche locale, soit par recherche globale.

La recherche locale s'appuie sur le gradient de la fonction ou champ à optimiser. De nombreux travaux, parmi lesquels (Ögren et al., 2004, Choi et al., 2007, Williams and Sukhatme, 2012), utilisent de telles approches pour trouver le maximum en utilisant des systèmes multi-agents.

Les méthodes de recherche globale ne s'appuient pas uniquement sur le gradient de la fonction à optimiser. Cela prend en compte les méthodes de recherche

aléatoire (cf. (Solis and Wets, 1981)), les méthodes de gradient généralisé (cf. (Griewank, 1981)), les algorithmes génétiques (cf. (Golberg, 1989)) ou encore les méthodes par exploration globale du champ. Ces dernières utilisent des algorithmes par division de l'espace de recherche en intervalles telle que celle présentée dans (Hansen et al., 2003) ou l'algorithme DIRECT présenté dans (Jones et al., 1993).

Enfin, les méthode de représentation de la fonction à optimiser permettent de transformer le problème d'optimisation en un problème parallèle plus facilement solvable. Les méthodes d'estimation présentées précédemment peuvent être utilisées à cette fin. La recherche se fait ensuite sur le modèle ainsi créé qui peut s'avérer moins cher à évaluer. Plusieurs méthodes d'optimisation utilisant le krigeage sont présentées dans (Sasena, 2002).

En nous basant sur les travaux existants, nous allons maintenant présenter les contributions faites dans cette thèse pour la mission de recherche de maximum par système multi-agents.

0.2 Présentation du problème et des agents

Le but est de trouver la position du maximum $\mathbf{x}_M$ du champ ϕ dans la zone $D \subset \mathbb{R}^n$, $n = 2, 3$.

$$\mathbf{x}_M = \arg\max_{\mathbf{x} \in D} \left(\phi(\mathbf{x})\right) \tag{1}$$

Un groupe de N agents identiques est considéré. La position de l'agent i à l'instant t est noté $\mathbf{x}_i(t)$. La dynamique des agents est la suivante :

$$M\ddot{\mathbf{x}}_i(t) + C\left(\mathbf{x}_i(t), \dot{\mathbf{x}}_i(t)\right)\dot{\mathbf{x}}_i(t) = \mathbf{u}_i(t) \tag{2}$$

où $\mathbf{u}_i(t)$ est la commande appliquée à l'agent i à l'instant t, M est la masse d'un agent et $C\left(\mathbf{x}_i(t), \dot{\mathbf{x}}_i(t)\right)$ est un coefficient de friction positif.

Chaque agent est équipé d'un capteur lui permettant de mesurer la valeur du champ ϕ. Ce capteur a deux états η possibles, il peut être dans un état sain ($\eta = 0$) ou défaillant ($\eta = 1$). L'état du capteur d'un agent $\eta_i(t_k)$ peux varier entre deux instants t_k et t_{k+1} de manière probabiliste. Les mesures sont faites à temps discret, tous les agents étant synchronisés entre eux.

L'équation de mesure d'un agent est :

$$y_i(t_k) = \phi(\mathbf{x}_i(t_k)) + n_i(\eta, t_k) \tag{3}$$

Où $n_i(\eta, t_k)$ modélise le bruit de mesure du capteur de l'agent i. Les $n_i(\eta, t_k)$ sont des réalisations indépendantes d'une variable gaussienne de moyenne nulle et de variance $\sigma^2_{\eta_i(t_k)}$, avec $\sigma^2_{\eta_i(t_k)=0} \ll \sigma^2_{\eta_i(t_k)=1}$.

Le rayon de communication entre deux agents est appelé R. Le voisinage de l'agent i est défini par :

$$\mathcal{N}_i(t) = \{j \mid \|\mathbf{x}_i(t) - \mathbf{x}_j(t)\| \leqslant R\}\,. \tag{4}$$

Soit $\mathcal{M}(t_k)$ l'ensemble des agents ayant effectué une mesure à l'instant t_k. Les informations disponibles pour l'agent i à l'instant t_k sont notées $S_i(t_k)$ et définies par :

$$S_i(t_k) = \bigcup_{\ell=0}^{k} \{[y_j(t_\ell), \mathbf{x}_j(t_\ell)] \mid j \in \mathcal{N}_i(t_\ell) \cap \mathcal{M}(t_\ell)\}\,. \tag{5}$$

0.3 Estimation coopérative par système multi-agents

La première partie de la thèse présente une solution locale au problème de recherche de maximum. Le système multi-agents va estimer coopérativement le gradient du champ.

0.3.1 Estimation du champ et de son gradient

Une estimation par moindres carrés est utilisée pour estimer le champ et son gradient. Le champ peut être écrit sous la forme d'un développement de Taylor d'ordre deux à la position $\widehat{\mathbf{x}}_i^k$ tel que:

$$\phi_i(\mathbf{x}) = \phi\left(\widehat{\mathbf{x}}_i^k\right) + \left(\mathbf{x} - \widehat{\mathbf{x}}_i^k\right)^{\mathrm{T}} \nabla\phi\left(\widehat{\mathbf{x}}_i^k\right) + \frac{1}{2}\left(\mathbf{x} - \widehat{\mathbf{x}}_i^k\right)^{\mathrm{T}} \nabla^2\phi(\boldsymbol{\chi}_i)\left(\mathbf{x} - \widehat{\mathbf{x}}_i^k\right). \tag{6}$$

Où $\boldsymbol{\chi}_i$ est un point du segment reliant $\mathbf{x}$ et $\widehat{\mathbf{x}}_i^k$. Le vecteur des paramètres à estimer est :

$$\boldsymbol{\alpha}_i^k = \begin{pmatrix} \phi\left(\widehat{\mathbf{x}}_i^k\right) \\ \nabla\phi\left(\widehat{\mathbf{x}}_i^k\right) \end{pmatrix} \tag{7}$$

Le champ est ensuite approximé par

$$\bar{\phi}_i\left(\mathbf{x}\right) = \phi\left(\widehat{\mathbf{x}}_i^k\right) + \left(\mathbf{x} - \widehat{\mathbf{x}}_i^k\right)^{\mathrm{T}} \nabla\phi\left(\widehat{\mathbf{x}}_i^k\right), \tag{8}$$

et l'erreur de modélisation est définie comme:

$$\begin{aligned} e_i\left(\mathbf{x}\right) &= \phi_i\left(\mathbf{x}\right) - \bar{\phi}_i\left(\mathbf{x}\right) \\ &= \frac{1}{2}\left(\mathbf{x} - \widehat{\mathbf{x}}_i^k\right)^{\mathrm{T}} \nabla^2\phi(\boldsymbol{\chi}_i)\left(\mathbf{x} - \widehat{\mathbf{x}}_i^k\right), \end{aligned} \tag{9}$$

La mesure de l'agent j peut s'exprimer en utilisant le développement précédent comme :

$$y_j\left(t_k\right) = \begin{pmatrix} 1 & \left(\mathbf{x}_j\left(t_k\right) - \widehat{\mathbf{x}}_i^k\right)^{\mathrm{T}} \end{pmatrix} \boldsymbol{\alpha}_i^k + e_i\left(\mathbf{x}_j\left(t_k\right), \widehat{\mathbf{x}}_i^k\right) + n_j\left(t_k\right). \tag{10}$$

L'agent i peut maintenant rassembler toutes les mesures de $\mathcal{N}_i(t_k)$ à l'instant t_k avec $\mathcal{N}_i(t_k) = \{i_1, \ldots, i_{N_i}\}$ et les mettre sous la forme matricielle suivante:

$$\mathbf{y}_{i,k} = \bar{\mathbf{R}}_{i,k}\boldsymbol{\alpha}_i^k + \mathbf{n}_{i,k} + \mathbf{e}_{i,k} \tag{11}$$

avec

$$\begin{aligned} \mathbf{y}_{i,k} &= \left(y_{i_1}\left(t_k\right), \ldots, y_{i_{N_i}}\left(t_k\right)\right)^{\mathrm{T}}, \\ \bar{\mathbf{R}}_{i,k} &= \begin{pmatrix} 1 & \left(\mathbf{x}_{i_1}\left(t_k\right) - \widehat{\mathbf{x}}_i^k\right)^{\mathrm{T}} \\ \vdots & \vdots \\ 1 & \left(\mathbf{x}_{i_{N_i}}\left(t_k\right) - \widehat{\mathbf{x}}_i^k\right)^{\mathrm{T}} \end{pmatrix}, \\ \mathbf{n}_{i,k} &= \left(n_{i_1}\left(t_k\right), \ldots, n_{i_{N_i}}\left(t_k\right)\right)^{\mathrm{T}}, \end{aligned} \tag{12}$$

et

$$\mathbf{e}_{i,k} = \begin{pmatrix} \frac{1}{2}\left(\mathbf{x}_{i_1}(t_k) - \widehat{\mathbf{x}}_i^k\right)^{\mathrm{T}} \nabla^2\phi(\boldsymbol{\chi}_{i1})\left(\mathbf{x}_{i_1}(t_k) - \widehat{\mathbf{x}}_i^k\right) \\ \vdots \\ \frac{1}{2}\left(\mathbf{x}_{i_{N_i}}(t_k) - \widehat{\mathbf{x}}_i^k\right)^{\mathrm{T}} \nabla^2\phi(\boldsymbol{\chi}_{iN})\left(\mathbf{x}_{i_{N_i}}(t_k) - \widehat{\mathbf{x}}_i^k\right) \end{pmatrix}. \tag{13}$$

En considérant la matrice de pondération $\mathbf{W}_{i,k}$ définie par

$$\mathbf{W}_{i,k} = \mathrm{diag}\left(\sigma^{-2}_{\theta_1(t_k)} \exp\left(\frac{-||\mathbf{x}_1(t_k) - \widehat{\mathbf{x}}_i^k||_2^2}{k_{\mathrm{w}}}\right), \ldots, \right.$$
$$\left. \sigma^{-2}_{\theta_N(t_k)} \exp\left(\frac{-||\mathbf{x}_N(t_k) - \widehat{\mathbf{x}}_i^k||_2^2}{k_{\mathrm{w}}}\right)\right), \tag{14}$$

avec k_{w} un paramètre de réglage, on obtient l'estimée par moindres carrés suivante :

$$\widehat{\boldsymbol{\alpha}}_i^k = \left(\bar{\mathbf{R}}_{i,k}^{\mathrm{T}} \mathbf{W}_{i,k} \bar{\mathbf{R}}_{i,k}\right)^{-1} \bar{\mathbf{R}}_{i,k}^{\mathrm{T}} \mathbf{W}_{i,k} \mathbf{y}_{i,k}. \tag{15}$$

0.3.2 Placement optimal de capteurs

Une fois l'estimée $\widehat{\boldsymbol{\alpha}}_i^k$ obtenue, nous allons étudier différents critères de placement optimal de capteurs.

Placement optimal par minimisation de la variance d'estimation

Nous cherchons à trouver les positions de capteurs qui minimiseront la variance de l'estimation :

$$\widehat{\boldsymbol{\Sigma}}_{\alpha_i^{k+1}} = \left(\bar{\mathbf{R}}_{i,k+1}^{\mathrm{T}} \mathbf{W}_{i,k+1} \bar{\mathbf{R}}_{i,k+1}\right)^{-1}. \tag{16}$$

Deux critères seront évalués, le T-optimal et le D-optimal. Le critère T-optimal s'écrit :

$$(\mathbf{x}_i(t_{k+1}) \ldots \mathbf{x}_N(t_{k+1})) = \arg \max_{(\mathbf{x}_1,\ldots,\mathbf{x}_N)} \mathrm{tr}\left(\bar{\mathbf{R}}_{i,k+1}^{\mathrm{T}} \mathbf{W}_{i,k+1} \bar{\mathbf{R}}_{i,k+1}\right) \tag{17}$$

$$\text{sous la contrainte } \|\mathbf{x}_i - \mathbf{x}_j\|_2^2 \geqslant R^2_{\text{safety}},\ j > i. \tag{18}$$

Deux solutions analytiques peuvent être trouvées à ce problème en relaxant la

contrainte et en utilisant les multiplicateurs de Lagrange :

$$\mathbf{x}_i(t_{k+1}) = \widehat{\mathbf{x}}_i^{k+1} \tag{19}$$

ou

$$\left\|\mathbf{x}_i\left(t_{k+1}\right) - \widehat{\mathbf{x}}_i^{k+1}\right\|_2^2 = k_{\mathrm{w}} - 1 \tag{20}$$

La première solution place les agents sur la position d'estimation alors que la seconde les place sur un cercle centré en $\widehat{\mathbf{x}}_i^{k+1}$ de rayon $\sqrt{k_{\mathrm{w}} - 1}$.

Le critère D-optimal s'écrit:

$$\left(\mathbf{x}_i\left(t_{k+1}\right) \ldots \mathbf{x}_N\left(t_{k+1}\right)\right) = \arg \max_{(\mathbf{x}_1,\ldots,\mathbf{x}_N)} \det\left(\bar{\mathbf{R}}_{i,k+1}^{\mathrm{T}} \mathbf{W}_{i,k+1} \bar{\mathbf{R}}_{i,k+1}\right) \tag{21}$$

$$\text{sous la contrainte } \|\mathbf{x}_i - \mathbf{x}_j\|_2^2 \geqslant R_{\text{safety}}^2,\ j > i. \tag{22}$$

De la même manière que précédemment, on trouve que le critère est minimum pour les agents situés à la position $\widehat{\mathbf{x}}_i^{k+1}$ ou lorsqu'ils sont situés sur un cercle centré en $\widehat{\mathbf{x}}_i^{k+1}$ de rayon $\sqrt{\frac{2k_{\mathrm{w}}}{3}}$.

Ces solutions ne sont valables que lorsque les contraintes les permettent quel que soit l'état des capteurs. Des solutions numérique sont présenter pour illustrer le cas où les agents ne peuvent pas tenir sur les cercles sans violer la contrainte(Voir Figures 2,3,4 et 5).

Ces résultats numériques montrent que lorsque les agents ne peuvent tenir sur le cercle trouver analytiquement tout en vérifiant la contraintes d'évitement de collision, alors :

- Les agents défaillants se placent plus loin de la position d'estimation que les agents sains.
- Dans le cas du T-optimal, les agents se placent dans une formation qui tente de mettre tout les agents sur le même cercle
- Dans le cas du D-optimal, les agents se placent dans une formation qui tente de réduire la distance inter-agents au maximum et qui se centre sur la position d'estimation.

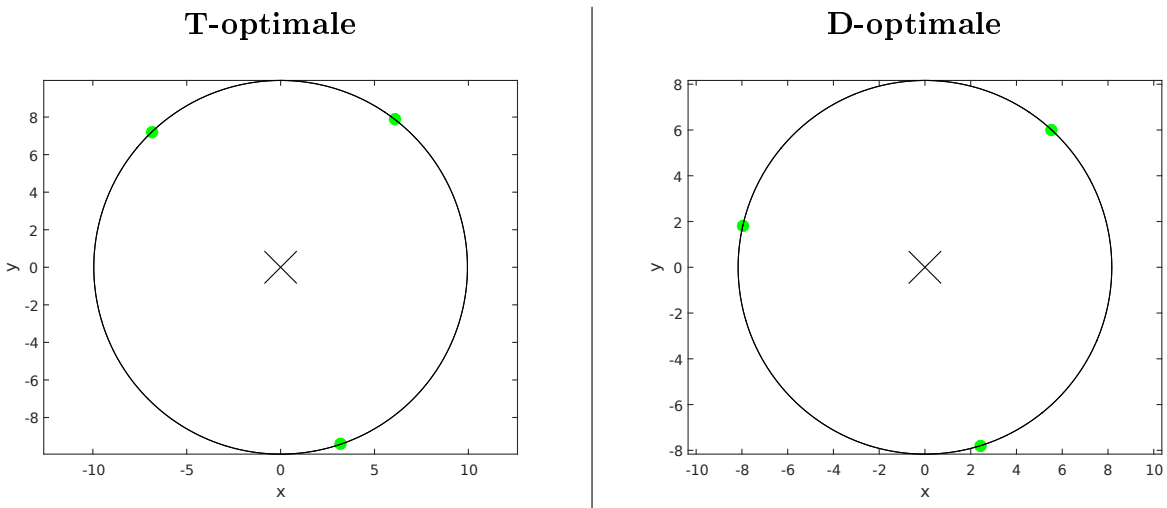

Figure 2: Formation pour 3 agents sans défaillance

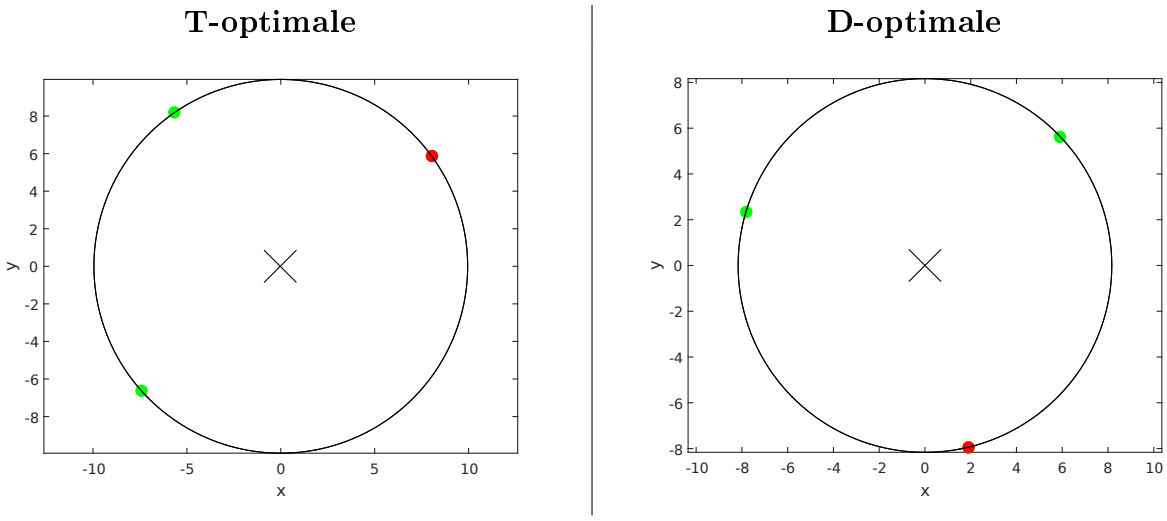

Figure 3: Formation pour 3 agents dont 1 défaillant

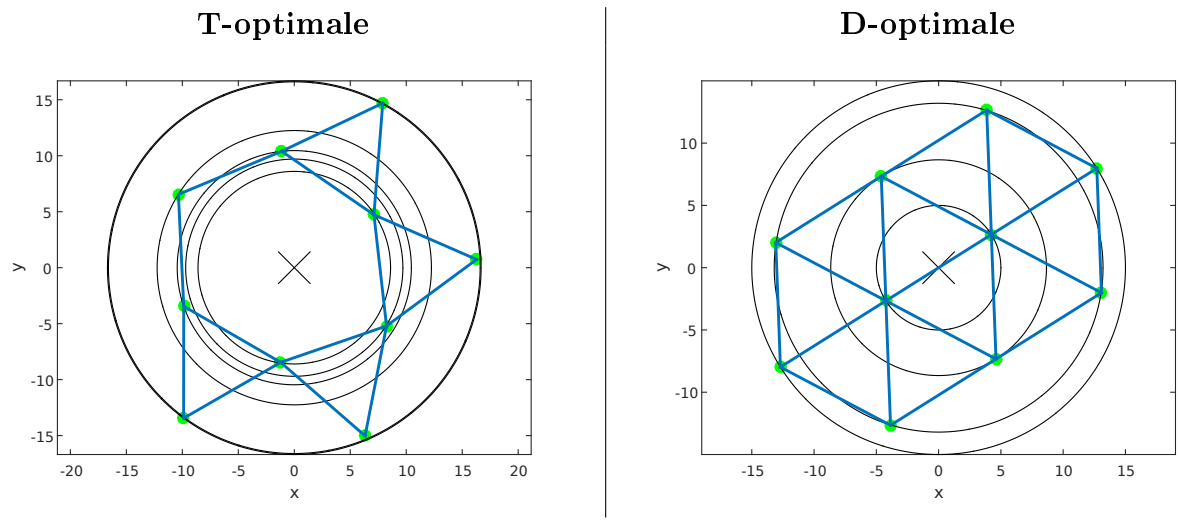

Figure 4: Formation pour 10 agents sans défaillance

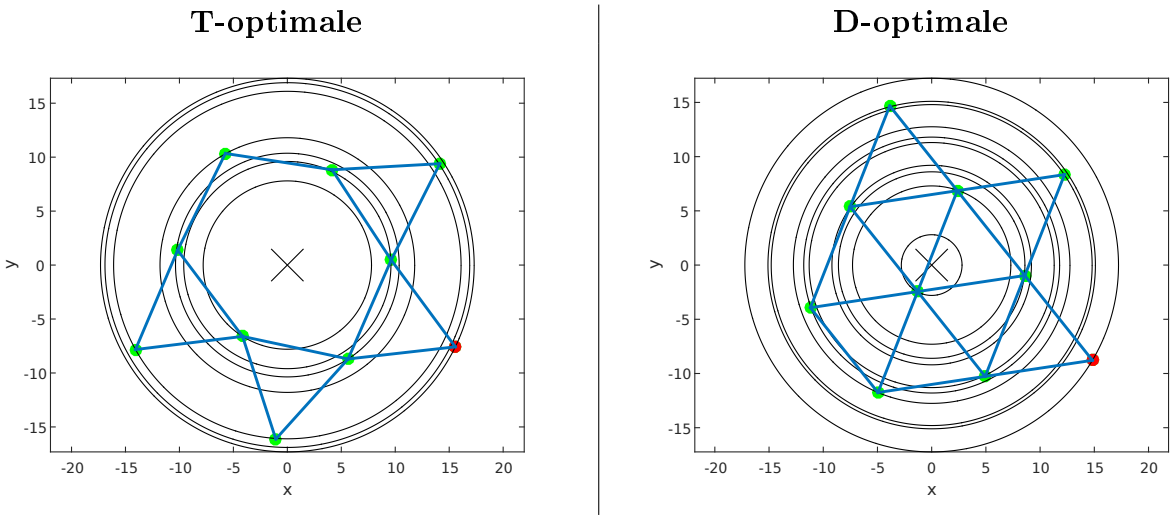

Figure 5: Formation pour 10 agents dont 1 défaillant

Placement optimal par minimisation de l'erreur de modèle

Un autre critère pour le placement optimal de capteurs est de minimiser l'erreur de modèle. Cette erreur de modèle provoque un biais sur le résultat de l'estimation comme le montre:

$$E\left[\widehat{\boldsymbol{\alpha}}_i^k\right] - \boldsymbol{\alpha}_i^k = \left(\bar{\mathbf{R}}_{i,k}^{\mathrm{T}} \mathbf{W}_{i,k} \bar{\mathbf{R}}_{i,k}\right)^{-1} \bar{\mathbf{R}}_{i,k}^{\mathrm{T}} \mathbf{W}_{i,k} \mathbf{e}_{i,k} \tag{23}$$

Nous cherchons donc les positions minimisant $\mathbf{e}_{i,k}$: $\mathbf{x}_i^d = \arg\min_{\tilde{\mathbf{x}}_i} e_i\left(\tilde{\mathbf{x}}_i\right)$ Par maximisation de $\mathbf{e}_{i,k}$, on trouve que minimiser l'erreur de modèle revient à minimiser $\frac{1}{2}||K||\ ||\tilde{\mathbf{x}}_i - \widehat{\mathbf{x}}_i^k||^2$ ou K est la constante de Lipschitz du gradient du champ sur D :

$$\left(\mathbf{x}_i\left(t_{k+1}\right) \ldots \mathbf{x}_N\left(t_{k+1}\right)\right) = \arg \min_{(\mathbf{x}_1,\ldots,\mathbf{x}_N)} \frac{1}{2}||K||\ ||\tilde{\mathbf{x}}_i - \widehat{\mathbf{x}}_i^k||^2 \tag{24}$$

$$\text{sous la contrainte } \left\|\mathbf{x}_i - \mathbf{x}_j\right\|_2^2 \geqslant R_{\text{safety}}^2,\ j > i. \tag{25}$$

Les positions minimisant ce critère créent une formation minimisant la distance inter-agents centré autour de $\widehat{\mathbf{x}}_i^k$.

0.3.3 Détection et identification de défauts

Une méthode de détection de défauts est proposée. Elle se base sur une analyse d'un résidu r_i construit comme $r_i = \hat{\phi}_i(\mathbf{x}_i) - y_i$.

Le résidu construit par l'agent i, considérant que l'agent j subit un biais de mesure d_j, est:

$$r_i(d_j) = \mathbf{h}_i \mathbf{n}_i + \mathbf{h}_i \mathbf{e}_i - n_i + \mathbf{h}_i[j] d_j, \tag{26}$$

Où $\mathbf{h}_i = [1\ 0\ 0]\left(\mathbf{R}_{i,k}^{\mathrm{T}} \mathbf{W}_{i,k} \mathbf{R}_{i,k}\right)^{-1} \mathbf{R}_{i,k}^{\mathrm{T}} \mathbf{W}_{i,k}$ est un vecteur et $\mathbf{h}_i[j]$ est la j-ème entrée du vecteur.

Le seuil adaptatif proposé est le suivant:

$$|r_i - \mathbf{h}_i \mathbf{e}_i| < k_{\text{FDI}} \sqrt{\sigma_0^2\left(1 + \mathbf{h}_i \mathbf{h}_i^T - 2\mathbf{h}_i[i]\right) + \mathbf{h}_i^T \mathbf{U}_i \mathbf{h}_i} \tag{27}$$

Où k_{FDI} est un paramètre de réglage. Des simulations numériques sont présentées

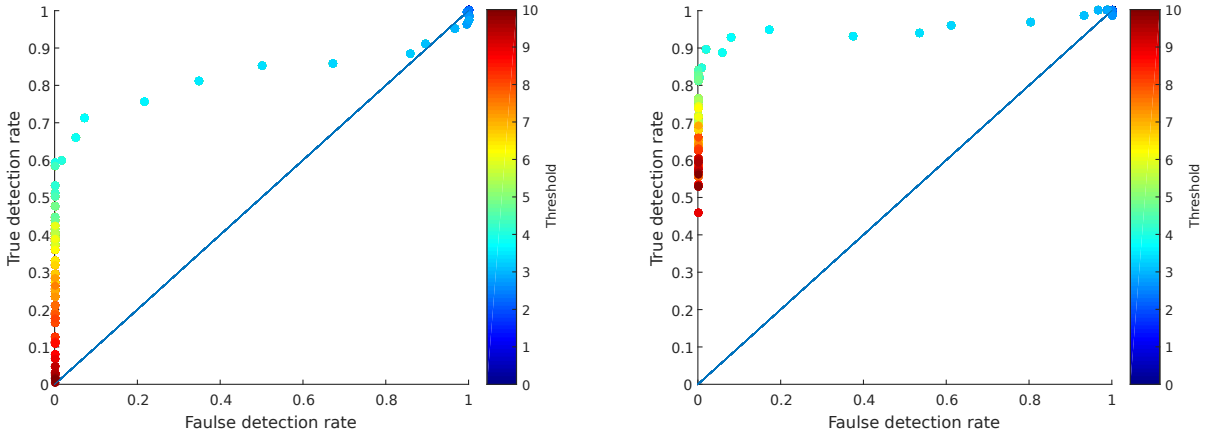

Courbe ROC pour $N = 15$ et $d = 1$ Courbe ROC pour $N = 15$ et $d = 3$

Figure 6: Courbe ROC de la détection de défauts

pour illustrer les performances de détection du seuil adaptatif proposé (Figure 6).

Pour parvenir à localiser le capteur défaillant, un système de banc de filtres est appliqué, suivi par un vote qui détermine, pour le système multi-agents, quel est l'agent dont le capteur est défaillant.

0.4 Loi de guidage reconfigurable pour recherche locale de maximum

Maintenant que la méthode d'estimation a été présentée et que les positions optimales où effectuer des mesures ont été définies, nous allons présenter une loi de guidage permettant de remplir la mission.

Les objectifs de la loi de guidage sont les suivants:

- Amener les agents dans la formation désirée.
- Éviter les collisions entre les agents.
- Déplacer les agents vers la position du maximum

Pour ce faire, une loi de guidage en deux parties a été conçue. Une partie bas-niveau a pour mission de regrouper les agents en formation et une partie

haut-niveau déplace la formation en suivant la direction du gradient. La partie bas-niveau correspond à la commande des agents :

$$\begin{aligned}\mathbf{u}_i(t) =& M\ddot{\widehat{\mathbf{x}}}_i(t) + C(\mathbf{x}_i(t), \dot{\mathbf{x}}_i(t))\dot{\mathbf{x}}_i(t) - k_1\left(\dot{\mathbf{x}}_i(t) - \dot{\widehat{\mathbf{x}}}_i(t)\right) \\ &+ 2k_2\sum_{j=1}^{N}(\mathbf{x}_i(t) - \mathbf{x}_j(t))\exp\left(-\frac{(\mathbf{x}_i(t) - \mathbf{x}_j(t))^T(\mathbf{x}_i(t) - \mathbf{x}_j(t))}{q}\right) \\ &- k_3^i(\theta_i, t)(\mathbf{x}_i(t) - \widehat{\mathbf{x}}_i(t)),\end{aligned} \tag{28}$$

La partie haut-niveau correspond au déplacement de la position estimée du maximum :

$$\widehat{\mathbf{x}}_i^{k+1} = \widehat{\mathbf{x}}_i^k + \lambda_i^k \widehat{\nabla\phi}\left(\widehat{\mathbf{x}}_i^k\right) \,/\, \left\|\widehat{\nabla\phi}\left(\widehat{\mathbf{x}}_i^k\right)\right\|_2. \tag{29}$$

avec λ_i^k le pas de la montée de gradient à l'instant t_k. Ce pas est adapté de la façon suivante :

$$\lambda_i^k = \begin{cases} \min\left\{\lambda_{\max}, 2\lambda_i^{k-1}\right\} & \text{si } \widehat{\phi}\left(\widehat{\mathbf{x}}_i^k\right) > \widehat{\phi}\left(\widehat{\mathbf{x}}_i^{k-1}\right), \\ \lambda_i^{k-1}/4 & \text{sinon} \end{cases} \tag{30}$$

0.4.1 Étude de stabilité de la commande

La stabilité de la commande bas-niveau est démontrée en utilisant la méthode de Lyapunov en considérant la fonction suivante :

$$\begin{aligned}V(\mathbf{x}(t)) = \frac{1}{2}\sum_{i=1}^{N}\Bigg[&(\dot{\mathbf{x}}_i(t) - \dot{\widehat{\mathbf{x}}}(t))^T M(\dot{\mathbf{x}}_i(t) - \dot{\widehat{\mathbf{x}}}(t)) + (\mathbf{x}_i(t) - \widehat{\mathbf{x}}(t))^T k_3^i(\mathbf{x}_i(t) - \widehat{\mathbf{x}}(t)) \\ &+ k_2\sum_{j=1}^{N}\exp\left(-\frac{(\mathbf{x}_i(t) - \mathbf{x}_j(t))^T(\mathbf{x}_i(t) - \mathbf{x}_j(t)}{q}\right)\Bigg]\end{aligned} \tag{31}$$

La dérivée de cette fonction est :

$$\dot{V} = -\sum_{i=1}^{N}\left[k_1(\dot{\mathbf{x}}_i - \dot{\widehat{\mathbf{x}}})^T(\dot{\mathbf{x}}_i - \dot{\widehat{\mathbf{x}}})\right] \leq 0 \tag{32}$$

Le résultat $\dot{V} \leq 0$ garantit que la position des agents converge asymptotiquement

vers un équilibre correspondant à une formation compacte centrée en $\widehat{\mathbf{x}}$.

0.4.2 Méthode de reconfiguration

Une fois la loi de guidage de base établie, nous avons cherché à la modifier pour prendre en compte les capteurs défaillants. Le but étant, d'après les résultats du placement optimal, de mettre les agents sains au centre de la formation et les défaillants en périphérie de celle-ci. Cette reconfiguration est effectuée en modifiant la commande des agents défaillants. Le gain k_3 de la commande bas niveau est modifié pour être dépendant de l'état du capteur. Un nouveau gain adaptatif $k_3^i\left(\theta_i(t_k)\right)$ remplace k_3.

En prenant $k_3^i\left(\theta_i = 0\right) > k_3^i\left(\theta_i = 1\right)$ les agents défaillants seront placés en bordure de la formation. La Figure 7 illustre la reconfiguration à différents instants. Les agents verts sont sains. Lorsque le capteur d'un agent au centre est détecté défaillant, son gain $k_3^i\left(\theta_i(t_k)\right)$ est adapté et il se déplace à la limite de la formation.

La méthode de recherche locale du maximum avec l'estimation coopérative et la reconfiguration en cas de capteurs défaillants est illustrée en Figure 8. L'agent défaillant est représenté en noir. Malgré la détection d'un agent défaillant, la flotte se reconfigure et parvient à rejoindre le maximum du champ.

La recherche de maximum par montée de gradient connait plusieurs limitations. Premièrement, le système multi-agents n'est pas sûr de converger vers le maximum global du champ, mais uniquement vers le premier maximum rencontré. Deuxièmement, le fait de restreindre les agents à se déplacer dans une formation limite l'intérêt d'avoir plusieurs agents. En se dispersant dans la zone, le maximum pourrait être localisé plus rapidement.

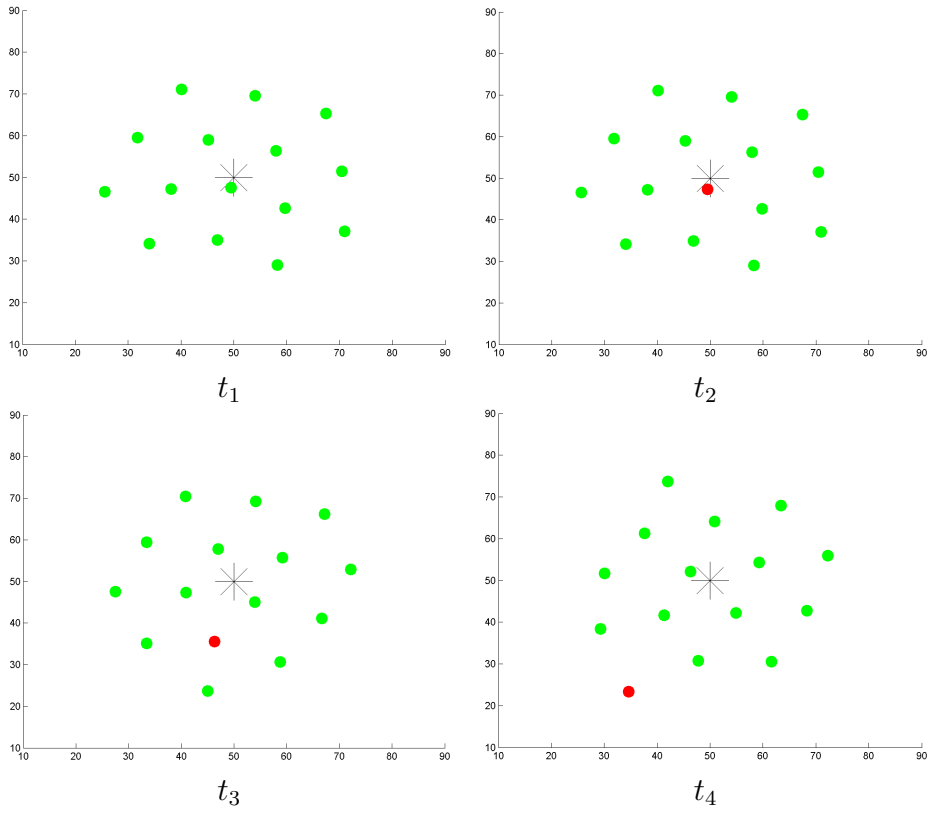

Figure 7: Illustration de la technique de reconfiguration

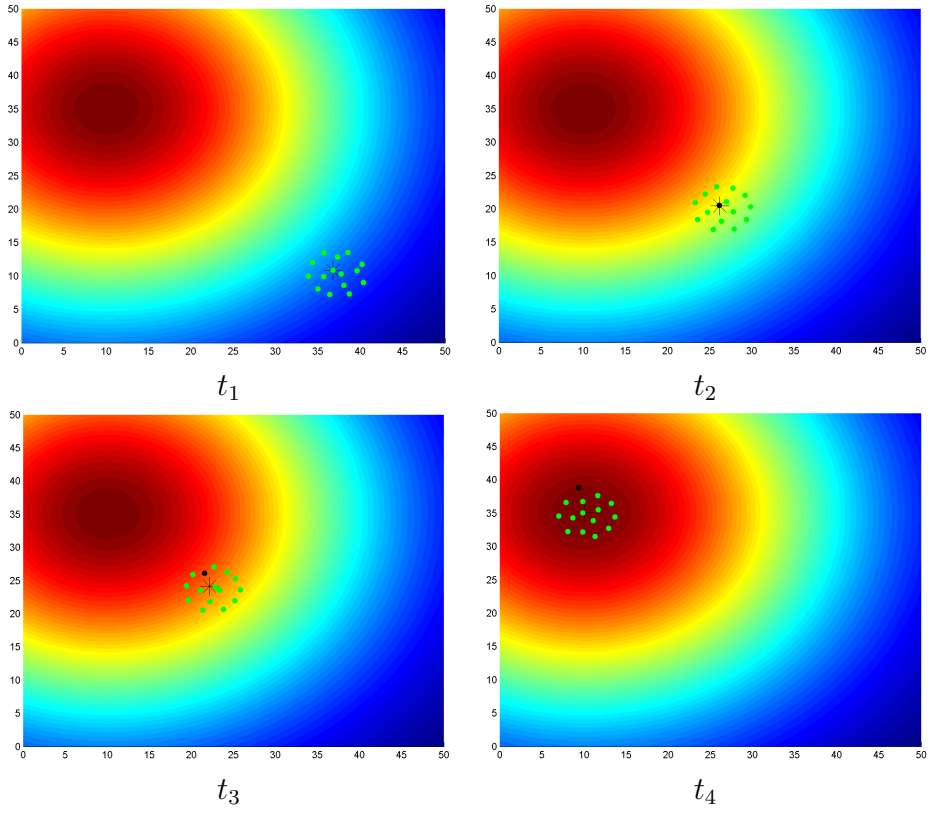

Figure 8: Illustration de la montée de gradient avec reconfiguration

Contributions

Les contributions à la recherche locale de maximum sont :

- Étude de nouveaux critères de placement optimal de capteurs pour l'estimation coopérative du gradient.
- Présentation d'un mécanisme de détection de défauts basé sur un seuil adaptatif dépendant des erreurs de modèle et de mesure.
- Développement d'une loi de guidage à deux niveaux pour :
  - Amener les agents à la formation désirée.
  - Déplacer la formation dans la direction du gradient.
  - Reconfigurer la formation en cas de capteurs défaillants.
- Preuve de stabilité de la commande proposée par la théorie de Lyapunov.

0.5 Recherche globale de maximum avec un modèle de krigeage

Pour dépasser les limites de la méthode de recherche locale, une méthode de recherche globale est proposée. Cette méthode s'appuie sur une modélisation du champ par un méta-modèle : le krigeage. Ce méta-modèle utilise les propriétés de covariance spatiale du champ qui s'avèrent très utiles pour notre application.

0.5.1 Présentation du krigeage et des critères d'échantillonnage existants

Le Krigeage représente la fonction à approximer par un processus gaussien.

Soit $f : \mathbf{p} \in D \subset \mathbb{R}^2 \rightarrow f(\mathbf{p}) \in \mathbb{R}$ le champ à modéliser et $Y(\mathbf{p}) = r(\mathbf{p})^T\boldsymbol{\beta} + Z(\mathbf{p})$ son modèle avec r un vecteur de régression, $\boldsymbol{\beta}$ un vecteur de paramètres et Z un processus gaussien de moyenne nulle et de covariance $C(Z(\mathbf{p}_1), Z(\mathbf{p}_2)) = \sigma_z^2\xi(\mathbf{p}_1, \mathbf{p}_2)$. ξ est la fonction de corrélation du champ.

A partir d'un ensemble de points d'échantillonnage de f, on peut écrire l'équation:

$$\mathbf{Y} = \begin{bmatrix} Y(\mathbf{p}_1) \\ ... \\ Y(\mathbf{p}_n) \end{bmatrix} = \underbrace{\begin{bmatrix} r^T(\mathbf{p}_1) \\ ... \\ r^T(\mathbf{p}_n) \end{bmatrix}}_{\mathbf{R}} \boldsymbol{\beta} + \underbrace{\begin{bmatrix} Z(\mathbf{p}_1) \\ ... \\ Z(\mathbf{p}_n) \end{bmatrix}}_{\mathbf{Z}} \tag{33}$$

et définir les vecteurs et matrices: $\mathbf{k}_p = [\xi(\mathbf{p}, \mathbf{p}_1), ..., \xi(\mathbf{p}, \mathbf{p}_n)]^T$, et $\mathbf{K}_{ij} = \xi(\mathbf{p}_i, \mathbf{p}_j)$.

Le modèle de krigeage fournit en tout point de l'espace une valeur moyenne du champ estimé

$$\mu(\mathbf{p}) = r(\mathbf{p})^T\boldsymbol{\beta} + \mathbf{k}_p^T\mathbf{K}^{-1}(\mathbf{Y} - \mathbf{R}\boldsymbol{\beta}) \tag{34}$$

et une variance de l'erreur de prédiction

$$\sigma^2(\mathbf{p}) = E[(\hat{Y}(\mathbf{p}) - \mathbf{a}_p\mathbf{Y})^2] = \sigma_z^2(1 - \mathbf{k}_p^T\mathbf{K}^{-1}\mathbf{k}_p)) \tag{35}$$

où σ_z^2 est la variance du champ f.

La recherche de maximum se fait sur le modèle de krigeage en cherchant la position d'échantillonnage. Différents critères ont déjà été proposés pour parvenir

à localiser le maximum. Le critère de Kushner présenté dans (Kushner, 1962), l'*Expected Improvement* utilisé par l'algorithme EGO dans (Jones et al., 1998) ou encore la '*Lower Confidence Bounding* function' proposer dans (Cox and John, 1997) sont autant de méthodes d'optimisation basées sur le krigeage. La limitation principale de ces méthodes est de ne pas avoir été conçues pour les systèmes multi-agents. Une seule position d'échantillonnage est donnée à chaque itération sans tenir compte des contraintes dynamiques des agents.

D'autres critères d'échantillonnage à base de krigeage ont été développés pour les systèmes multi-agents, notamment dans (Choi et al., 2008) et (Xu et al., 2011). Ces critères sont principalement adaptés pour l'exploration du champ par plusieurs véhicules. Une optimisation en deux temps est proposée, tout d'abord la zone est explorée pour minimiser la variance du modèle (i.e. l'incertitude) sur l'ensemble du champ, puis une fois la connaissance du champ établie, les agents se déplacent vers le maximum estimé.

0.5.2 Présentation du critère d'échantillonnage développé

Dans le cadre de cette thèse, un nouveau critère est proposé pour répondre à la mission de recherche de maximum par système multi-agents.

Ce critère a pour objectifs :

- Attribuer à chaque agent une position d'échantillonnage proche de sa position et l'éloignant des autres agents.
- Limiter la recherche aux seules zones de présence potentielle du maximum (définie par les caractéristiques du modèle de krigeage).
- Faire converger les agents vers la position du maximum global du champ.

Considérons le maximum des échantillons du champ $f^i_{\max}(t_k) = \max_{\mathbf{x}\in S_i(t_k)} \{\hat{\phi}_{i,k}(\mathbf{x})\}$.
Le critère proposé est le suivant:

$$\mathbf{x}^d_i(t_k) = \arg\min_{\mathbf{x}\in D} \left\{ J^{(k)}_i(\mathbf{x}) \right\} \tag{36a}$$

$$\text{s.c. } \hat{\phi}_{i,k}(\mathbf{x}) + b\sigma_{\phi,i,k}(\mathbf{x}) > f^i_{\max}(t_k) \tag{36b}$$

avec le coût $J_i^{(k)}$ définit par

$$J_i^{(k)}(\mathbf{x}) = \|\mathbf{x}_i(t_k) - \mathbf{x}\|^2 - \sum_{j \in \mathcal{N}_i(t_k)} \alpha \|\mathbf{x}_j(t_k) - \mathbf{x}\|^2, \tag{37}$$

où α et b sont des paramètres de réglage.

La contrainte (36b) définit les zones à explorer comme étant les zones potentielles de présence du maximum, c'est à dire les zones dont la moyenne du modèle plus l'incertitude du modèle est supérieure au maximum courant. L'effet désiré de la contrainte est un phénomène de montée des eaux provoquée par la mise à jour de $f_{\max}^i$ qui réduit les zones d'intérêts pour l'exploration.

La Figure 9 illustre le fonctionnement du critère sur un exemple simple à une dimension. Le vrai champ est représenté en bleu, la moyenne du modèle en rouge, et l'incertitude à trois fois l'écart-type en noir. Les points bleus représentent les points de mesure, la ligne pointillée verte la valeur de $f_{\max}^i$ et la ligne verte continue délimite le domaine strictement supérieur à $f_{\max}^i$ en introduisant un paramètre $\epsilon > 0$ tel que la contrainte est plus facilement satisfaite.

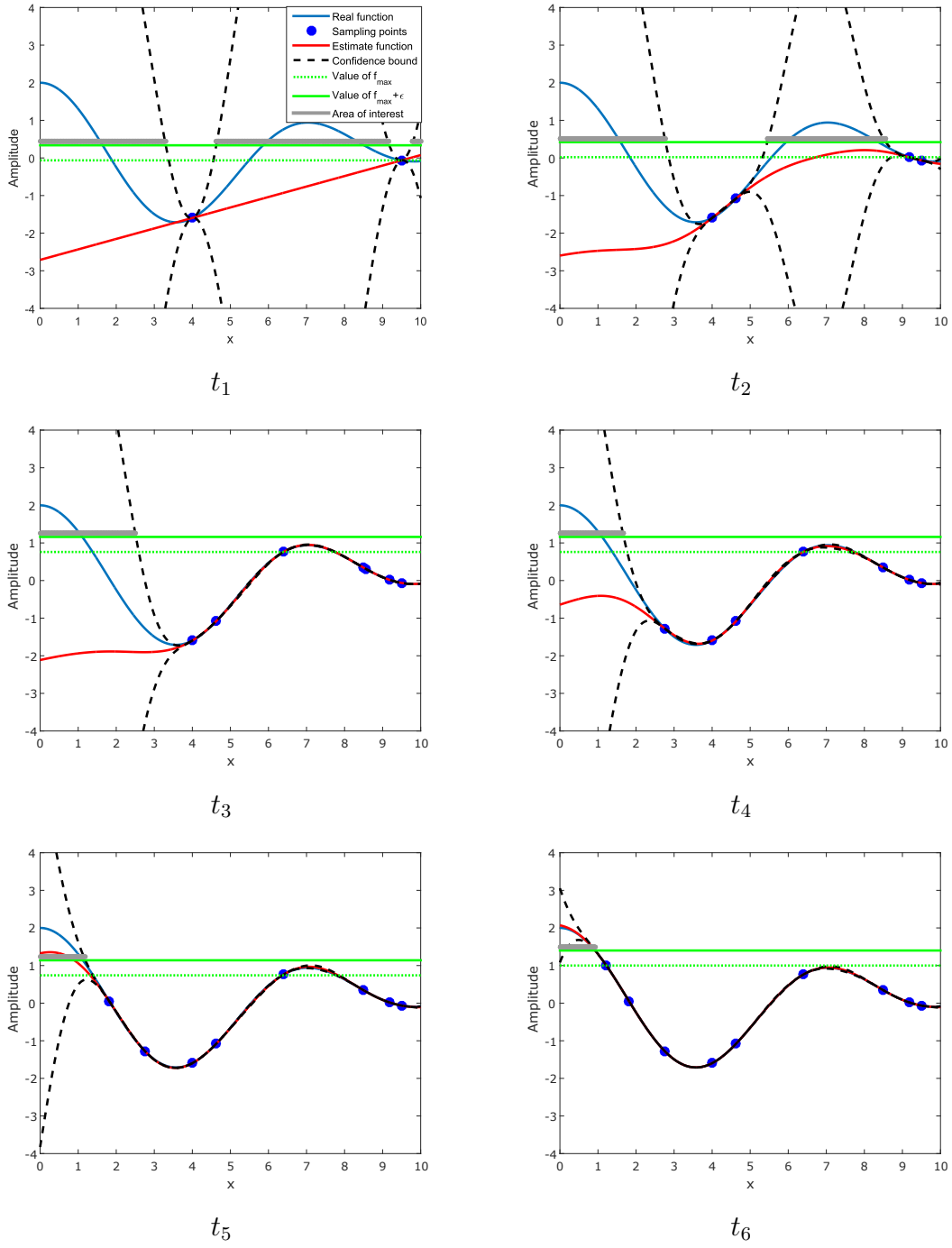

t_1 t_2 t_3 t_4 t_5 t_6

Figure 9: Illustration de fonctionnement du critère (36)

0.5.3 Adaptation de la loi de guidage pour la recherche globale

La loi de guidage proposée précédemment est reprise dans le contexte de recherche globale. Au lieu de faire converger tous les agents vers la position estimée du maximum $\widehat{\mathbf{x}}_i(t)$, la commande en position est donnée vers la position désirée $\mathbf{x}_i^{\mathrm{d}}(t)$. La position désirée $\mathbf{x}_i^{\mathrm{d}}(t)$ est calculée à partir du critère d'échantillonnage, et ne possède donc ni vitesse ni accélération.

La commande bas-niveau utilisée pour les agents est la suivante :

$$\begin{aligned}\mathbf{u}_i(t) =& C(\mathbf{x}_i(t), \dot{\mathbf{x}}_i(t))\dot{\mathbf{x}}_i(t) - k_1\dot{\mathbf{x}}_i(t) - k_3^i(\theta_i, t)\mathbf{x}_i(t) \\ &+ 2k_2\sum_{j=1}^{N}(\mathbf{x}_i(t) - \mathbf{x}_j(t))\, exp\left(-\frac{(\mathbf{x}_i(t) - \mathbf{x}_j(t))^T(\mathbf{x}_i(t) - \mathbf{x}_j(t))}{q}\right). \end{aligned} \quad (38)$$

Les modifications de la commande ne modifie pas le résultat de convergence asymptotique détaillé précédemment.

Algorithm 1 Algorithme de recherche globale de maximum

for à chaque instant t_k **do**
  for chaque agent i **do**
    if $||\mathbf{x}_i(t_k) - \mathbf{x}_i^{\mathrm{d}}(t_k)|| < \delta$ **then**
      Collecter une mesure y_i à la position $\mathbf{x}_i(t_k)$
    end if
    Echanger les informations avec les agents dans $\mathcal{N}_i(t_k)$
    Mettre à jour $S_i(t_k)$
    if $S_i(t_k) \neq S_i(t_{k-1})$ **then**
      Mettre à jour le modèle de krigeage (34) et (35)
      Minimiser le critère (36) pour trouver $\mathbf{x}_i^{\mathrm{d}}(t_{k+1})$
    end if
    Calculer la commande $\mathbf{u}_i(t_k)$ (38) qui :
    - Déplace les agents vers $\mathbf{x}_i^{\mathrm{d}}(t_k)$
    - Évite les collisions inter-agents
  end for
end for

Une simulation de recherche est effectuée sur le champ ϕ_{test} défini sur $D = [0,\ 50] \times [0,\ 50]$ et représenté en Figure 10

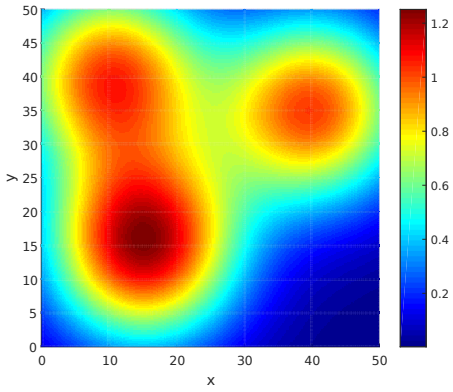

Figure 10: Fonction ϕ_{test}

Un système multi-agents de $N = 5$ agents est initialisé à des positions aléatoires dans D. Les paramètres de la simulation sont les suivants: le bruit de mesure des agents a une variance $\sigma_0^2 = 0.01$. Les paramètres de la loi de guidage sont $q = 0.1$, $k_1 = 47$, $k_2 = 50$, $k_3 = 1600$, $M = 1$ kg et $C = 0.001$ kg/s. La période d'échantillonnage est de $T = 0.01$s. Les paramètres du critère sont $b = 3$ et $\alpha = \frac{1}{N} = \frac{1}{3}$. Les paramètres du modèle sont $\theta = 50$ and $\sigma_k^2 = 0.5$.

Les Figures 11 et 12 illustrent la recherche du maximum. Le champ représenté correspond à la moyenne du modèle plus l'incertitude.

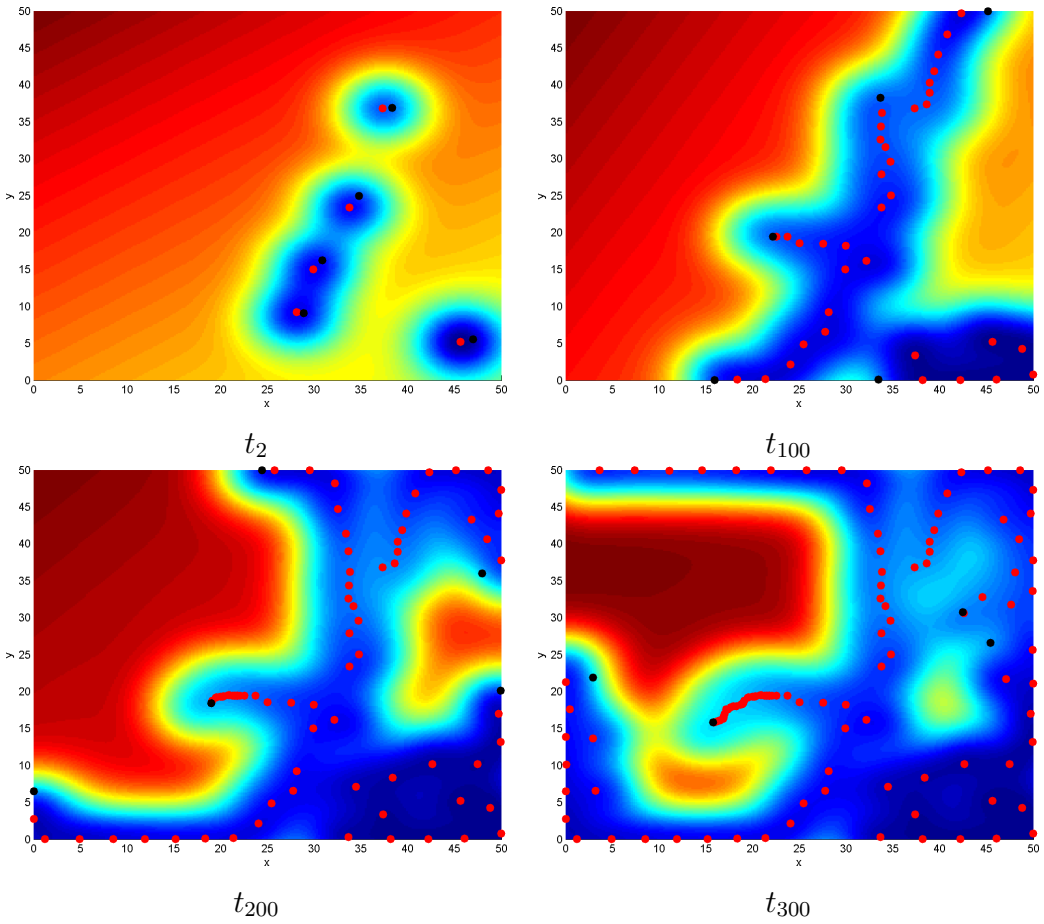

Figure 11: Illustration de la recherche de maximum sur ϕ_{test} par 5 agents

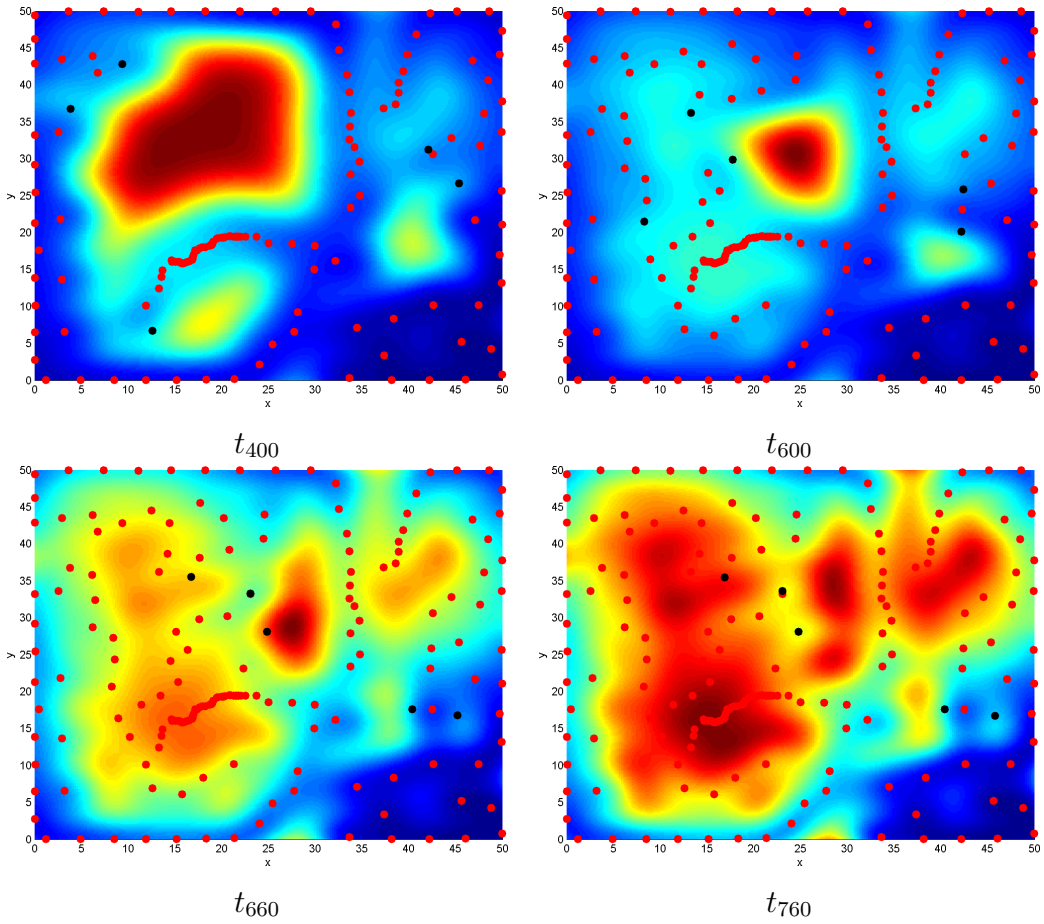

Figure 12: Illustration de la recherche de maximum sur ϕ_{test} par 5 agents

0.5.4 Comparaison avec une méthode de l'état de référence

Le critère proposé a été comparé à celui proposé dans (Xu et al., 2011). Ce critère nécessite un pas d'échantillonnage paramètré. Deux valeurs de ce pas ont été testées : $\tau_1 = 5T$ et $\tau_2 = 20T$. Les deux critères seront notés Xu5 et Xu20. Les résultats présentés sont obtenus sur plusieurs jeux de simulations. Les Figures 13 et 14 montrent que le critère proposé converge vite (autour de 300 itération en moyenne) vers la position du maximum avec une erreur faible et pour un nombre de mesure faible (inférieur à 100 mesures). Le critère Xu20 converge lui aussi rapidement (dans les 300 itérations) mais avec une erreur finale au alentour de 5m en moyenne. Le critère Xu5 converge lui plus lentement (autour des 500 itérations

en moyenne) mais a aussi une erreur faible.

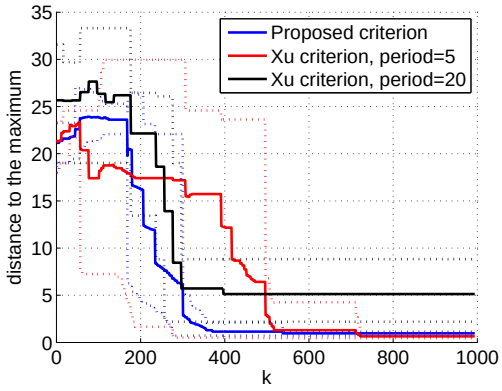

Figure 13: Distance au maximum par rapport au nombre d'itérations

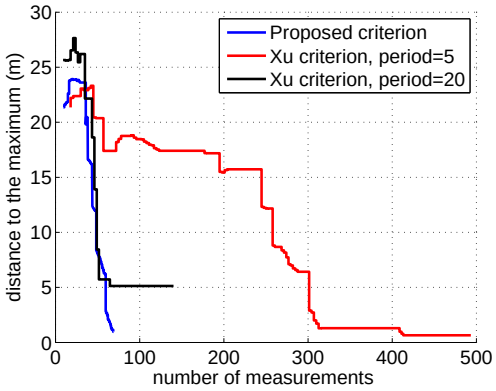

Figure 14: Distance au maximum par rapport au nombre de mesures effectuées

La méthode proposée permet une convergence plus rapide vers la position du maximum avec une faible erreur de position par rapport aux méthodes de l'état de l'art. Cela tient au fait que le critère proposé est construit pour limiter l'exploration globale aux seules zones d'intérêt alors que le critère de référence s'appuie sur une première phase d'exploration exhaustive du champ.

Contributions

Les contributions à la recherche globale de maximum sont :

- Définition d'un critère d'échantillonnage pour l'optimisation à base de krigeage permettant :
  - La dispersion des agents pour l'exploration.
  - L'assignation de positions de mesure prenant en compte la dynamique des agents.
  - La limitation de l'exploration aux seules zones d'intérêt.

0.6 Conclusion et perspectives

0.6.1 Approche locale

Pour répondre au problème de localisation du maximum d'un champ inconnu avec un système multi-agents, nous avons commencé par proposer une méthode de recherche locale par montée de gradient.

Pour parvenir au maximum, une estimation coopérative du gradient par moindres carrés pondérés est effectuée. Les contributions de la méthode proposée relèvent du placement optimal de capteurs. Plusieurs critères d'optimalité ont été proposés et leur solutions présentées. Nous nous sommes aussi intéressés à la détection de mesures aberrantes. Après une analyse de l'influence des perturbations sur notre estimation, un seuil adaptatif est proposé pour détecter les capteurs défaillants. Une loi de commande à deux niveaux a été proposé pour rassemblé les agents en formation et les déplacer vers le maximum du champ. Une méthode de reconfiguration a été présenté afin de replacer les agents aux capteurs défaillant dans la formation. Des simulations et une expérimentation ont été faites pour appuyer les résultats trouvés et montré la faisabilité de la méthode proposée.

En perspective de ces travaux, nous pouvons poursuivre l'étude analytique des critères de placement optimal pour essayer de trouver une solution théorique lorsque les agents ne peuvent pas se repartir sur un cercle à cause de la contrainte d'évitement de collision. Concernant la détection de capteurs défaillants, la localisation de l'agent fautif est effectuée par un système de vote par tous les agents. D'autres approches basées sur les consensus locaux pourront être étudiées pour identifier l'origine de l'erreur dans le système.

0.6.2 Approche globale

Afin de répondre aux limitations de la méthode locale ne permettant qu'une convergence vers le premier maximum rencontré, une méthode de recherche globale est proposée. Cette méthode s'appuie sur un modèle du champ par krigeage pour décider quelles zones explorer. Un critère d'échantillonnage est proposé prenant en compte la mission de recherche de maximum, la dynamique des agents ainsi que les caractéristiques de moyenne et d'incertitude du modèle.

La loi de commande de la partie local est réadapté au problème de déplacement

des agents sans mise en formation. Des simulations ont été faites pour montré le fonctionnement de la méthode proposé.

Pour aller plus loin dans cette approche, une méthode de détection devrait être proposée pour prendre en compte la défaillance d'un agent. Une difficulté supplémentaire vient du fait que contrairement à la méthode locale, les mesures passées sont gardées et utilisées. En cas de capteur défaillant, il faut analyser les mesures passées pour purger les mesures aberrantes.

Part I

Introduction and problem statement

Chapter 1

Introduction

Humans have realised since decades that mobile unmanned systems such as robots, satellites, or drones may extend their possibility of actions. Such systems are highly suitable for operations in hazardous environments such as space, battle fields and toxic or radioactive areas. They are also convenient for executing repetitive tasks such as monitoring.

More recent developments (Choi et al., 2009b, Schwager et al., 2011) promote Multi-Agent System (MAS) as a flexible solution, potentially more robust to fault and cheaper than a single agent for an equivalent efficiency. A MAS is a system composed of several homogeneous or heterogeneous entities. Each entity is a subsystem equipped with actuators and/or sensors and is able to perform programmed tasks. This topic is a very active field of research where progress is constant. MAS can handle a large range of missions such as monitoring (Akyildiz et al., 2005), research and exploration (Ahmadzadeh et al., 2006). One of the main interest of MAS is the possibility of cooperation between the different agents to accomplish their goals.

When dealing with a mission of exploration or search in a zone, the cooperation between agents may consist in finding the trajectories of all agents so that the coverage of an area is obtained in a more efficient way, *e.g.*, faster or with less energy consumed. Most missions of interest require to collect measurements of some spatially and time-varying physical quantities. Consequently, the agents are equipped with sensors to measure their environment. The types of measurement

needed may vary depending on the mission. It can be a temperature sensor to detect fire in a forest, a chemical concentration sensor to detect leaks in an industrial area, a camera to explore an unknown area, *etc.*

In this thesis, we focus on the mission of extremum seeking of an unknown field in a delimited area. Agents collect scalar measurements of the field value at their positions. They may exchange this data to compute a model of the unknown field and to design a search strategy to reach the maximum.

The topics tackled in this thesis include cooperative estimation, optimal sensor placement, Fault Detection and Isolation (FDI), control law design for MAS, local and global field optimisation.

Cooperative estimation is a problem that has been considered for more than 10 years. Cooperation means here that several agents share their measurements or estimates in order to improve the accuracy or the reliability of the common result. Some solutions have been proposed in this context for field estimation. In (Ögren et al., 2004), a cooperative estimation of the gradient of the unknown field is performed. A single Kalman filter is used to compute the estimate from the measurements collected by all the agents. In (Cortés, 2009) cooperative estimation is performed using a weighted least-squares estimator and an interpolating method.

All these authors and others (Zhang et al., 2007, Choi et al., 2007) compute a local estimate of the gradient of the unknown field to perform an optimisation by gradient climbing. This search strategy is common and easy to carry out with MAS. It can determine a local maximum of the unknown field following the gradient direction but is not guaranteed to obtain the global optimum in multi-modal fields and can result in a dead-end in case of a null gradient.

Other cooperative estimation techniques use a global model of the unknown field rather than a local one to perform the search. It is the case of (Choi et al., 2008, 2009b, Schwager et al., 2008) where meta-models are used to represent the entire unknown field. Most of these approaches rely on Kriging. This method is based on spatial covariance, which is well-suited for spatially distributed MAS as it may be used to design a sampling criterion taking into account the agent positions. (Xu et al., 2011) and (Gu and Hu, 2012) propose sampling policies to move a MAS while performing exploration or optimisation of an unknown field.

Special care has to be taken with measurements since the search efficiency depends on their quality. The measurements may be collected by a defective sensor, thus misleading the system towards an erroneous result. The effects of an outlier can vary from the impossibility to find the maximum to the loss of the fleet. Fault Detection and Isolation (FDI) schemes have been developed to detect the occurrence of such defective sensors and to lessen their influence on the resulting estimates.

The sensor locations evolve with the positions of the agents. These locations can be optimized to improve the estimation process. In the case of a local estimation, (Ögren et al., 2004) suggests a formation strategy to optimise the sensor placements but does not consider the case of faulty sensors with degraded capability. For the global approach, when a Kriging model is used, the sampling criteria should be designed to optimise the position where the next measurement has to be performed.

In both cases, the agents are moved according to a designed control law that brings the agents into the desired formation and moves the agents to the desired positions. The control law presented in (Cheah et al., 2009) satisfies this objective and guarantees the stability of the MAS but does not allow reconfiguring the formation in case of faulty sensors.

The aim of this thesis is to define strategies allowing a MAS to find the position of the maximum of an unknown spatial field.

Firstly, local search strategies based on gradient climbing are investigated. The existing methods answer basic problems such as gradient estimation, control law computation, sensor placement or fault detection, but none of them are designed to treat all of these problems simultaneously. Three main contributions in the local approach proposed in this thesis are presented. An optimal sensor placement analysis with three criteria has been developed. A fault detection scheme based on a novel adaptive threshold has been defined to detect outliers. Finally, a distributed control law for formation control that enables reconfiguration to maintain the estimation performance in case of faults on sensors has been designed.

Secondly, gradient climbing as a local search strategy cannot find the global maximum in a multi modal field. To overcome this issue, we investigate global

search strategies with Kriging. We analyse the existing methods, most of them are not designed for MAS but only for numerical optimisation with possibility to sample the cost function anywhere at any time. The few of them conceived for MAS are proposed for exploration missions that can be adapted to the search problem. In this thesis, the main contribution for global optimisation based on Kriging-modelling is the design of a novel criterion. This criterion takes into account the agent positions and the Kriging model to select their next sampling positions. It aims at spreading the agents in the search area to perform a faster exploration. The areas to be explore are also limited to only zones that may contain the maximum of the unknown field.

Figure 1.1 presents the different topics and how they interact together. The initial mission goal is to find the maximum of the field with a MAS. This initial task leads to two problems, namely the control law design and the estimation method. The control law design should move the agents as requested by the search criteria while avoiding collision. The control laws for local and global approaches may have different objectives.

The estimation problem is related to the search method used. For the local approach, the estimation process should estimate the local gradient of the unknown field. For the global approach, the estimation process should design the Kriging model over the entire search space.

The estimation problem leads to two sub-tasks, the sensor placement and the fault detection and isolation. The sensor placement is used to determine at which positions the unknown field should be sampled. For the local approach, the answer to this sub-task is the optimal sensor placement analysis. For the global approach, the answer is the design of the new sampling criterion. A fault detection and isolation scheme, related to the estimation model used, should be designed to detect when a fault occur and identify the origin of the fault. The final answer for the local and global approaches merge the previous sub-tasks to propose a control law that leads the agents to the desired sampling positions and enable reconfiguration in case of fault in the system.

This thesis is organised as follows. In Part I, the main problems and assumptions are introduced.

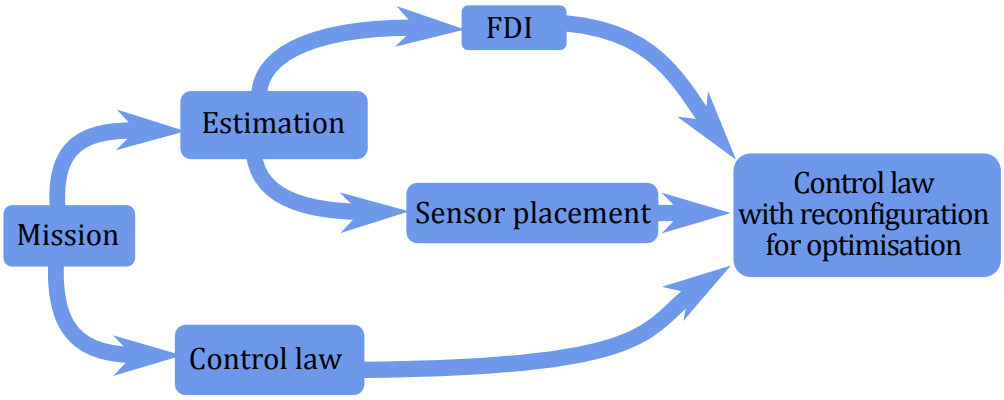

Figure 1.1: Steps to the proposed solution

Chapter 2 describes some previous works and literature related to the topics of interest. These topics integrate the presentation of a multi-agent system, the different methods of formation control, the existing fault detection and identification schemes, the estimation methods and the local and global optimisation strategies. The advantages and limitations of the existing solutions are presented.

Chapter 3 presents the main problem and describes the set of hypotheses and notation used in the rest of the thesis. The model of the agents and their sensors are defined.

The contributions presented in this thesis are divided in two parts. Part II focuses on the local search strategy. **Chapter 4** introduces the gradient estimation method, followed by three optimal sensor placement criteria. Analytical and numerical solutions for these criteria are investigated. A fault detection scheme with a novel adaptive threshold is introduced. Numerical simulations are performed to analyse the sensitivity of the proposed solution to its tuning parameters. A fault isolation strategy completes this chapter.

Chapter 5 presents a two-layer control law. The low-layer control drives the agents into a desired formation for estimation while a high-layer control moves the formation toward the maximum by gradient climbing. A stability analysis of the low-layer is performed using Lyapunov theory. Experiments on mobile robotic platforms illustrate the effectiveness of the estimation method and the high-layer control law. A reconfiguration scheme is proposed to take into account sensor faults by modifying the control law. The proposed local approach is illustrated by

numerical simulations.

The work presented in Part III overcomes some issues of the local approach. **Chapter 6** starts with a presentation of the Kriging modelling method, followed by a description of the existing criteria of the state-of-the-art for Kriging-based optimisation without MAS and exploration with MAS. After this presentation, we describe our new sampling criterion. This criterion uses the Kriging model to select the positions where the field should be measured while considering the dynamics of the MAS. The behaviour of the proposed criterion is illustrated on a basic example. The control law introduced in Chapter 5 is then adapted to the global search. Numerical simulations are reported to highlight the proposed solutions and how they compare to state-of-the-art criteria. Perspective work for a FDI scheme adapted to the global approach is presented.

A concluding **Chapter 7** summarizes the results presented in this thesis and proposes some directions for future works.

Author publications:

- (Kahn et al, 2013) Kahn, A., Marzat, J., Piet Lahanier, H. *Formation flying control via elliptical virtual structure*, IEEE International Conference on Networking, Sensing and Control, 158-163, Evry, France, (2013)

- (Piet-Lahanier et al, 2013) Piet Lahanier, H., Kahn, A., Marzat, J. *Cooperative guidance laws for maneuvering target interception*,IFAC Symposium on Automatic Control in Aerospace, 296-301, Würzburg, Germany, (2013)

- (Marzat et al, 2013) Marzat, J., Piet Lahanier, H., Kahn, A. *Cooperative guidance of Lego Mindstorms NXT mobile robots*, 12th International Conference on Informatics in Control, Automation and Robotics, 605-610, Vienne, Austria, (2013)

- (Bertrand et al, 2014) Bertrand S., Marzat J., Piet-Lahanier H., Kahn A., Rochefort Y., *MPC Strategies for Cooperative Guidance of Autonomous Vehicles*, Aerospace Lab Journal, 8, 1-18, (2014)

- (Kahn et al, 2015a) Kahn, A., Marzat, J., Piet Lahanier, H., Kieffer, M. *Cooperative estimation with outlier detection and fleet reconfiguration for multi-agent systems*, IFAC Workshop on Multi-Vehicule Systems, 11-16, Genova, Italy, (2015)

- (Kahn et al, 2015b) Kahn, A., Marzat, J., Piet Lahanier, H., Kieffer, M. *Global extremum seeking by Kriging with a multi-agent system*, 17th IFAC Symposium on System Identification, Bejing, China (2015)

Chapter 2

State-of-the-Art: From multi-agent systems to extremum seeking

Chapter goals

In this chapter, a presentation of some state-of-the-art methods is done for the following topics developed in this thesis.

- Multi-agent system: missions and control
- Fault detection and reconfiguration: outlier detection and resulting actions
- Optimisation: local and global models, different search approches
- Cooperative estimation: acquire knowledge on the field from measurements

This chapter presents existing works on the related topics addressed in this thesis.

First, multi-vehicle systems are introduced in Section 2.1. Description of their abilities and limitations is provided and approaches developed to overcome the main issues are discussed. Second, Section 2.2 presents the different control strategies to regroup a MAS into a formation. Third, Section 2.3 introduces the Fault Detection and Isolation (FDI) topic with some common methods used to detect faults. The kind of fault considered is occurrence of outliers within the measure-

ments (abrupt fault). Estimation methods and reconfiguration approaches are investigated afterwards.

Last, as the main objective in this study is to search for a maximum, local and global optimization techniques are presented in Section 2.5. Figure 2.1 describes the various topics considered in this thesis. To complete the initial mission, the control law and the estimation tasks can be designed independently but need to share information to operate. The first one is used to move the agents towards their future positions while avoiding collision. The second one deals with the collection of measurements and how they are combined to obtain the required characteristics of the field. This implies a sensor placement method to know where to perform the measurement and a FDI scheme to detect when a sensor is faulty. The control law linked with the sensor placement and the FDI scheme design a system with reconfiguration capabilities to find the maximum of a field.

2.1 Multi-agent system (MAS)

Thanks to developments in robotics and artificial intelligence, autonomous vehicles have widened their scope of application. They present a huge advantage for repetitive and time-consuming tasks like surveillance and monitoring (Sirigineedi et al., 2010, Merino et al., 2005). They allow humans to delegate these tasks as they are usually more efficient and faster to accomplishing them. Autonomous vehicles are also used in environments presenting risks for human operators, (Parker, 1998).

This thesis focuses on MAS consisting of multiple vehicles. The agents considered in our study are equipped with sensors and actuators to interact with the environment. Communication and computational capabilities are embedded in the agents to enable cooperation. The agents interact with each other by sharing information. In our study, the agents are mobile autonomous vehicles able to move in an unknown environment, and to measure some of its characteristics.

Deciding to use a MAS consists in finding the best trade-off between using a single and possibly complex vehicle which has a single task to perform and several less complex vehicles that require task division.

The efficiency of a system to perform a mission is usually quantified by some cost function. One can try to minimize the energy consumption of the agents by optimizing the trajectories, or one can try to minimize the estimation error or

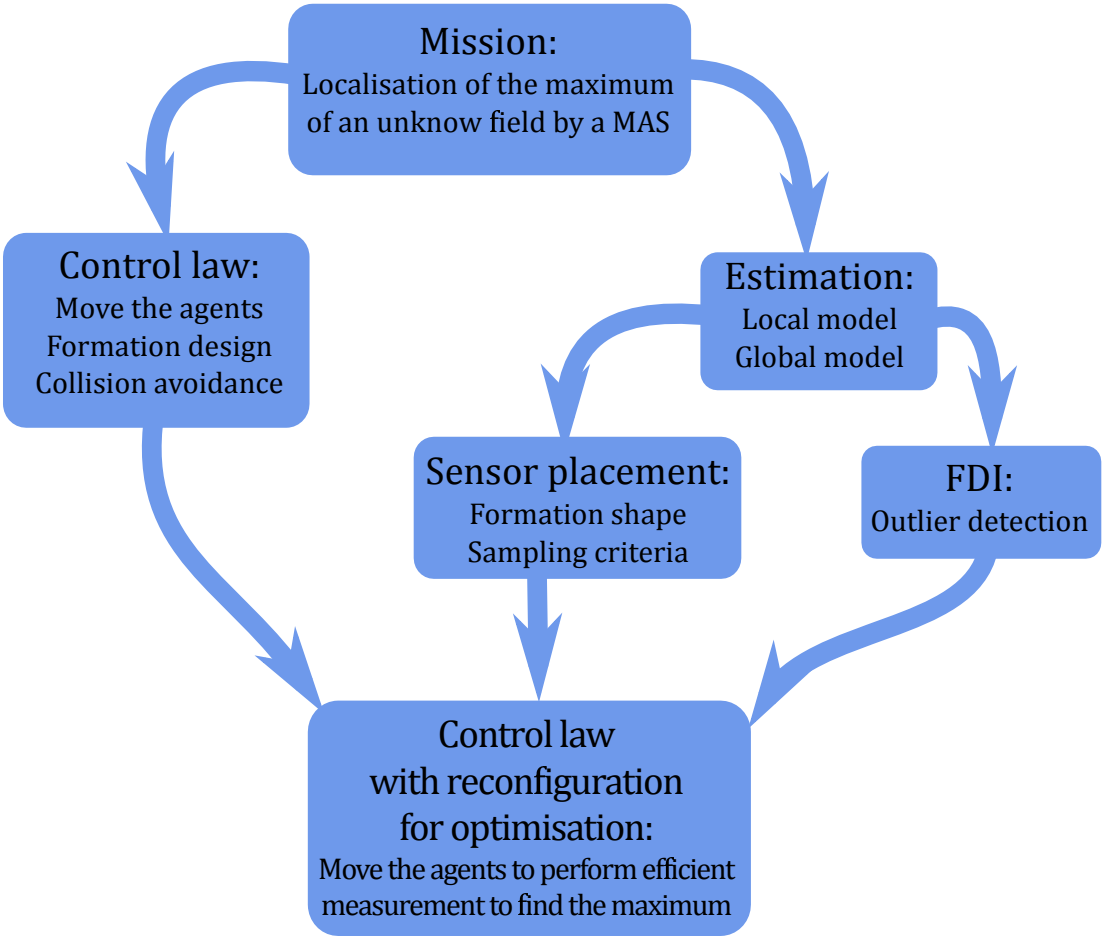

Figure 2.1: Steps followed to design the proposed maximum seeking solution with MAS

the exploration required to find the maximum. One single agent can perform a mission such as area exploration or extremum seeking of a spatial field, but a MAS may perform the same task more efficiently by using several agents cooperatively and spreading them in the area. Another advantage of MAS over a single agent system is its robustness to vehicle loss. However, the cooperative movements of several vehicles imply to take care of difficulties such as task sharing or collision avoidance.

2.1.1 Cooperation among the agents

A MAS aims to use cooperation among the agents composing the system to fulfil the mission. A MAS is justified when the global efficiency of the agents has to be greater than the sum of the efficiencies of each agent. The way cooperation in a MAS has to take place is particularly problem dependent.

For example, for missions such as surveillance and area exploration, several agents disseminated in the search space may reach the objective faster than a single agent. A search mission for forest fire detection by a fleet of heterogeneous UAV has been proposed by (Merino et al., 2005). Data association from different agents improves the cooperative detection and localisation. This cooperation between agents decreases the uncertainty of the fire location.

A fleet of UAVs (Sirigineedi et al., 2010) can carry out a surveillance mission of some interest area, e.g. an harbour. Allocation of the targeted surveillance points is done with respect to the importance of each position. The MAS checks areas with higher importance more often than areas with lower interest.

MAS are also relevant for multi-target tracking or for observation. The agents can be spread over several targets (Parker, 1999) and can attempt to maximize the time during which an agent is located in the vicinity of the targets.

Between exploration and surveillance, missions such as level curve tracking by MAS have been investigated (Williams and Sukhatme, 2012). Each agent transmits information to its neighbours to divide the global mapping problem into local problems. Analyses show that the performance of the mapping process increases with the number of agents in the system. More agents means a better spatial distribution and more observations.

2.1.2 Robustness to fault

A fault is an unexpected hardware or software event that occurs in a system and may disturb the system operation. Robustness of a system to faults is the ability to maintain the same level of performance after occurrence of a fault in the system.

MAS are considered more robust than a single agent system to the occurrence of critical faults as they provide larger flexibility in terms of reconfiguration. If the fault concerns one of the agent actuators, the dynamics of the agents are changed. In (Bošković and Mehra, 2002) the authors propose guidance laws for MAS by

a leader-follower technique. They study the case of actuator faults on a follower agent and propose a modification of the control law to maintain the formation.

A formation feedback control has been developed by (Ren and Beard, 2002) to adapt the control of every agent depending on the state and disturbance of the other agents to maintain the desired formation. This control keeps all vehicles in a formation and limits the influence of internal or external disturbances.

Instead of modifying the control law, other actions are possible to overcome an actuator fault. A modification of the initial trajectory can take into account the new constraints induced by the damaged agent dynamics (Chamseddine et al., 2012). The authors used a virtual structure control law to maintain the formation of fleet of quadrotor UAV. The trajectories are defined by Bézier curves. When an actuator of an agent becomes faulty, different cases may be considered, (i) the damaged agent is not able to continue the mission and remaining agents continue without it; (ii) the damaged agent can continue the mission but with degraded performance, decisions have thus to be taken to choose whether the fleet continues with or without the faulty agent.

2.1.3 Task assignment for the agents

When using a MAS instead of a single agent, the problem of task assignment must be tackled. Planning and task division share the set of tasks of the initial mission between several agents. To increase the capabilities of a MAS compared to a single agent, the mission must be divisible into smaller tasks that can be performed in parallel by the agents of the MAS.

The division of the mission cooperatively over the agents is problem dependent. Trajectory definition or path planning of the agents are common tasks for vehicle MAS.

To move a fleet of agents, it could be preferable to bring the vehicles in formation. Moving the formation will require one single control law, while the control of each vehicle should maintain the formation. The fleet coordination can be divided in subtasks such as geometric pattern formation, orientation alignment of the agents, coordination of the agents within the group, motion and formation stability (Chen and Luh, 1994). Each agent has to carry out its subtask to perform

formation control of the MAS.

Some work (Chamseddine et al., 2012) proposes, a first planning of the trajectory of the MAS before the mission starts, then a second planning takes place when a fault modifies the initial dynamics of an agent.

Trajectory planning is also related to problems such as rendez-vous and constrained paths. In (Tsourdos, 2005), Dubins paths generate trajectories of equal length for a MAS of UAVs. The rendez-vous problem is also treated by using Voronoi tessellation of the space to determine the path of each agent (Jiang et al., 2007).

Aside from trajectory and path planning, task allocation concerns any other action that the agents may have to fulfil. In (Tang and Parker, 2007), task division and allocation are taken in a broader sense and behavioural repartition methods are proposed. This requires tasks to be divided in a tree of subtasks so that a group of heterogeneous agents can perform them.

2.1.4 Architecture of the system

The problem of planning and task allocation is treated differently depending on the MAS architecture. Three of them are possible.

- The centralised architecture where all the information is gathered in a master node. Only one element performs the computations and the decisions for all the agents.
- The distributed architecture where each agent acquires its own information or shares it with neighbours and treats it by itself to perform computation and decision.
- The hybrid architecture where some parts are centralised (information from all the system for instance) and some parts are distributed (computation of the control law for instance)

The centralised approach requires the availability of the information from the whole system at a central processing point. This architecture is easier to implement (communication problem apart) because a single entity is in charge of all actions. (Zhang et al., 2010a) present a centralised fault diagnosis method. A

bank of filters isolates the faulty entry to identify the origin of a fault among all the inputs in the system.

A centralised architecture is also used for the formation control of a MAS in (Beard et al., 2000). A supervisor performs a high-level control over the formation depending on a set of events.

Hybrid architecture can be a solution to deal simultaneously with local problems such as collision avoidance, and global goals such as the determination of the motion of the formation. A double layer control is proposed for formation control by (Wang et al., 2007). The control architecture switches between two control strategies to allow each agent to avoid obstacles while moving within a MAS.

The decentralised or distributed architecture is more complicated to implement than the centralised one. The combination of individual actions and knowledge of each agent must converge toward the same result. This kind of architecture is used for control and motion planning as in (Sugihara and Suzuki, 1990), where each robot of a MAS is controlled individually with local information to perform a global task, such as spatial repartition. In (Julian et al., 2011), a distributed control law moves the agents of a MAS towards a region of interest to explore it and in (Zavlanos and Pappas, 2007), a distributed control law aims at creating a formation and moving it towards a desired position. These approaches deal with another relevant question in distributed architecture: achieving consensus among the agents. A consensus method is used to propagate an information among the agents. (Julian et al., 2011) present a consensus method to estimate some quantities from the measurements among the MAS and aims at unifying the knowledge of the environment between the agents. (Zavlanos and Pappas, 2007) propose a consensus scheme to move the agents in the same direction with the same velocity.

Distributed architectures and consensus have other applications. In sensor network studies, distributed estimation of a spatial field and fault detection and isolation of faulty sensors are proposed. Mechanisms to detect and identify faulty sensors in the network are proposed for instance by (Wang et al., 2009). A Bayesian estimation of a parameter of interest is performed in a distributive way using the measurements of the non-faulty sensors. A distributed Kalman filter is used for the estimation and Bayesian learning is employed to detect and isolate faulty measure-

ments from sensors (Zheng et al., 2010). In (Delouille et al., 2006), graph theory tools are used to model the distributed architecture. A sensor network transmits local estimates obtained in a neighbourhood via connected agents to share information. The proposed sub-graph method is robust to communication errors and faulty sensors. In (Schwager et al., 2008), a consensus on the estimated field ensures the movement of a fleet of agents to cover an area of interest. The consensus process makes the local estimation of a spatial field of each agent converge to a unique global value.

Apart from communication and computation architecture, different architectures also exist for the control of MAS. The design of the control law to move a MAS is more complex than for a single agent. The coordination of several agents implies more complex control laws to avoid collisions or take into account initial goals and sub-task of the mission.

2.2 Formation control

Different methods can be applied to control a MAS. All the control orders can be computed centrally or each agent may compute its own control input. This control is designed for reaching a goal that can be either a given desired position or a local equilibrium resulting from attractive and repulsive forces in the fleet.

Among all the different control laws for vehicles, we focus on formation control methods. Formation control allows moving a MAS in an environment while avoiding collisions between the vehicles. Three main classes of formation control can be identified. First, Leader-following where an agent has more importance than the others. The leader trajectory is decided independently from the others with different knowledge and goals. One agent is the leader of the formation, all the others are followers that should track its trajectory. The second class is formation control via a virtual structure where geometric, spatial or communication patterns link the agents together. No agent has a predominant position regarding the others. The third class is called control via behavioural rules. Each agent moves according to some rules and takes action depending on its environment.

2.2.1 Leader-follower formation control

In this architecture, all agents follow the trajectory of the leader of the formation. While the trajectory of the leader has to fulfil the mission requirement, a follower only needs a basic control law to follow it. Orientation and velocity matching between leader and followers has been used in (Bošković and Mehra, 2002). Exchange of information between the agents is mandatory to obtain the leader-follower formation. Investigation on communication delays in such systems and consensus conditions have been proposed in (Liu and Liu, 2010).

Let us consider heterogeneous MAS consisting of agents with different actuators, sensors or dynamics. In such a system, the leader can be different from the other agents. In (Bıyık and Arcak, 2008), the leader is the only agent equipped with a sensor and performs a gradient climbing. To compute the estimate of the gradient, it has to move slightly around its position to obtain the required measurements. Then the leader moves according to the direction of the gradient. The problem for the followers is to track the gradient climbing displacement without taking care of the slight movement of the leader for data collection. Different solutions to track the leader smoothly are proposed for the followers.

To create the formation with the leader, the control law of the followers can be combined with some behavioural rules to reconfigure the formation of the followers in case of obstacles or when a follower loses the formation (Carpin and Parker, 2002). The leader follows a human or is remotely driven and the followers form a line to chase the leader.

The propagation of information from the leader to the followers (Leader to formation stability) is analysed in (Tanner et al., 2004) using tools from graph theory. It quantifies the control error coming from leaders in an interconnected system and can be used to test different connections among agents in leader-following formation control.

2.2.2 Virtual structure formation control

To overcome the issues encountered in the leader following scheme when the leader suffers from a failure, the virtual structure is a formation control method where all the agents have the same importance in the group.

A sub category of virtual structure, derived from leader following scheme is

called virtual leader (Rochefort et al., 2011). Instead of a real vehicle used as the leader of the formation, a virtual vehicle described by its current position and sometimes speed, is created to guide the other agents and move the formation.

Virtual leader and potential fields (the potential field are used to create repulsive and attractive forces between the vehicles) are used to create a formation and move a fleet of agents in (Leonard and Fiorelli, 2001, Ögren et al., 2004). In (Ögren et al., 2004), virtual leaders move the MAS toward the maximum of a field by gradient climbing. To compute the gradient, a least-square estimate and a Kalman filter are used with measurements of all the agents. The geometric pattern of the formation is analysed and optimal formations are proposed.

Another method proposes to decompose the fleet in several layers depending on the place of each agent with respect to the virtual leader (Longhi et al., 2008). Each agent may follow its own leader. The formation can be modified without consideration about the leader in case of a fault, it only modifies the architecture of the formation.

Without a leader to shape the formation, the geometrical links between the agents can be stated by a virtual structure. Virtual structures can also represent the connection among the agents in a formation.

The virtual structure control can treat the MAS as a rigid body (Tan and Lewis, 1996). The agents are linked together and move as if they compose a rigid body. This control method does not allow any kind of flexibility in the movement of the agents or any deformation of the formation.

In (Ren and Beard, 2002, 2004), a virtual structure method for spacecraft formation is proposed. Their control scheme can be decentralized and agents aim at matching a desired place in the formation and to maintain it.

Potential fields are used to create a formation with some desired shape in (Yan et al., 2011, 2012). A part of the control law called regulation control force is applied to prevent the agents from being stuck in a local minimum of the formation shape. Shapes such as squares, triangles or other polygons can be obtained. Lyapunov method is used to demonstrate the stability of the proposed control law.

Potential field control can be mixed with sliding mode control to define a formation for the agents and move them toward a target (Yao et al., 2007).

In (Cheah et al., 2009), a control law is presented to create formations of different shapes. Some areas are defined and the agents move and spread homo-

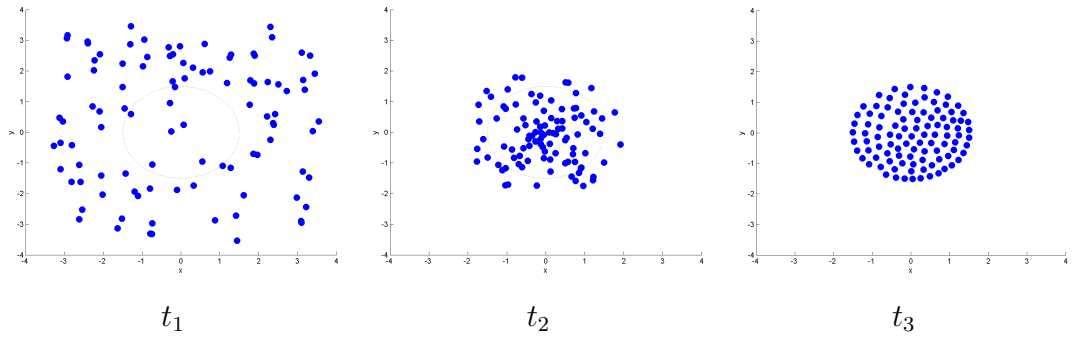

Figure 2.2: Illustration of the control law of (Cheah et al., 2009), formation control by Lyapunov method

geneously inside. By moving this area, the formation moves while preserving its shape. Gradient descent attracts the agents inside the area then a sliding mode control switches the agent commands to keep them within the delimited area. Lyapunov method is used to demonstrate the stability of the proposed control and ensure that the agents will reach the inside of the target area while avoiding collision. Figure 2.2 illustrates the proposed control law. The positions of the agents are plotted with blue spots and the desired formation is shown by the dashed black circle. The first simulation time t_1 shows the agent initial positions. At t_2 a transition phase corresponding to the agents moving in the desired area is shown. The figure at time t_3 shows the agents reaching a stable formation in the desired shape.

To spread the agents over a desired area with points or zones of interest, some authors have used the Voronoi repartition, such as (Cortés et al., 2002). A coverage control moves the agents to the area of interest and treats at the same time the allocation problem to create the formation. An interest function with a maximum is defined and known by the agents. Each agent computes the mean of this interest function over its Voronoi cell defined by its neighbours. Then each agent moves toward the barycentre of its cell. Repeating this process, the fleet moves toward the maximum of the interest function and creates a formation around. The authors propose also a scheme to force the shape of the formation with the same method. Figure 2.3 illustrates the evolution of the MAS considering the proposed control law. The agent positions are plotted with blue spots and the Voronoi tessellation by red lines. At time t_1 the agents are in their initial positions. At time t_2 there is

a transition phase where the agents move to cover the area. At time t_3, the agents have reached a stable formation in the desired shape.

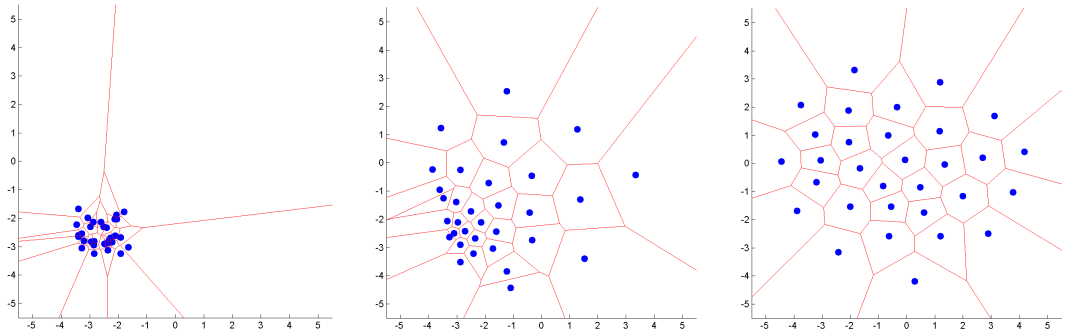

t_1 t_2 t_3

Figure 2.3: Illustration of the control law of (Cortés et al., 2002), formation control by Voronoi tessellation

Following the same idea, (Schwager et al., 2007, 2008, 2009b) present a Voronoi repartition to allocate the positions of the agents. They complement the previous work with a learning and consensus scheme to allow the agents to learn and construct a model of the field of interest. Simulations and experiments have been performed with multi-modal functions of interest. This problem is related to the position allocation of a MAS. The same authors have worked with flying quadrotor UAVs for vision coverage of an area (Schwager et al., 2009a). They propose a distributed control strategy built to optimise the location of the agents with multiple cameras.

2.2.3 Behavioural-rule formation control

In behaviour-rule formation control, each agent has a set of rules that it has to follow and the combination of these rules lead to some desired behaviour.

Swarm control (or flocking) is a part of formation control halfway between virtual structures and control based on behavioural rule.

The Reynolds rules defined in (Reynolds, 1987) present the foundations of swarm control. Each agent obeys to three rules. The first one is the collision avoidance, a repulsive term between agents. The second is the velocity matching,

a unity term that forces the velocity of each agent to converge to a common value. The third one is the flock centring to keep the agents together and avoid dispersion. By using this kind of control, the fleet reaches a consensus in direction and velocity.

In (Olfati-Saber, 2006) is presented an approach derived from swarm control theory to keep the formation in a predefined geometric shape. Simulations in 2D and 3D are presented and obstacle avoidance with splitting and re-joining manoeuvres are described.

Behavioural rules depend on the close environment of the agents. If a modification happens in the agent direct environment, then the control input computed by behavioural rule may be modified. This makes the behavioural rule control sensitive to change in its neighbourhood.

The architecture *ALLIANCE* developed in (Parker, 1998) is an example of control via behavioural rules. It defines for each agent a set of behaviours or actions that can be performed. Depending on the knowledge of their environment coming from their sensors or collected from their neighbours, the agents decide which action to take. This architecture is fault tolerant because if an agent fails to perform an action, one of its neighbours may achieve it.

The evolution of the previous architecture result in the *ASyMTRe* architecture presented in (Tang and Parker, 2005, Zhang and Parker, 2010). It proposes a cooperation among robots to perform a given task. This kind of architecture is appropriate for heterogeneous groups of agents where all the robots are not equipped with the same sensors and actuators.

Manoeuvre of a MAS relying on behavioural rules and several strategies are shown for the problem of maintaining a formation during the movement of a group of vehicles in (Lawton et al., 2003).

2.3 Fault Detection and Isolation (FDI)

After this presentation of the different formation control strategies, this section provides some elements from the state-of-the-art in fault detection and isolation.

MAS can be subject to faults during their missions. These faults can have external or internal sources but may disturb the behaviour of the MAS. It is important to detect when such faults occur to take the appropriate actions. Figure 2.4 shows a representation of a system with different possible faults and a fault detection

and isolation (FDI) scheme.

The usual method to detect an error is to compare the output of the system y with the desired output or its estimate $\hat{y}$. This comparison is computed by construction of a residual r

$$r = y - \hat{y}. \tag{2.1}$$

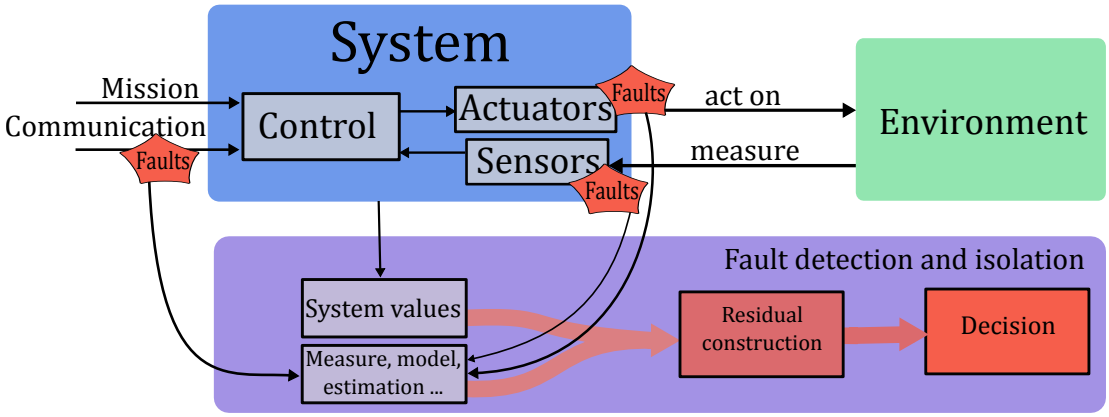

Figure 2.4: Illustration of a system with a FDI scheme

The study of the value of r allows to decide if the system is faulty or not. The residual is compared to a threshold to detect the presence of faults. The threshold can be static or adaptive (Zhang et al., 2004).

In a complex system such as a fleet of vehicles, different types of errors or faults can take place. One may identify actuator faults that can modify the dynamics of the vehicles, sensor faults that can disturb the measurement of an agent or communication errors such as delays or loss during transmission.

2.3.1 Actuator fault

The survey (Marzat et al., 2012) on FDI methods for aerospace systems classifies the FDI methods depending on the type of vehicles concerned and introduces a reminder of the commonly used methods.

In case of faults that modify the dynamics of one agent, mission such as rendez-vous may fail. To compensate actuator faults in one vehicle, the others could reconfigure their trajectories to achieve the mission nonetheless (Jiang et al., 2007).

A FDI scheme that ensures the stability of a formation of vehicles under the possibility of the sudden breakdown of an agent is proposed in (Seo et al., 2012). The method is based on a distributed control scheme with output feedback. It also considers the possibility of a loss of communication.

Different strategies for FDI are possible to overcome actuator faults, either centralized, semi-decentralized or decentralised architecture as presented in (Meskin and Khorasani, 2009, 2011). They treat the problem of FDI among several agents with perfect or imperfect communication. They study the FDI for MAS with dependent fault signatures. Due to the redundancy of agents and actuators, the isolation of faults can be hard to perform and a fault signature can be the result of several causes. The authors propose different architectures to perform the FDI. They claim that the semi-decentralised architecture has the same detection rate than the centralised one with less computational requirements.

Theorems and conditions to determine the kind of systems and faults that are detectable and identifiable are presented in (Zhang et al., 2010a). The authors build a fault detection estimator to detect when a fault occurs in the system but not where it happen. A bank of fault isolation estimators identifies then the source of the fault.

2.3.2 Wireless Sensor Network fault: outlier detection

In a MAS, communication between the agents can be subject to errors such as losses of data, delay or inability to maintain contact. The sensors of the agents can also provide some faulty measurements.

Communication faults

Communication issues among the MAS are frequently encountered in WSN. A WSN has to deal with delay and losses during the transmission of data (Song et al., 2013). A control law designed to move the MAS while taking into account the communication range of the agents is described in (Li et al., 2011). Conditions to guarantee a consensus for tracking with a MAS and delay in communication are presented in (Li and Fang, 2012). In (Liu and Liu, 2011), a MAS is subject to input and communication delays. The sufficient conditions to converge to a consensus in position are analysed with the generalized Nyquist stability criterion

and the linear fractional transformation.

The detection of a communication loss or delay may be tackled with some checking bits added to each transferred packages. (Seiler and Sengupta, 2001) study the influence of communication loss in the feedback loop of a control system. Conditions are presented to design a stable control for a given packet loss rate. To construct the residual needed for FDI, a consensus method may be used to obtain a basis for comparison. These methods are useful for communication error detection. (Ren et al., 2005) presents a survey on the consensus problems for MAS and reviews topics such as consensus convergence analysis, or systems with a changing communication topology in case of errors. The consensus is usually performed by sharing information with the close neighbours of the agent and by repeating this transmission with all the agents, until information is spread in the entire network (Schwager et al., 2008).

Sensor faults

The second issue with WSN concerns the use of the sensors. The sensors measure a characteristic value of the unknown environment. Sensors may be subject to faults and can produce faulty measurements, or outliers. An outlier is a measurement whose value cannot be explained by the sole effects of noise.

The survey on outlier detection for WSN (Zhang et al., 2010b) classifies the outlier detection methods in different categories depending on the input sensor data (abnormal value or non-correlated value), the type of outliers (local outlier or global outlier), the sources of the outliers (error or event) and the importance of the outliers (binary decision or outlier score). An exhaustive list of outlier detection techniques is presented with the pros and cons of each of them.

Neighbour comparison A common way to perform outlier detection in a WSN consists in comparing the measurements of a sensor with those obtained by its neighbours. It assumes that the measured field has some spatial or temporal correlation. This scheme is used to detect locally the state of the sensor (faulty or not) and adapt the network to deal with this information (Choi et al., 2009a). The comparison of a sensor measurement with those of its neighbours is equivalent to analyse the distance variations between measurements. Several types of distances exist to detect outliers. In (Angiulli et al., 2006), outlier distance-based detection

techniques are investigated. A method and scale analysis for the distance between measurements are proposed. Some of the common distances used to evaluate a measurement compared to a set of values are the Cook distance (Cook, 1986), or Mahalanobis distance (Nurunnabi and West, 2012).

The scattering of the data set can be evaluated to determine the presence of outliers as in (Ibacache-Pulgar et al., 2014). It uses likelihood score functions such as Cook distance or Mahalanobis distance to determined the consistency of the measurements. (Lange et al., 1989) perform a cooperative estimation of a field from the data of a WSN. They propose to weight the estimation with the probability of each sample to be an outlier.

Clustering An important outlier detection technique is built from cluster theory. From a set of data, to detect an abnormal value, it is first needed to represent the normal value distribution. Clustering methods classify the measurements into several classes. These techniques may not require prior knowledge on the data set. A learning phase identifies the normal values and creates the model. New data is added to the clustering system and it determines the membership to the normal value cluster or other clusters.

A clustering technique is proposed to detect outliers based on swarm intelligence control in (Alam et al., 2010). A set of parameters of the clusters evolve in the parameter space in the same way as a swarm by manoeuvring while staying close to each other. The outlier threshold for the data depends on the parameters of the clusters. At each time step, a data point can be included in a cluster or considered as a potential outlier. The number of outliers is closely related to the parameterisation of the outlier threshold.

The authors of (Poonam and Dutta, 2012) analyse other clustering algorithms used for outlier detection such as Clustering Large Application and Clustering Large Application based Randomized Search. They aim to perform the outlier detection at the same time as the clustering operation. The clusters formed by a small number of values are considered as outliers and removed from the database.

Some classification algorithms need a training phase to build a model of the system under normal functioning (Li and Parker, 2007). From this model, a classification cluster algorithm is applied before the mission and updated during the mission. The new data points are added to the database using the clustering algo-

rithm. The cluster outputs (aka classification result) allow the detection of faults in the system such as measurement outliers.

The outliers may also come from attacks on the sensors. In (Bishop and Savkin, 2011), the WSN considered performs an estimation of an unknown spatial field. Some of the sensors of the network can be subject to attacks that disturb the estimation. A detection scheme is employed to isolate the faulty measurements and avoid disturbance on the estimation. A trade-off is presented between the robustness of the system under outliers and the sensitivity to faulty measurements of the system for estimation.

2.4 Cooperative estimation

WSN obtain information on their environment from their sensors. The kind of mission they are used for can be the monitoring of a physical field, the estimation of an unknown value, or the search for some particular point (e. g. a maximum).

To construct the model of the unknown field, different estimation tools can be used. As stated before, the estimation has to deal with outliers, measurement errors from the sensors as well as communication errors.

Least squares are a common tool for such estimation (Panigrahi et al., 2011) as well as weighted least squares with weights spatially correlated to the position of the sensors (Cortés, 2009) or a priori knowledge to weight the measurements (Wang et al., 2009). These algorithms can be used on distributed systems as in (Delouille et al., 2006) which uses graph theory tools to decentralize the problem over local neighbourhoods or (Wang et al., 2009) which uses knowledge of the field distribution and Bayesian theory to compute a distributed estimation.

Kalman filters are also widely used to perform the estimation. A distributed version of the basic filter has been introduced in (Olfati-Saber, 2005, 2007), and modified to deal with faulty data in (Zheng et al., 2010) or analysed to guarantee the convergence of the filter under communication conditions in (Zhang and Leonard, 2010). Some works (Cortés, 2009, Le Ny and Pappas, 2009) have fused the Kalman filter algorithm with some other estimation algorithm (such as Kriging) to obtain a better estimate of characteristic value of the estimated field.

The Kriging estimator (or Gaussian process regression) is a meta-model approach which computes the best linear unbiased prediction of the intermediate

values between sampling points (Matheron, 1971, Schonlau, 1997, Sasena, 2002). The Kriging model of an unknown function is a Gaussian process, defined at any point of the space by mean and covariance functions. The Kriging estimator provides an estimation of these two functions for the unknown field based on sampling points and prior knowledge on the covariance. It will be more precisely introduced in Section 2.5.2. Kriging estimators have been used for MAS to estimate spatial unknown fields (Graham and Cortés, 2010, Choi et al., 2008, 2009b, Cortés, 2009). Some methods have been developed to distribute the Kriging estimation on the agents (Gu and Hu, 2012, Xu et al., 2011).

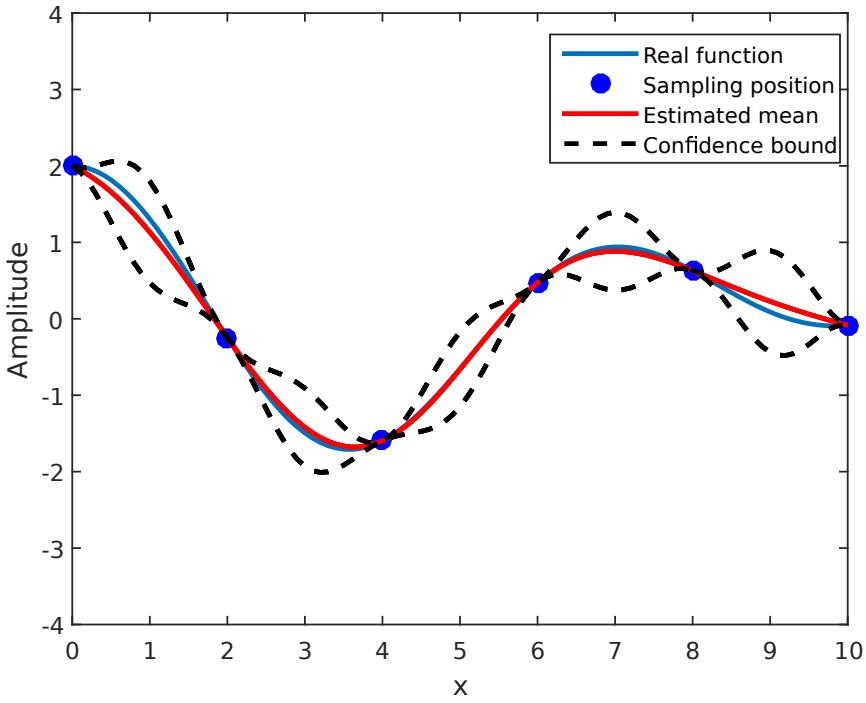

Figure 2.5: Illustration of the Kriging model

The output of a Kriging model is illustrated on Figure 2.5. The blue line represents the real function. The blue spots are the points where measurements have been taken. The red line represents the mean of the Kriged model and the black dashed line represents the confidence bounds at 68.2% computed from the covariance of the model.

In cooperative estimation of a spatial field, the positions of the agents (and sensors) can have a significant impact on the quality of the estimation. Sensor placement techniques may be used to perform such estimation.

Sensor placement

The sensor placement technique is an answer to two concerns encountered by MAS.

The first one is about the communication range of each agent to share information with the others. Depending on the environment, or communication technologies and capabilities (Akyildiz et al., 2005), the communication range adds constraints on the sensor placement.

The second one is about the location of the sensors for estimation. The optimal sensor placement can be determined using different tools to obtain the best estimation with regard to some criteria.

One of them is Experiment Design where optimal positions for the sensor are searched for using a precision criterion (Walter and Pronzato, 1990). A potential approach consists in finding the locations where measurements have to be taken to maximize a function of the Fisher information matrix derived from the model structure and measurement noise distribution (Pronzato and Walter, 1988).

Sensor placement for MAS has been proposed in (Leonard et al., 2007) to estimate the gradient of an unknown field. Unlike usual sensor placement problems, the sensors are embedded on vehicles and able to move. Thus, the sensor placement optimisation must be taken into account in the control law of the agents (Ögren et al., 2004, Lynch et al., 2008). The shape of the formation can be adjusted to minimise estimation uncertainty (Zhang and Leonard, 2010).

Another idea is to compute the trajectories of the agents in such a way that entropy of the estimation information is maximised along the displacement (Ucinski and Chen, 2005, Tricaud et al., 2008). A maximisation of the entropy means that the measurements increase the level of available information and thus result in an improved estimation.

Once an optimal sensor placement has been found, the control law should guide the agents at this position. The sensor placement optimisation can also be used to reconfigure the MAS when an error occurs on an agent.

Recover from fault: Reconfiguration

FDI schemes presented previously can be used to detect faults and identify which agent is defective. Once these steps have been performed, actions have to be taken to recover or attenuate the faults.

An actuator fault can modify the agents' dynamics. To maintain the formation, the control of the other agents has to be modified as well (Bošković and Mehra, 2002, Ren and Beard, 2002, Zhaohui and Noura, 2013) or the trajectories changed (Chamseddine et al., 2012).

For sensor faults, the outlier detection techniques aim at isolating the faulty values from the measurement set. Alternatively, robust estimators can handle these faults without degrading the results. The outlier detection technique based on learning (Alam et al., 2010, Li and Parker, 2007) also offers a reconfiguration. After the detection of a fault, the algorithm learns to adapt the classification to the outlier. The change can go from the removal of a value from the set (Bishop and Savkin, 2011), to the removal of a sensor from the network (Curiac et al., 2009).

Recent works propose to test ahead the response of the system to different control input with respect to an evaluation function (Cully et al., 2015). The evaluation is performed prior to the mission due to the huge amount of computation needed, only the result is stored in a *behaviour map* on the system during the mission that defines the possible behaviour of the system for predetermined control inputs. When an error occurs during the mission, a reconfiguration scheme is used to replace the control by a new control approach selected in the *behaviour map*. This method allows the system to recover from different kinds of errors without the need to analyse the set of all possible errors.

2.5 Extremum seeking: Local search vs. global search

The problem considered in this thesis is to find the position of the maximum of an unknown spatial field (or objective function). The search strategy can be local or global with different methods for each strategy. We focus on the search methods for MAS of vehicles. This limitation implies to consider constraints for reaching

the points where the criterion value should be computed. The criterion to optimize is the value of the spatial field obtained in our case from the measurement of the embedded sensors. From these measurements, a model of the unknown field is designed. Sampling positions for optimisation have to be selected with respect to the dynamics and positions of the agents. The position of the maximum is sought for by applying a search strategy to the model. Local search uses only local information and a local part of the model while global search uses information from the whole model.

2.5.1 Local search: Gradient climbing

The search for the maximum of the spatial field can be performed by a local estimation of the field. Then, the agents have to move along the direction of the gradient (Bıyık and Arcak, 2008). The gradient value can be derived from a polynomial model of the field. Various approaches have been used for estimating the gradient field direction either with a least-square estimator (Ögren et al., 2004), Kalman filter (Zhang and Leonard, 2010) or Kriging estimator (Choi et al., 2007). The gradient of the unknown field may be computed using any estimation technique described in Section 2.4. Other works (Dantu and Sukhatme, 2007, Zhang et al., 2007, Williams and Sukhatme, 2012) look for strategies to move the vehicles along level curves where the value of the field is constant. The problem of level curve tracking is similar to the problem of gradient climbing. Both need to estimate the gradient to move either toward its direction or perpendicularly to its direction.

Numerous methods are used to search for the maximum using the gradient value, such as Newton's or quasi-Newton method, interior point methods, conjugate gradients and subgradient methods among others (Hurtado et al., 2004).

The local search for maximum seeking has several issues. The main one is the convergence of the system to the closest local maximum encountered, which may lead to miss the global one. More efficient search strategies have to be used to ensure the convergence to the global maximum position.

2.5.2 Global search:

To overcome the limitations of local search, global optimisation methods can be applied. These global methods do not rely only on the gradient to perform the

search. A classification of the global optimisation methods has been proposed in (Torn and Zilinskas, 1989).

Direct methods

These methods only use some local information of the objective function.

Random search Three basic random search methods exist. The first one consists in performing k samplings of the objective function and selecting the optimum among them. The second one consists in randomly selecting a position and performing a local search from this point until convergence. The third one selects several random points and performs local search from all of them. The estimated global optimum is the best one among the local optimal found (Solis and Wets, 1981).

Pattern search This method evaluates the objective function on a defined pattern around an initial search point. The search point moves then toward the optimum direction evaluated by the pattern (Torczon, 1997). Basic patterns are often selected as a fixed cross, but more complex patterns may change size and orientation or number of evaluation points of the pattern.

Clustering These methods start with a random search and define a cluster around each local optimum of the objective function found. Once the cluster delimits an area, new random searches are initialised in the area without this cluster. Once the search space is explored and the optimum of each area is found, the estimated global extremum is found among them (Becker and Lago, 1970).

Generalised descent As the clustering methods, the generalised descent methods start with a random search with descent steps. These methods are introduced in (Griewank, 1981). When an optimum is found, the objective function is modified to avoid the next descent step to converge to the same optimum. To avoid this, a modification of the trajectory during the descent step can be used, as well as a penalisation of the objective function.

Evolutionary strategies and genetic algorithms These methods require a high number of evaluations of the objective function but can be applied to complex problems with large search spaces, constraints and non linearities (Golberg, 1989). They iterate the following steps:

1. Random initialisation of a population in the search space.
2. Evaluation of the objective function for the population
3. Selection of the best members of the population
4. Crossover and mutation of the population best members to generate new members
5. Go back to Step 2

In (Hansen et al., 2003) the CMAES (Complexity of the Derandomized Evolution Strategy with Covariance Matrix Adaptation) algorithm is proposed. CMAES is a highly parallel algorithm that uses an evolution strategy to adapt the covariance matrix of the members of the population to reduce the number of generations needed to converge to the maximum.

Indirect methods

These methods use sets of sampling points to design a model of the objective function and select iteratively new sampling points to refine the optimum estimate.

Covering methods These methods are based on subdivision of the search space and exclusion of sub-areas that do not contain the optimum. These methods contain the interval-based methods (Hansen and Walster, 2003) that offer guarantees on the convergence. In the same idea, the DIRECT algorithm (Jones et al., 1993) divides the search space in rectangles to optimise the cost function by local and global search at the same time.

Methods approximating the objective function The objective function may be expensive to evaluate. To avoid repetitive call to the objective function, a model of the objective function less expensive to evaluate is designed. The

optimisation is done on the model by selecting sampling position for the objective function.

To acquire knowledge on the objective function for finding the extremum, an accurate model should be designed. Interpolation methods construct an estimation of the unknown field from a set of measurements at spatial sampling positions. Different methods exist using linear, polynomial, or spline representations. Linear interpolation is the simplest to evaluate but may result in large errors in the evaluation of the real objective function. Polynomial interpolation is more flexible and thus can adapt to a wider range of functions. Its drawbacks are the cost of evaluation for high degree polynomials and the potential occurrence of oscillations. Spline descriptions present the same advantage as polynomial but are easier to evaluate. The last interpolation method that we describe is Gaussian process regression (or Kriging) (Sasena, 2002, Schonlau, 1997). Compared to the other interpolation methods, Kriging provides the best linear unbiased prediction of the field between the sampling points.

Using the interpolated model, the extremum search is performed by selecting new measurements to be collected with a sampling criterion. Criteria developed for optimisation with Kriging are presented in Section 6.3 of this thesis. In the case of MAS, the sampling criterion cannot be separated from the control law of the agents.

2.6 Conclusions

MAS are a solution to the issues raised by the use of single agent systems with potential faults. The task division of the initial mission is a difficulty which is compensated by the cooperation among the agents. Behavioural-rule control depends too much on the environment and the mission to be adapted on several problems. On the other hand, leader-follower techniques are more sensitive to deal with a fault in the leader. Moreover, leader-follower offers less possibility to the formation for sensor placement than virtual structures. The control law scheme used in this thesis will be based on virtual structure because of its adaptability and its redesign capabilities.

Maximum seeking of an unknown field has been treated by several methods.

Local search is the first and most straightforward way to find the position of a maximum. Yet, its main limitation is that it may lead to a MAS being stuck at the first maximum encountered. Global search with Kriging deals well with the constraint of our problem (sensors embedded on vehicles so constrained dynamically and characteristics of Gaussian process for optimisation). Several criteria exist for optimisation with Kriging. Some recent ones have been developed for MAS with dynamics of the agents and control law taken into account. We have developed a new criterion for maximisation of a unknown field by a MAS and compared its efficiency with existing ones.

As the mission implies measurements to perform an estimation, sensor faults are considered and FDI schemes applied to detect and treat the faults by appropriate solutions. Many outliers detection techniques exist for WSN but most assume that the sensors are fixed. We propose a reconfiguration of the sensors after detection of a fault by modifying the spatial repartition of the agents.

Summary

In this chapter, the state-of-the-art has been presented with the existing methods for our problems. We have highlighted MAS with their advantages and issues. The different control laws for formation control have been shown. The estimation tools and models design have been introduced, as well as optimisation methods.
The next chapters will present our contributions to the following topics:

- Optimal sensor placement for cooperative estimation
- FDI scheme with adaptive threshold for outliers detection
- Formation control law with guaranteed stability
- Reconfiguration of the formation in case of fault
- Sampling criterion for global search via Kriging model

Chapter 3

Maximum seeking: a mission for a multi-agent system

Chapter goals

In this chapter, the spatial field maximisation problem using a MAS is stated. The characteristics of the agents are also detailed.
For this purpose, the following subjects are treated:

- Type of mission for the agents: Control laws are problem dependent, focus is put on maximum seeking.
- Characteristics of an agent: Dynamics and measurement model.
- Characteristics of the system: Relation between the agents among the fleet.

In the literature, MAS are employed in tasks such as surveillance, monitoring, search or exploration (Sirigineedi et al., 2010, Merino et al., 2005). This thesis considers problems where MAS are used to find the global maximum of some unknown spatial field.

Consider some unknown and time-invariant scalar field ϕ defined over a compact space $D \subset \mathbb{R}^n$, $n = 2, 3$ which has to be maximized. The field ϕ may present several local extrema but is assumed to have a unique argument of its global max-

imum $\mathbf{x}_M \in D$ define as $\mathbf{x}_M = \arg\max_{\mathbf{x}\in D} (\phi(\mathbf{x}))$ The field ϕ is assumed to be twice-continuously differentiable over D.

Different strategies are used to determine the localisation of the maximum in Parts II and III. The next section describes a model of the agents considered in this thesis.

3.1 Characteristics of agents

A group of N identical agents is considered. The position of agent i in D at time t is denoted by $\mathbf{x}_i(t)$. The position of each agent evolves according to the following model introduced in (Wang, 1991):

$$M\ddot{\mathbf{x}}_i(t) + C\left(\mathbf{x}_i(t), \dot{\mathbf{x}}_i(t)\right)\dot{\mathbf{x}}_i(t) = \mathbf{u}_i(t) \tag{3.1}$$

where $\mathbf{u}_i(t)$ is the control input applied to agent i at time t, M is the mass of the agent, and $C\left(\mathbf{x}_i(t), \dot{\mathbf{x}}_i(t)\right)$ is a non-negative friction coefficient.

The position and the velocity compose the state vector of an agent. At each time step, we assume that each agent has a perfect knowledge of its own state vector. State estimation is not considered in this thesis.

The continuous time t is sampled with a period T to get discrete time instants t_k. All the agents are synchronized on the same discrete time. The computations such as the model construction or evaluation of the control input are performed at discrete time instants.

Each agent i is equipped with a sensor able to perform a pointwise measurement $y_i(t_k)$ of the field ϕ at the position $\mathbf{x}_i(t_k)$ at time t_k. The sensor may be in two states (or conditions), normal ($\eta = 0$) or faulty ($\eta = 1$). This state $\eta_i(t_k)$ is time varying. A Markov chain with transition probabilities between two subsequent instants t_k and t_{k+1} ($t_k < t_{k+1}$) can model the evolution of the state of each sensor:

$$p_{01} = \Pr\left(\eta_i\left(t_{k+1}\right) = 1 | \eta_i\left(t_k\right) = 0\right) \tag{3.2}$$

$$p_{10} = \Pr\left(\eta_i\left(t_{k+1}\right) = 0 | \eta_i\left(t_k\right) = 1\right) \tag{3.3}$$

and $p_{00} = 1 - p_{01}$ and $p_{11} = 1 - p_{10}$.

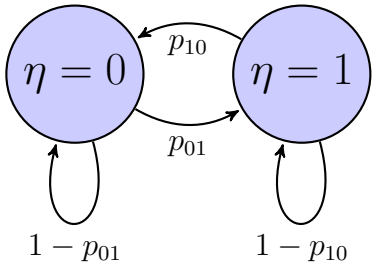

Figure 3.1: Modelling of the state transition of a sensor

The measurement equation is assumed to be

$$y_i(t_k) = \phi(\mathbf{x}_i(t_k)) + n_i(\eta_i(t_k), t_k) \tag{3.4}$$

where $n_i(\eta_i(t_k), t_k)$ models the measurement noise of the sensor of agent i. The $n_i(\eta_i(t_k), t_k)$s are realisations of independently distributed zero-mean Gaussian variables with state-dependent variance $\sigma^2_{\eta_i(t_k)}$, where $\sigma^2_{\eta_i(t_k)=0} \ll \sigma^2_{\eta_i(t_k)=1}$.

The hypothesis on the measurement noise for healthy sensor is $n_i(0, t_k) \sim \mathcal{N}(0, \sigma_0^2)$. When $\eta_i = 1$, the sensor of agent i is considered as faulty; the measurement noise does not follow the same normal distribution $n_i(1, t_k) \sim \mathcal{N}(\nu, \sigma_1^2)$. The measurement error of the faulty sensor has a Gaussian distribution with a bias and a higher variance, resulting in a higher additional disturbance on the measurement $y_i(t_k)$. The measurement of the faulty sensor may be unusable for the mission. Other assumptions could be considered on the measurement noise such as coloured noise.

3.2 Communications between agents of the MAS

A time-varying communication graph $\mathcal{G}(t_k)$ is defined to represent the communication between the agents. The communications are assumed to be lossless and without delay. Two agents are assumed to be able to communicate when their distance is smaller than R. $\mathcal{G}$ is undirected and time-varying. The set of neighbours of agent i at time t is denoted by

$$\mathcal{N}_i(t) = \{j \mid \|\mathbf{x}_i(t) - \mathbf{x}_j(t)\| \leqslant R\}. \tag{3.5}$$

When two agents are neighbours, they can share information such as position or measurements. The set of all information available at agent i at time t_k is denoted $S_i(t_k)$.

Let $\mathcal{M}(t_k)$ be the set of agents that collect a measurement at time t_k. The set $S_i(t_k)$ is then defined as

$$S_i(t_k) = \bigcup_{\ell=0}^{k} \{[y_j(t_\ell), \mathbf{x}_j(t_\ell)] \mid j \in \mathcal{N}_i(t_\ell) \cap \mathcal{M}(t_\ell)\} . \tag{3.6}$$

Each agent then computes its own model of the unknown field and its control input using $S_i(t_k)$.

3.3 Model of the unknown field

The field ϕ to model can be uni-modal or multi-modal. The estimation of ϕ is performed from the measurements of the agents.

The proposed local approach models the field at each point $\mathbf{x}$ using a second-order Taylor expansion of ϕ. The parameters of this expansion may be obtained by each agent using least-square estimation with $S_i(t_k)$ as input of the estimator.

The global approach builds a more elaborate meta-model of the unknown field and an estimation at each $\mathbf{x} \in D$ of the mean and the variance of this metamodel is performed to find the maximum. The meta-model method used is Kriging (or Gaussian process regression) as it presents interesting characteristics for global search (See Chapter 6).

3.4 Estimation and control law for an extremum search mission

The initial problem is to find the position of the maximum of an unknown spatial field. To reach this goal, two search strategies are presented. In both cases, the model is built by estimating the characteristics of the real field. To perform this estimation, desired sampling positions are defined. The control law should be designed to move the agents to desired sampling positions and avoid collision.

The goal of the search strategies is to:

- Define iteratively desired sampling positions to locate the maximum of the field.

The goal of the modelling methods is to:

- Compute an accurate approximation of the unknown field from desired sampling points.

The objectives of the control law are double:

- Move the agents to the desired sampling positions.
- Avoid collision between the agents.

All these steps can be performed in a centralised or distributed way. To avoid collisions between agents, a safety radius R_{safety} is defined as the minimum admissible space between two agents. In this thesis, the control law computation and the model estimation are distributed on each agent but with information on their neighbourhood (positions of the agents in $\mathcal{N}_i(t_k)$ and $S_i(t_k)$).

To perform the most accurate estimation of the model, different strategies are used to define the sampling positions. For the local search, optimal sensor positions are analysed to move the agents in the best formation shape to perform measurements. For the global search, a sampling criterion is designed to optimise the search and use global information from the model. The measurements available for the estimation are noisy and can be subject to outliers as defined in Section 3.1. To deal with potential outliers, FDI schemes are proposed for the local approach. The redundancy provided by the MAS compared to the use of a single agent system is used to perform a reconfiguration of the MAS in case of a faulty agent.

Summary

In this chapter, the maximum seeking mission has been introduced and assumptions on the agents have been established:

- Dynamics of the agents
- Sensor model of the agents
- Communication among the MAS

The next Part will present a local approach to fulfil the mission based on a gradient climbing. A cooperative estimation scheme will be presented, optimal sensor placement will be considered and a control law will be proposed.

A third Part will present a global search method based on Kriging. A new sampling criterion is developped to improve exploration capabilities.

Part II

Local approach

Chapter 4

Cooperative estimation by a MAS for maximum seeking

Chapter goals

In this chapter, a local approach is proposed to localize the maximum of a field. For that purpose, the following topics are considered:

- Cooperative estimation: Unknown field value and its spatial gradient are estimated from the measurements of the agents.
- Fault detection and identification: Collected measurements are analysed to detect whether one or several sensors are faulty.
- Agent placement: At each step, an optimal location of the agents is evaluated to obtain the best estimation.

The local search approach for finding the location of the maximum of a field is performed using gradient climbing method. The field and its variations are described using a local second-order Taylor expansion model. Weighted least-square estimation of the parameters of this model is carried out to reconstruct the gradient of the field from the measurements of the agents. The agents move along the gradient direction to reach the maximum. During these steps, the consistency of the available measurements is checked to detect the presence of outliers.

4.1 Proposed solution

The proposed local approach consists in:

- Gathering the agents together in a formation that maximizes the estimation accuracy,
- Moving the agents toward the field local maximum.

The displacement toward the maximum is operated using a gradient climbing method as in (Bıyık and Arcak, 2008, Cortés, 2009). Cooperative estimates of the field and its gradient have to be obtained from the collected measurements of the agents at time t_k. As the precision of the resulting estimates varies with the locations of the collected measurements, the best agent locations regarding to the estimation precision have been evaluated. Optimal sensor placement schemes for parameter estimation of unknown field have been presented by several authors. (Ögren et al., 2004) presents an optimal formation shape to minimise a least-square estimation error of the field on one time step. (Ucinski and Chen, 2005) finds the optimal trajectory for its agents that maximises the determinant of the Fisher Information Matrix on an horizon of several time steps.

The method developed in this thesis aims to find the optimal sensor locations while taking into account the state of the sensor of each agent. When an agent sensor turns out to be faulty, an analysis performed earlier provides a new location for the faulty agent to lower the discrepancy on the results induced by the fault. Once the faulty agent is isolated, a tuning parameter can be modified to lead the agents to their new desired positions using a distributed control law (see 5).

As the scheme requires to detect the occurrence of a fault on one of the sensors, a fault detection and identification scheme is proposed to estimate the state of each sensor.

Each agent i has it own position of estimation $\widehat{\mathbf{x}}_i^k$ where it computes the estimate of the unknown field. This position of estimation is updated to move along the gradient direction to reach the real position of the maximum.

A six-step approach is considered in each time interval of the form $[t_k, t_{k+1}]$:

1. Each agent collects a measurement $y_i(t_k)$ of the field at its current location $\mathbf{x}_i(t_k)$.

2. The measurement and the current agent location are broadcast to the other agents located within its neighbourhood.

3. Each agent i computes an estimate of the field and of its gradient at its current position of estimation $\widehat{\mathbf{x}}_i^k$.

4. Each agent estimates the state of its embedded sensor and of the sensors of its neighbours using the shared measurements.

5. All agents move towards the optimal localisation defined in the control law depending on the state of their sensor.

6. The position $\widehat{\mathbf{x}}_i^k$ is then updated to get $\widehat{\mathbf{x}}_i^{k+1}$, and each agent determines its control inputs from its available information to move towards $\widehat{\mathbf{x}}_i^{k+1}$ while avoiding collisions.

4.2 Field estimation

A local model ϕ_i is derived from a second-order Taylor expansion of ϕ centered at $\widehat{\mathbf{x}}_i^k$

$$\phi_i(\mathbf{x}) = \phi\left(\widehat{\mathbf{x}}_i^k\right) + \left(\mathbf{x} - \widehat{\mathbf{x}}_i^k\right)^{\mathrm{T}} \nabla\phi\left(\widehat{\mathbf{x}}_i^k\right) + \frac{1}{2}\left(\mathbf{x} - \widehat{\mathbf{x}}_i^k\right)^{\mathrm{T}} \nabla^2\phi(\boldsymbol{\chi}_i)\left(\mathbf{x} - \widehat{\mathbf{x}}_i^k\right). \tag{4.1}$$

where $\boldsymbol{\chi}_i$ belongs to the segment joining $\mathbf{x}$ and $\widehat{\mathbf{x}}_i^k$. The vector of parameters to be estimated is

$$\boldsymbol{\alpha}_i^k = \begin{pmatrix} \phi\left(\widehat{\mathbf{x}}_i^k\right) \\ \nabla\phi\left(\widehat{\mathbf{x}}_i^k\right) \end{pmatrix} \tag{4.2}$$

using the measured field values $y_j(t_k)$, $j \in \mathcal{N}_i(t_k)$ provided by the agents in the neighbourhood of i. One may approximate ϕ_i in (4.1) as follows

$$\bar{\phi}_i(\mathbf{x}) = \phi\left(\widehat{\mathbf{x}}_i^k\right) + \left(\mathbf{x} - \widehat{\mathbf{x}}_i^k\right)^{\mathrm{T}} \nabla\phi\left(\widehat{\mathbf{x}}_i^k\right), \tag{4.3}$$

introducing the approximation error

$$\begin{aligned} e_i(\mathbf{x}) &= \phi_i(\mathbf{x}) - \bar{\phi}_i(\mathbf{x}) \\ &= \frac{1}{2}\left(\mathbf{x} - \widehat{\mathbf{x}}_i^k\right)^{\mathrm{T}} \nabla^2\phi(\boldsymbol{\chi}_i)\left(\mathbf{x} - \widehat{\mathbf{x}}_i^k\right), \end{aligned} \tag{4.4}$$

which corresponds to the neglected second-order term of (4.1).

The model (4.3) could be extended to take into account the second-order term using a third-order Taylor expansion. However, various examples provided by (Zhang and Leonard, 2010) illustrate the fact that the estimation of the Hessian matrix $\nabla\phi\left(\widehat{\mathbf{x}}_i^k\right)$ from noisy field measurements is difficult and results in poor-quality estimates.

The measurement noise $n_j(\eta_j, t_k)$ will be denoted $n_j(t_k)$ for the sake of simplicity as the impact of the sensor state η_j is not considered in a first time. Using (4.1), agent i models the measurement $y_j(t_k)$ provided by agent j as follows

$$\begin{aligned} y_j(t_k) &= \phi(\mathbf{x}_j(t_k)) + n_j(t_k) \\ &= \phi\left(\widehat{\mathbf{x}}_i^k\right) + \left(\mathbf{x}_j(t_k) - \widehat{\mathbf{x}}_i^k\right)^{\mathrm{T}} \nabla\phi\left(\widehat{\mathbf{x}}_i^k\right) \\ &+ \frac{1}{2}\left(\mathbf{x}_j(t_k) - \widehat{\mathbf{x}}_i^k\right)^{\mathrm{T}} \nabla^2\phi(\boldsymbol{\chi}_{ij})\left(\mathbf{x}_j(t_k) - \widehat{\mathbf{x}}_i^k\right) + n_j(t_k), \end{aligned} \tag{4.5}$$

where $\boldsymbol{\chi}_{ij}$ belongs to the segment joining $\widehat{\mathbf{x}}_i^k$ and $\mathbf{x}_j(t_k)$. Then, using (4.2) and (4.5),

$$y_j(t_k) = \begin{pmatrix} 1 & \left(\mathbf{x}_j(t_k) - \widehat{\mathbf{x}}_i^k\right)^{\mathrm{T}} \end{pmatrix} \boldsymbol{\alpha}_i^k + e_i(\mathbf{x}_j(t_k)) + n_j(t_k). \tag{4.6}$$

Agent i collects all the measurements from the agents located within its neighbourhood $\mathcal{N}_i(t_k)$ at t_k with $\mathcal{N}_i(t_k) = \{i_1, \ldots, i_{N_i}\}$,to obtain

$$\mathbf{y}_{i,k} = \bar{\mathbf{R}}_{i,k}\boldsymbol{\alpha}_i^k + \mathbf{n}_{i,k} + \mathbf{e}_{i,k} \tag{4.7}$$

where

$$\begin{aligned} \mathbf{y}_{i,k} &= \left(y_{i_1}(t_k), \ldots, y_{i_{N_i}}(t_k)\right)^{\mathrm{T}}, \\ \bar{\mathbf{R}}_{i,k} &= \begin{pmatrix} 1 & \left(\mathbf{x}_{i_1}(t_k) - \widehat{\mathbf{x}}_i^k\right)^{\mathrm{T}} \\ \vdots & \vdots \\ 1 & \left(\mathbf{x}_{i_{N_i}}(t_k) - \widehat{\mathbf{x}}_i^k\right)^{\mathrm{T}} \end{pmatrix}, \end{aligned} \tag{4.8}$$

$$\mathbf{n}_{i,k} = \left(n_{i_1}\left(t_k\right), \ldots, n_{i_{N_i}}\left(t_k\right)\right)^{\mathrm{T}},$$

and

$$\mathbf{e}_{i,k} = \begin{pmatrix} \frac{1}{2}\left(\mathbf{x}_{i_1}\left(t_k\right) - \widehat{\mathbf{x}}_i^k\right)^{\mathrm{T}} \nabla^2\phi(\boldsymbol{\chi}_{i1})\left(\mathbf{x}_{i_1}\left(t_k\right) - \widehat{\mathbf{x}}_i^k\right) \\ \vdots \\ \frac{1}{2}\left(\mathbf{x}_{i_{N_i}}\left(t_k\right) - \widehat{\mathbf{x}}_i^k\right)^{\mathrm{T}} \nabla^2\phi(\boldsymbol{\chi}_{iN})\left(\mathbf{x}_{i_{N_i}}\left(t_k\right) - \widehat{\mathbf{x}}_i^k\right) \end{pmatrix}. \tag{4.9}$$

The measurement noise vector $\mathbf{n}_{i,k}$ is assumed to be a realisation of a zero-mean Gaussian vector with diagonal covariance matrix

$$\boldsymbol{\Sigma}_{i,t_k} = \operatorname{diag}\left(\sigma^2_{\eta_{i_1}(t_k)}, \ldots, \sigma^2_{\eta_{i_{N_i}}(t_k)}\right). \tag{4.10}$$

If one neglects $\mathbf{e}_{i,k}$, the maximum likelihood estimate of $\boldsymbol{\alpha}_i^k$ would correspond to the argument of the minimum of

$$J_0\left(\boldsymbol{\alpha}\right) = \left(\mathbf{y}_{i,k} - \bar{\mathbf{R}}_{i,k}\boldsymbol{\alpha}\right)^{\mathrm{T}} \boldsymbol{\Sigma}_{i,t_k}^{-1}\left(\mathbf{y}_{i,k} - \bar{\mathbf{R}}_{i,k}\boldsymbol{\alpha}\right). \tag{4.11}$$

Accounting for the impact of $\mathbf{e}_{i,k}$ is more complicated. The jth component of $\mathbf{e}_{i,k}$ is a function of $\left\|\mathbf{x}_j\left(t_k\right) - \widehat{\mathbf{x}}_i^k\right\|_2^2$, where $\|\cdot\|_2$ is the Euclidian norm. The model error grows thus quadratically with the distance between $\mathbf{x}_j\left(t_k\right)$ and $\widehat{\mathbf{x}}_i^k$. Measurements provided by agents far from $\widehat{\mathbf{x}}_i^k$ should play a less important role in the estimation of $\boldsymbol{\alpha}$ than measurements collected close to this position as the modelling error increases with the distance. The following weighting matrix is thus chosen to account for both the measurement noise and the modelling error,

$$\begin{aligned} \mathbf{W}_{i,k} = \operatorname{diag}\Bigg(&\sigma^{-2}_{\eta_1(t_k)} \exp\left(\frac{-||\mathbf{x}_1\left(t_k\right) - \widehat{\mathbf{x}}_i^k||_2^2}{k_{\mathrm{w}}}\right), \ldots, \\ &\sigma^{-2}_{\eta_{N_i}(t_k)} \exp\left(\frac{-||\mathbf{x}_{N_i}\left(t_k\right) - \widehat{\mathbf{x}}_i^k||_2^2}{k_{\mathrm{w}}}\right)\Bigg), \end{aligned} \tag{4.12}$$

where k_{w} is some tuning parameter to be adjusted depending on the assumed spatial correlation of ϕ. This value should be small if the spatial variations of the field are assumed to be large around the current estimated location. On the contrary, if the spatial variations are assumed to be small, larger values of k_{w} could be chosen. The weighted least-square estimate of $\boldsymbol{\alpha}_i^k$ with weighting matrix $\mathbf{W}_{i,k}$

is obtained as

$$\widehat{\boldsymbol{\alpha}}_i^k = \left(\bar{\mathbf{R}}_{i,k}^{\mathrm{T}} \mathbf{W}_{i,k} \bar{\mathbf{R}}_{i,k}\right)^{-1} \bar{\mathbf{R}}_{i,k}^{\mathrm{T}} \mathbf{W}_{i,k} \mathbf{y}_{i,k}. \tag{4.13}$$

4.3 Optimal agent placement

In this section, two criteria are considered to quantify the quality of the estimates obtained for a given repartition of the agents. The first one is the variance of the resulting estimation error presented in Section 4.2. The second one is the amplitude of the modelling error of the unknown field. The two optimisations are performed in a centralised way by minimizing these criteria. The resulting locations should be reached by the formation using an appropriate control law.

4.3.1 Minimisation of the variance of estimation error

In this section, one determines at each time step the agent locations that minimise the variance of the estimation error of $\widehat{\boldsymbol{\alpha}}_i^{k+1}$ at $\widehat{\mathbf{x}}_i^{k+1}$. As the sensors are embedded on vehicles, safety requirements have to be fulfilled. They can be translated as a lower bound on the relative distance between two sensors. From (4.13), an approximation[1] of the covariance of $\widehat{\boldsymbol{\alpha}}_i^{k+1}$ at $\widehat{\mathbf{x}}_i^{k+1}$ is given by

$$\widehat{\boldsymbol{\Sigma}}_{\alpha_i^{k+1}} = \left(\bar{\mathbf{R}}_{i,k+1}^{\mathrm{T}} \mathbf{W}_{i,k+1} \bar{\mathbf{R}}_{i,k+1}\right)^{-1}. \tag{4.14}$$

Different scalar measures, such as the trace, the determinant or the maximum of the eigenvalues, can be used for the covariance matrix, which lead to different expressions of the criterion to be maximised. The T-optimal placement consists in maximising the trace of $\bar{\mathbf{R}}_{i,k+1}^{\mathrm{T}} \mathbf{W}_{i,k+1} \bar{\mathbf{R}}_{i,k+1}$. The positions of the agents corresponding to this maximum must also fulfil an additional constraint representing the limited tolerance on their relative distances for collision avoidance.

The D-optimal placement consists in maximising the determinant of $\bar{\mathbf{R}}_{i,k+1}^{\mathrm{T}} \mathbf{W}_{i,k+1} \bar{\mathbf{R}}_{i,k+1}$ under the same additional constraint on the relative distances. In the following, every agent has the same position of estimation $\widehat{\mathbf{x}}_i^{k+1}$.

[1] $\widehat{\boldsymbol{\alpha}}_i^{k+1}$ is assumed unbiased, even if it not the case in general, due to the presence of $\mathbf{e}_{i,k}$. Close to $\mathbf{x}_M$, more specifically, the components of $\mathbf{e}_{i,k}$ are likely to be negative.

Analytical T-optimal solution

Minimization of the trace of $\widehat{\mathbf{\Sigma}}_{\alpha_i^{k+1}}$ translates into the following constrained optimization problem

$$\left(\mathbf{x}_1\left(t_{k+1}\right)\ldots\mathbf{x}_N\left(t_{k+1}\right)\right) = \arg\max_{(\mathbf{x}_1,\ldots,\mathbf{x}_N)} \operatorname{tr}\left(\bar{\mathbf{R}}_{i,k+1}^{\mathrm{T}}\mathbf{W}_{i,k+1}\bar{\mathbf{R}}_{i,k+1}\right) \tag{4.15}$$

$$\text{with the constraint } \|\mathbf{x}_i-\mathbf{x}_j\|_2^2 \geqslant R_{\text{safety}}^2,\ \forall\{i,j\}, j>i. \tag{4.16}$$

To solve this problem, one introduces the Lagrangian associated to (4.15) and uses (4.8) and (4.12)

$$\begin{aligned}\mathcal{L}\left(\mathbf{x}_1,\ldots,\mathbf{x}_N,\boldsymbol{\mu}\right) = &\sum_{i=1}^{N}\sigma_{\theta_i(t_{k+1})}^{-2}\exp\left(\frac{-||\mathbf{x}_i-\widehat{\mathbf{x}}_i^{k+1}||_2^2}{k_{\mathrm{w}}}\right)\\ &\cdot\left(1+\left\|\mathbf{x}_i-\widehat{\mathbf{x}}_i^{k+1}\right\|_2^2\right)+\sum_{j>i}\mu_{ij}(\|\mathbf{x}_i-\mathbf{x}_j\|_2^2-R_{\text{safety}}^2).\end{aligned} \tag{4.17}$$

where the $\mu_{i,j}$s are Lagrange multipliers. Taking the partial derivatives of (4.17) with respect to $\mathbf{x}_i$, one gets

$$\begin{aligned}\frac{\partial\mathcal{L}}{\partial\mathbf{x}_i} = &-\frac{2\sigma_{\theta_i(t_{k+1})}^{-2}}{k_{\mathrm{w}}}\left(\mathbf{x}_i-\widehat{\mathbf{x}}_i^{k+1}\right)\exp\left(\frac{-||\mathbf{x}_i-\widehat{\mathbf{x}}_i^{k+1}||_2^2}{k_{\mathrm{w}}}\right)\left(1+\left\|\mathbf{x}_i-\widehat{\mathbf{x}}_i^{k+1}\right\|_2^2\right)\\ &+2\sigma_{\theta_i(t_{k+1})}^{-2}\left(\mathbf{x}_i-\widehat{\mathbf{x}}_i^{k+1}\right)\exp\left(\frac{-||\mathbf{x}_i-\widehat{\mathbf{x}}_i^{k+1}||_2^2}{k_{\mathrm{w}}}\right)\\ &+2\sum_{j\neq i}\mu_{ij}\left(\mathbf{x}_i-\mathbf{x}_j\right).\end{aligned} \tag{4.18}$$

$$\begin{aligned}\frac{\partial\mathcal{L}}{\partial\mathbf{x}_i} = &\ 2\sigma_{\theta_i(t_{k+1})}^{-2}\left(\mathbf{x}_i-\widehat{\mathbf{x}}_i^{k+1}\right)\exp\left(\frac{-||\mathbf{x}_i-\widehat{\mathbf{x}}_i^{k+1}||_2^2}{k_{\mathrm{w}}}\right)\\ &\left(1-\frac{1}{k_{\mathrm{w}}}\left(1+\left\|\mathbf{x}_i-\widehat{\mathbf{x}}_i^{k+1}\right\|_2^2\right)\right)+2\sum_{j\neq i}\mu_{ij}\left(\mathbf{x}_i-\mathbf{x}_j\right).\end{aligned} \tag{4.19}$$

Assuming first that $\mu_{ij}=0$ for all $i\neq j$, meaning that the safety distance constraint is satisfied, one may easily show that one should have either

$$\mathbf{x}_i(t_{k+1}) = \widehat{\mathbf{x}}_i^{k+1} \tag{4.20}$$

or

$$\left\|\mathbf{x}_i\left(t_{k+1}\right)-\widehat{\mathbf{x}}_i^{k+1}\right\|_2^2=k_{\mathrm{w}}-1 \tag{4.21}$$

which is possible only provided that $k_{\mathrm{w}}>1$. In this case, $\mathbf{x}_i\left(t_{k+1}\right)$ has to be located on a circle of radius $\sqrt{k_{\mathrm{w}}-1}$ centred in $\widehat{\mathbf{x}}_i^{k+1}$. The condition $k_{\mathrm{w}}>1$ corresponds to a modelling error increasing slowly with the distance to the point where the Taylor expansion has been performed, which is satisfied when ϕ varies slowly.

Influence of the parameters The parameters k_{w} and R_{safety} are along with the number of agents N, the three parameters that carry an influence on the circle where the agents should be located.

R_{safety} is a physical constraint that ensures the safety of the agents by defining a safety area around them to avoid collision. This parameter depends on the agent characteristics.

k_{w} depends on the unknown field model and is a term of the weighting matrix $\mathbf{W}_{i,k}$. A small value of k_{w} results in a fast decrease of the weight when the distance $||\mathbf{x}_i-\widehat{\mathbf{x}}_i^{k+1}||_2^2$ increases. Only the agents close to $\widehat{\mathbf{x}}_i^k$ should have an influence on the estimation. On the other side, for large values of k_{w}, the agents far from the position of estimation still have an influence on the estimation.

Figure 4.1 illustrates the evolution of the weight composing the matrix $\mathbf{W}_{i,k}$ in (4.12) for parameter $\sigma_{\eta_0}^2=0.01$ and several values of k_{w}.

For the estimation of the unknown field without previous knowledge, the worst case must be considered which corresponds to a field with fast spatial variations. In this case, the parameter k_{w} should be chosen small to minimise the influence of the measurements collected from remotely located sensors.

The distance between two agents located on the circle is $2r\sin(\alpha/2)$ where r is the radius of the circle and α is the center angle between two agents and the center of the circle. As $r=\sqrt{k_{\mathrm{w}}-1}$ and $\alpha=\frac{2\pi}{N}$, the smallest relative distance between two agents is $2\sqrt{k_{\mathrm{w}}-1}\sin(\frac{\pi}{N})$. A necessary condition for all agents to coexist on this circle while complying with the constraint of distance (4.16) is thus

$$2\sqrt{k_{\mathrm{w}}-1}\sin(\frac{\pi}{N})>\ R_{\mathrm{safety}}. \tag{4.22}$$

The condition (4.22) may not be fulfilled for some values of the N, k_{w} and R_{safety} parameters. When N becomes large, the condition can be approximated by

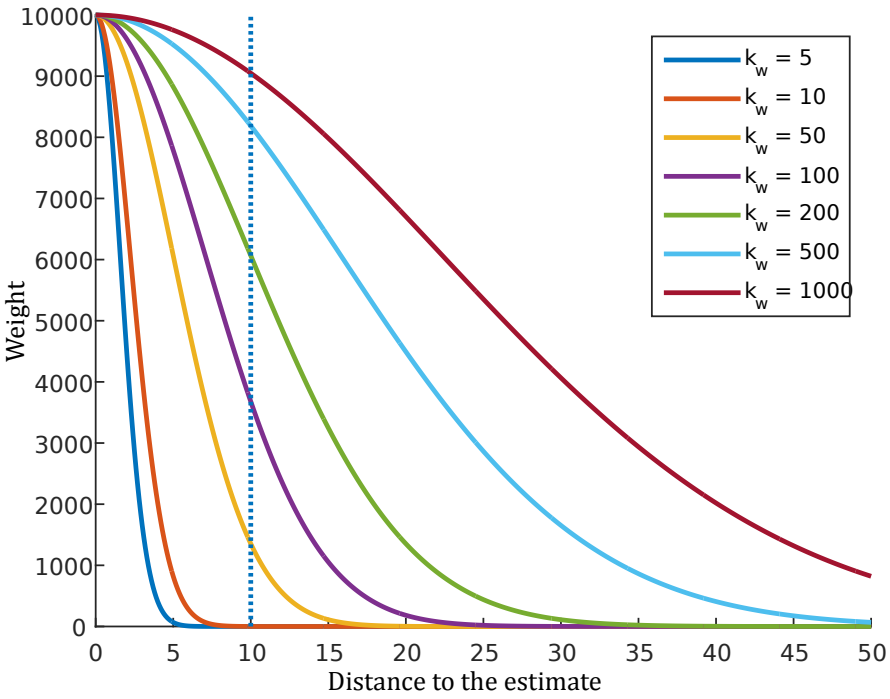

Figure 4.1: Influence of k_{w} on the weight

$\sqrt{k_{\mathrm{w}}-1} > \frac{N\,R_{\mathrm{safety}}}{4\pi}$. Thus k_{w} should increased quadratically with the number of agents and the relative safety distance. As stated previously, parameter k_{w} reflects the hypotheses on the field variations, it cannot be chosen to allow all agents to remain on a given circle. Its enlargement depends on the available knowledge on the field.

The cooperative estimation is computed with measurements collected from several sensors. A compromise must thus be found between the selection of the weights and the safety distance to ensure that several agents will participate efficiently to the estimation. The dashed line in Figure 4.1 represents a safety distance of 10m. Sensors located at least at the safety distance from $\widehat{\mathbf{x}}_i^k$ should be taken into account for the estimation. A value of $k_{\mathrm{w}} = 100$ ensures that the agents located at R_{safety} from another one located at the estimation position have a weight of about 40% of the other weights. Agents farther than $2R_{\mathrm{safety}}$ have a weight close to 0 and do not influence the estimation.

From this analysis of the parameters, one can notice that the agents are re-

quired to fit on a circle depending on N, R_{safety} and k_{w} while respecting the constraint (4.16). Therefore, the parameters cannot be changed if the constraints are not feasible. In the case where the agents cannot fit on a circle, no analytical solution has been found. Some numerical solutions are proposed for the optimal placement problem.

For the T-optimal solution, $k_{\text{w}} = 100$ corresponds to a circle of radius 9.95. Using a safety distance $R_{\text{safety}} = 10$, up to 5 agents can be located on the same circle without violating the constraint. When the fleet is composed of 6 agents or more, the agents cannot be located on the circle of radius $\sqrt{k_{\text{w}} - 1}$ while satisfying condition (4.22).

Analytical D-optimal solution

The D-optimal placement is obtained by maximizing the determinant of $\widehat{\boldsymbol{\Sigma}}_{\alpha_i^{k+1}}$. This is translated in the following constrained optimization problem

$$(\mathbf{x}_i\,(t_{k+1}) \dots \mathbf{x}_N\,(t_{k+1})) = \arg \max_{(\mathbf{x}_1,\dots,\mathbf{x}_N)} \det\left(\bar{\mathbf{R}}_{i,k+1}^{\mathrm{T}} \mathbf{W}_{i,k+1} \bar{\mathbf{R}}_{i,k+1}\right) \tag{4.23}$$

$$\text{with the constraint } \|\mathbf{x}_i - \mathbf{x}_j\|_2^2 \geqslant R_{\text{safety}}^2,\ \forall\{i,j\}, j > i. \tag{4.24}$$

The optimisation procedure is identical to the one used for T-optimal placement. The Lagrangian is defined as

$$\mathcal{L}\,(\mathbf{x}_1, \dots, \mathbf{x}_N, \boldsymbol{\mu}) = \det(\bar{\mathbf{R}}_{i,k+1}^{\mathrm{T}} \mathbf{W}_{i,k+1} \bar{\mathbf{R}}_{i,k+1}) + \sum_{j>i} \mu_{ij} (\|\mathbf{x}_i - \mathbf{x}_j\|_2^2 - R_{\text{safety}}^2). \tag{4.25}$$

Assume first that $\mu_{ij} = 0$ for all $i \neq j$, meaning that the safety distance constraint is satisfied. The expanded expression of the determinant obtained for

N agents is

$$\begin{aligned}\det(\bar{\mathbf{R}}_{i,k+1}^{\mathrm{T}}\mathbf{W}_{i,k+1}\bar{\mathbf{R}}_{i,k+1}) = &\sum_i^N w_{i,k}\sum_i^N X_i^2 w_{i,k}\sum_i^N Y_i^2 w_{i,k} - \sum_i^N w_{i,k}\left(\sum_i^N X_i Y_i w_{i,k}\right)^2 \\ &- \sum_i^N Y_i^2 w_{i,k}\left(\sum_i^N X_i w_{i,k}\right)^2 - \sum_i^N X_i^2 w_{i,k}\left(\sum_i^N Y_i w_{i,k}\right)^2 \\ &+ 2\sum_i^N w_{i,k}X_i\sum_i^N w_{i,k}Y_i\sum_i^N w_{i,k}X_iY_i\end{aligned} \tag{4.26}$$

Where X_i and Y_i denote respectively $(\mathbf{x}_i|_{x_1} - \widehat{\mathbf{x}}_i^{k+1}|_{x_1})$ and $(\mathbf{x}_i|_{x_2} - \widehat{\mathbf{x}}_i^{k+1}|_{x_2})$. $w_{i,k}$ denotes the weight composing the diagonal matrix $\mathbf{W}_{i,k}$. Let R_i and χ_i define the polar coordinates centred on $\widehat{\mathbf{x}}_i^{k+1}$ by $X_i = R_i\cos(\chi_i)$ and $Y_i = R_i\sin(\chi_i)$. Let $\det(\bar{\mathbf{R}}_{i,k+1}^{\mathrm{T}}\mathbf{W}_{i,k+1}\bar{\mathbf{R}}_{i,k+1})$ be denoted by det. The expression of the determinant becomes

$$\begin{aligned}\det = &\sum_i^N \sigma_i^2\exp\left(\frac{-R_i^2}{k_{\mathrm{w}}}\right)\sum_i^N R_i^2\sigma_i^2\exp\left(\frac{-R_i^2}{k_{\mathrm{w}}}\right)\cos^2(\chi_i)\sum_i^N R_i^2\sigma_i^2\exp\left(\frac{-R_i^2}{k_{\mathrm{w}}}\right)\sin^2(\chi_i) \\ &- \sum_i^N \sigma_i^2\exp\left(\frac{-R_i^2}{k_{\mathrm{w}}}\right)\left(\sum_i^N R_i\cos(\chi_i)R_i\sin(\chi_i)\sigma_i^2\exp\left(\frac{-R_i^2}{k_{\mathrm{w}}}\right)\right)^2 \\ &- \sum_i^N R_i^2\sin^2(\chi_i)\sigma_i^2\exp\left(\frac{-R_i^2}{k_{\mathrm{w}}}\right)\left(\sum_i^N R_i\cos(\chi_i)\sigma_i^2\exp\left(\frac{-R_i^2}{k_{\mathrm{w}}}\right)\right)^2 \\ &- \sum_i^N R_i^2\cos^2(\chi_i)\sigma_i^2\exp\left(\frac{-R_i^2}{k_{\mathrm{w}}}\right)\left(\sum_i^N R_i\sin(\chi_i)\sigma_i^2\exp\left(\frac{-R_i^2}{k_{\mathrm{w}}}\right)\right)^2 \\ &+ 2\sum_i^N \sigma_i^2\exp\left(\frac{-R_i^2}{k_{\mathrm{w}}}\right)R_i\cos(\chi_i)\sum_i^N \sigma_i^2\exp\left(\frac{-R_i^2}{k_{\mathrm{w}}}\right)R_i\sin(\chi_i) \\ &\sum_i^N \sigma_i^2\exp\left(\frac{-R_i^2}{k_{\mathrm{w}}}\right)R_i^2\cos(\chi_i)\sin(\chi_i)\end{aligned} \tag{4.27}$$

If one is searching for optimal location on a common circle, thus $R_i = R\ \forall i$. The

determinant simplifies into

$$\begin{aligned}\det = &\exp\left(\frac{-3R^2}{k_\mathrm{w}}\right) R^4 \sum_i^N \sigma_i^2 \sum_i^N \sigma_i^2 \cos^2(\chi_i) \sum_i^N \sigma_i^2 \sin^2(\chi_i) \\ &- \exp\left(\frac{-3R^2}{k_\mathrm{w}}\right) R^4 \sum_i^N \sigma_i^2 \left(\sum_i^N \cos(\chi_i)\sin(\chi_i)\sigma_i^2\right)^2 \\ &- \exp\left(\frac{-3R^2}{k_\mathrm{w}}\right) R^4 \sum_i^N \sin^2(\chi_i)\sigma_i^2 \left(\sum_i^N \cos(\chi_i)\sigma_i^2\right)^2 \\ &- \exp\left(\frac{-3R^2}{k_\mathrm{w}}\right) R^4 \sum_i^N \cos^2(\chi_i)\sigma_i^2 \left(\sum_i^N \sin(\chi_i)\sigma_i^2\right)^2 \\ &+ 2\exp\left(\frac{-3R^2}{k_\mathrm{w}}\right) R^4 \sum_i^N \sigma_i^2 \cos(\chi_i) \sum_i^N \sigma_i^2 \sin(\chi_i) \\ &\quad \sum_i^N \sigma_i^2 \cos(\chi_i)\sin(\chi_i)\end{aligned} \tag{4.28}$$

$$\begin{aligned}\det = &\exp\left(\frac{-3R^2}{k_\mathrm{w}}\right) R^4 \Bigg[\sum_i^N \sigma_i^2 \sum_i^N \sigma_i^2 \cos^2(\chi_i) \sum_i^N \sigma_i^2 \sin^2(\chi_i) \\ &- \sum_i^N \sigma_i^2 \left(\sum_i^N \cos(\chi_i)\sin(\chi_i)\sigma_i^2\right)^2 - \sum_i^N \sin^2(\chi_i)\sigma_i^2 \left(\sum_i^N \cos(\chi_i)\sigma_i^2\right)^2 \\ &- \sum_i^N \cos^2(\chi_i)\sigma_i^2 \left(\sum_i^N \sin(\chi_i)\sigma_i^2\right)^2 \\ &+ 2\sum_i^N \sigma_i^2 \cos(\chi_i) \sum_i^N \sigma_i^2 \sin(\chi_i) \sum_i^N \sigma_i^2 \cos(\chi_i)\sin(\chi_i) \Bigg]\end{aligned} \tag{4.29}$$

Deriving the Lagrangian with respect to R, with the constraints verified ($\mu_{ij} = 0$) results in

$$\frac{\partial \mathcal{L}}{\partial R} = \left(4R^3 \exp\left(\frac{-3R^2}{k_\mathrm{w}}\right) - \frac{6}{k_\mathrm{w}} R^5 \exp\left(\frac{-3R^2}{k_\mathrm{w}}\right)\right) \Bigg[- \sum_i^N \cos^2(\chi_i)\sigma_i^2 \left(\sum_i^N \sin(\chi_i)\sigma_i^2\right)^2 - \sum_i^N \sigma_i^2 \left(\sum_i^N \cos(\chi_i)\sin(\chi_i)\sigma_i^2\right)^2 - \sum_i^N \sin^2(\chi_i)\sigma_i^2 \left(\sum_i^N \cos(\chi_i)\sigma_i^2\right)^2 + \sum_i^N \sigma_i^2 \sum_i^N \sigma_i^2 \cos^2(\chi_i) \sum_i^N \sigma_i^2 \sin^2(\chi_i) + 2\sum_i^N \sigma_i^2 \cos(\chi_i) \sum_i^N \sigma_i^2 \sin(\chi_i) \sum_i^N \sigma_i^2 \cos(\chi_i)\sin(\chi_i) \Bigg] \tag{4.30}$$

$$\frac{\partial \mathcal{L}}{\partial R} = \left(4 - \frac{6}{k_\mathrm{w}} R^5\right) R^3 \exp\left(\frac{-3R^2}{k_\mathrm{w}}\right) \Bigg[- \sum_i^N \cos^2(\chi_i)\sigma_i^2 \left(\sum_i^N \sin(\chi_i)\sigma_i^2\right)^2 - \sum_i^N \sigma_i^2 \left(\sum_i^N \cos(\chi_i)\sin(\chi_i)\sigma_i^2\right)^2 - \sum_i^N \sin^2(\chi_i)\sigma_i^2 \left(\sum_i^N \cos(\chi_i)\sigma_i^2\right)^2 + \sum_i^N \sigma_i^2 \sum_i^N \sigma_i^2 \cos^2(\chi_i) \sum_i^N \sigma_i^2 \sin^2(\chi_i) + 2\sum_i^N \sigma_i^2 \cos(\chi_i) \sum_i^N \sigma_i^2 \sin(\chi_i) \sum_i^N \sigma_i^2 \cos(\chi_i)\sin(\chi_i) \Bigg] \tag{4.31}$$

which is equal to 0 for $R = 0$ or $R = \sqrt{\frac{2k_\mathrm{w}}{3}}$. Note first that the second solution does not impose any restriction on the value of k_w. Secondly, note that the result cannot be proved to be the optimal location result as the search domain for the solutions is restricted to a circle. Discussion similar to the one presented for T-optimal placement on the influence of the parameter values leads to the same type of conclusions on the relative values of k_w, N and R_safety.

Numerical solution

Numerical solutions are investigated for D-optimal and T-optimal sensor placements in the general case.

A numerical solution can be found to (4.15) and (4.23). A possible optimisation technique is CMAES (Hansen et al., 2003), which is an evolutionary algorithm that allows a random initialisation of the sensor agent positions. By hypothesis, all the agents have the same estimation position $\widehat{\mathbf{x}}_i^{k+1} = \widehat{\mathbf{x}}_j^{k+1} = \widehat{\mathbf{x}}^{k+1}$.

The set of parameters used are: $\sigma^2_{\eta=0} = 0.01$, $\sigma^2_{\eta=1} = 2\sigma^2_{\eta=0} = 0.02$, $k_{\mathrm{w}} = 100$, $R_{\mathrm{safety}} = 10$. The position of estimation is $\widehat{\mathbf{x}}^{k+1} = [0\ 0]$. The maximum number of iterations of the solver is set to $N.10^6$.

One searches for the solution of (4.15) and (4.23) with the constraints (4.16) and (4.24). The original criterion is penalized with a weighted sum of the constraints in order to find the solutions with the CMAES algorithm. The cost (4.15) takes values up to 10^{17}, therefore the weighted constraint consists in an additive term defined as $10^{17} \max(-\left\|\mathbf{x}_i - \mathbf{x}_j\right\|_2 + R_{\mathrm{safety}},\ 0)$, for $j > i$.

The results are presented for different numbers N of agents. For each value of N, both scenarios, with only healthy sensors and with one faulty sensor, are presented. An histogram illustrates the distance between the estimation position and the positions of the agents. This histogram results from 1000 runs of the solver with sensors randomly initialised over the search space. The best solution satisfying the constraint obtained when the iteration budget is consumed is selected as the optimum. For each histogram, an example is provided to illustrate the sensor formation. An infinity of formation positions can be considered as the argument of the optimal value of the criterion since the criterion value remains unchanged after a rotation centred on the position of estimation and permutation of agents with identical sensor states. Agents with fault-free sensors are plotted in green while agents with defective sensors are plotted in red. The estimation position is represented by a black cross. When two sensors are at a distance equal to R_{safety} to each other, a blue line is represented between the sensors. The distances represented on the histogram are shown on the formation plot by black circles. In the histograms, a different color represents an agent. The dark blue bar represents the faulty sensor.

For $N = 3$ sensors Figure 4.2 shows the optimal sensor placement for $N = 3$ sensors without fault. One can notice that the sensors are located on a circle at equal distance to the position of estimation, while respecting the collision avoidance constraint.

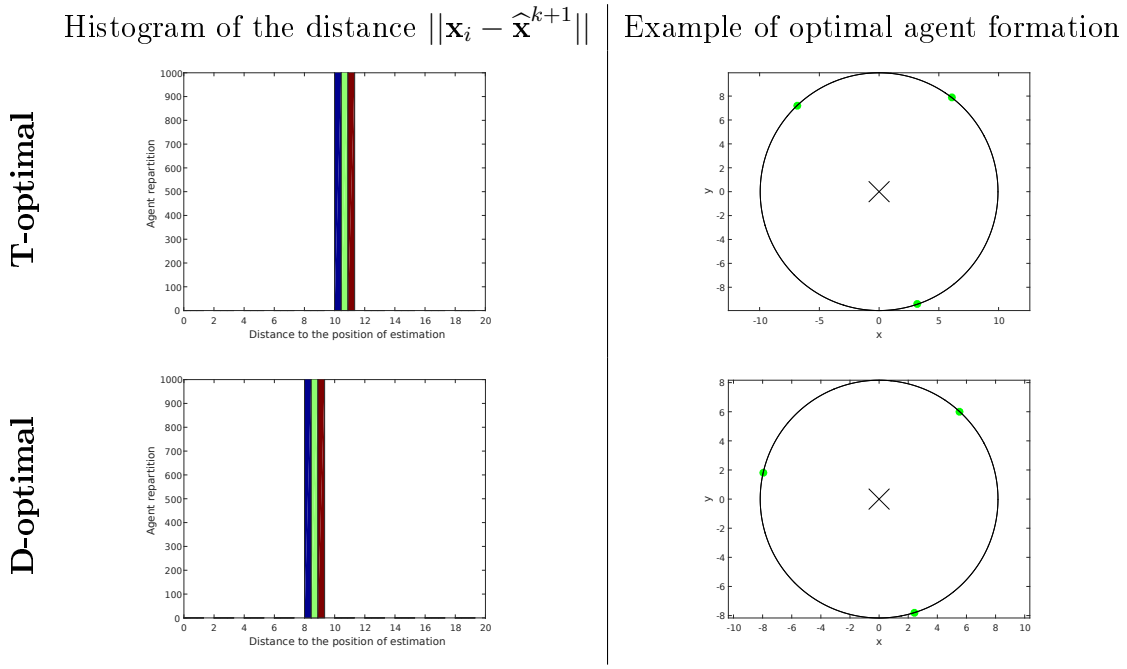

Figure 4.2: Illustration of the optimal positions for 3 healthy sensors

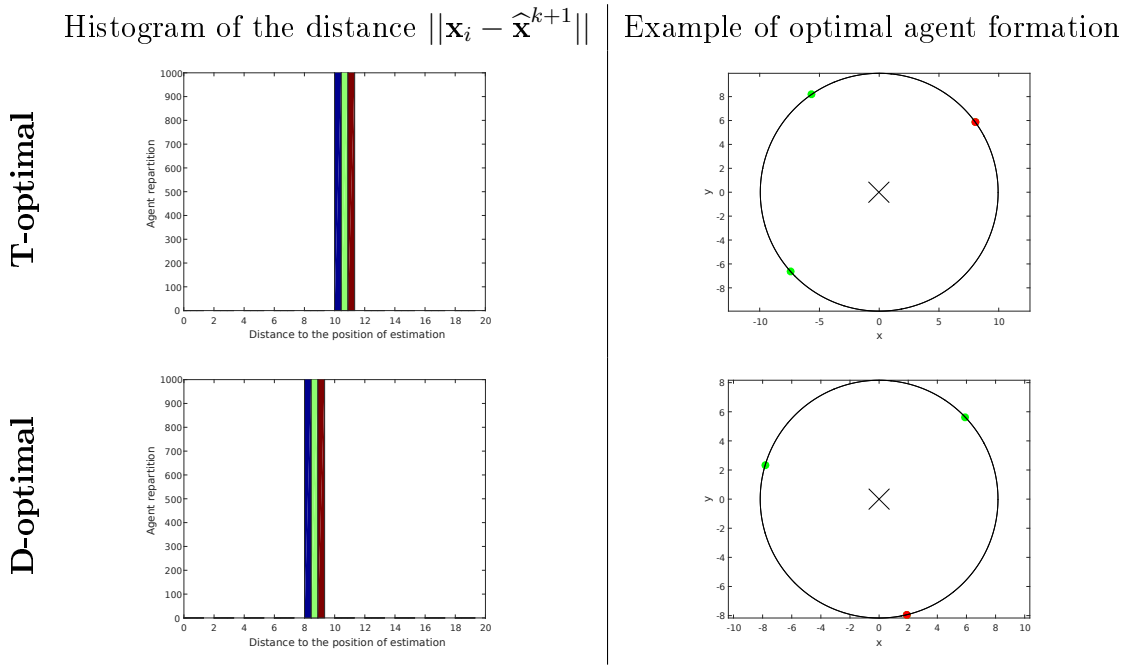

Figure 4.3: Illustration of the optimal positions for 3 sensors, 2 healthy and 1 faulty

Figure 4.3 illustrates the optimal sensor placement for $N = 3$ sensors with one faulty sensor. One can notice that the sensors are located on a circle at equal distance to the position of estimation, while respecting the collision avoidance constraint. The radius of this circle is the same that the radius calculated in the analytical part.

$4 \leq N \leq 10$ **sensors** Figures 4.4, 4.5, 4.6, 4.7, 4.8 show the optimal sensor placement respectively for $N = 4, 5, 7, 8$, and 10 sensors without fault. One can notice that the sensors are located on a circle at equal distance to the estimation position, while respecting the collision avoidance constraint.

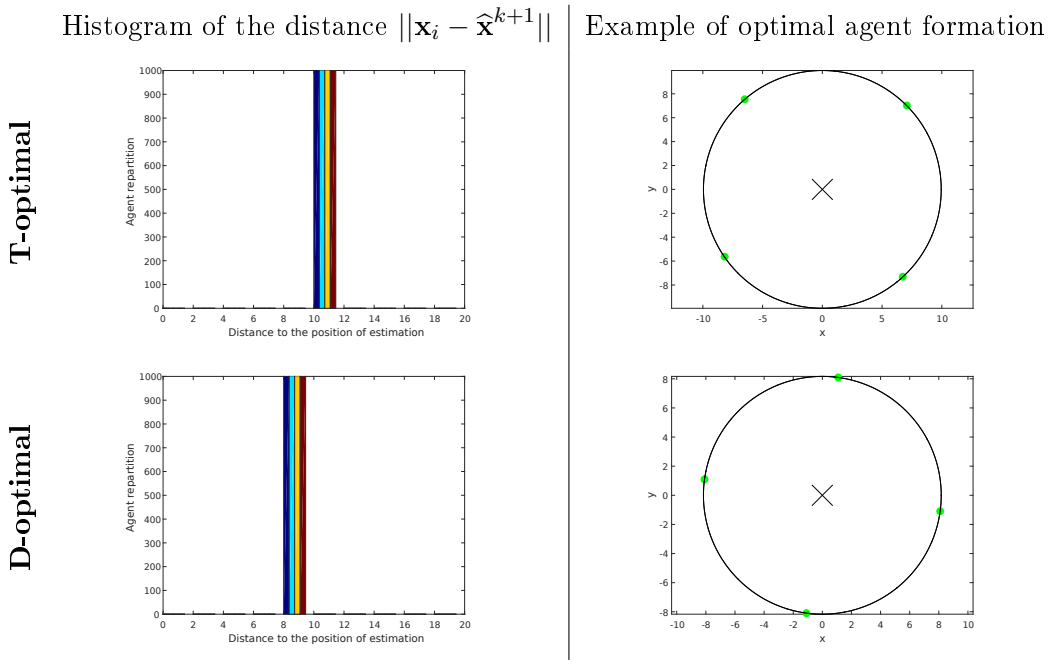

Figure 4.4: Illustration of the optimal positions for 4 healthy sensors

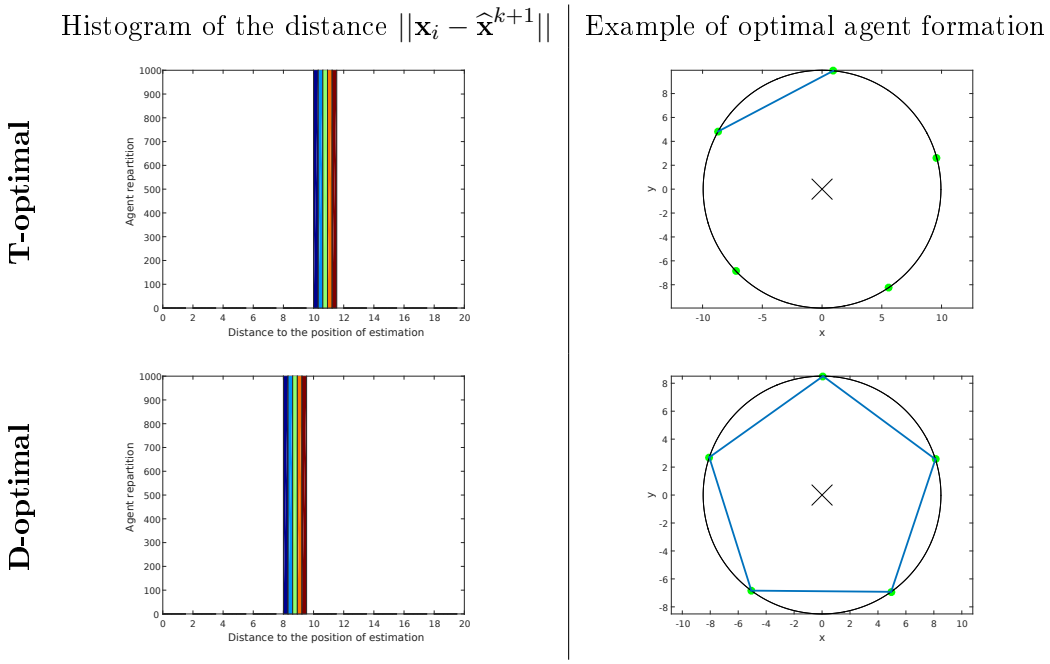

Figure 4.5: Illustration of the optimal positions for 5 healthy sensors

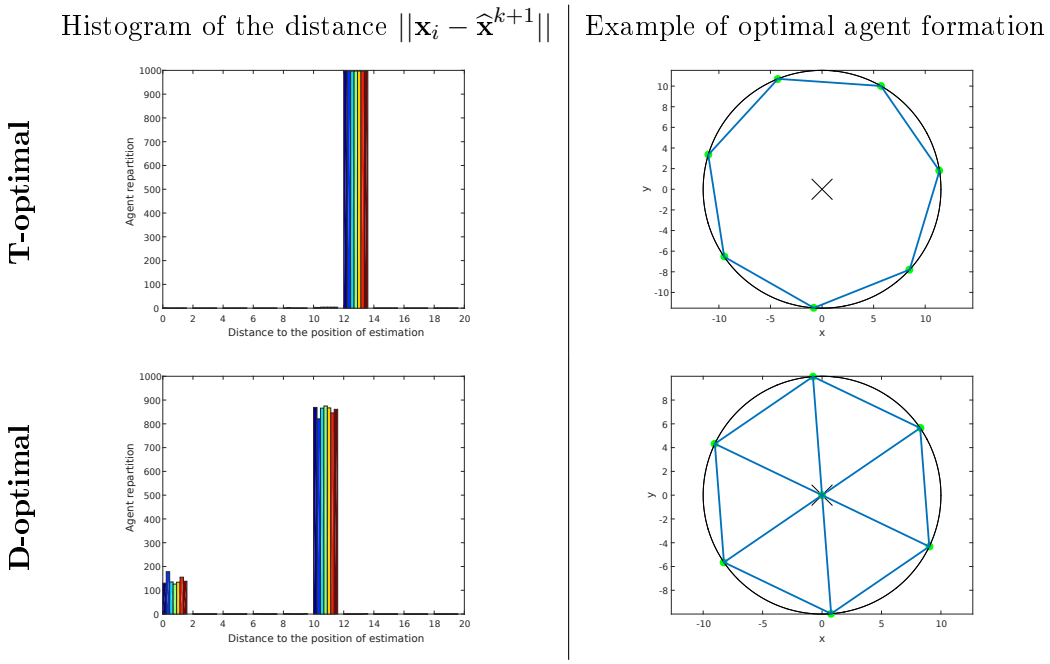

Figure 4.6: Illustration of the optimal positions for 7 healthy sensors

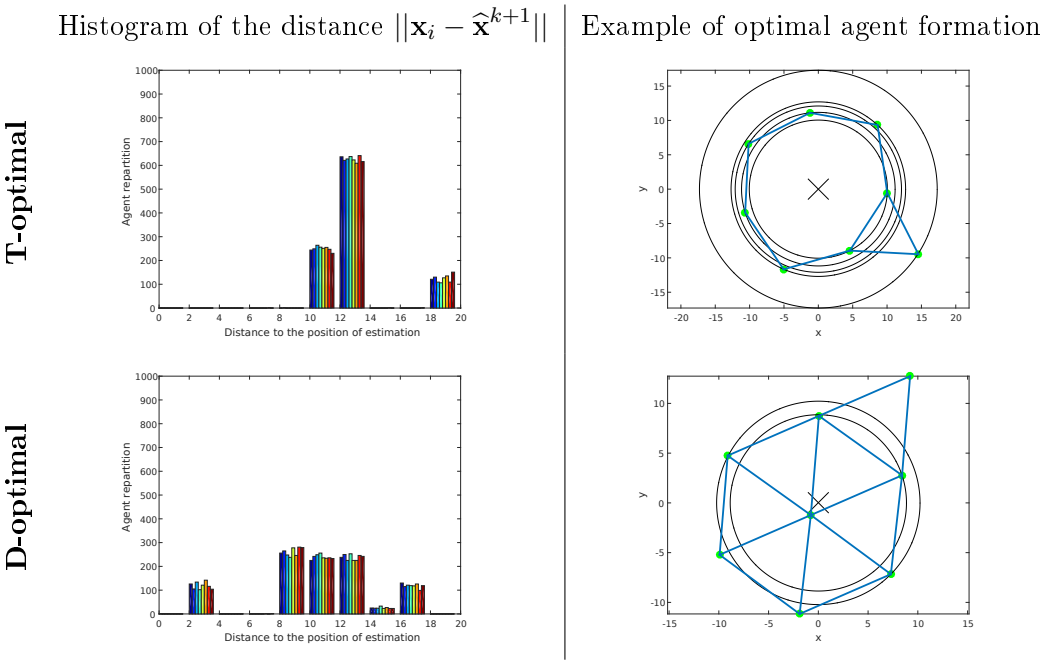

Figure 4.7: Illustration of the optimal positions for 8 healthy sensors

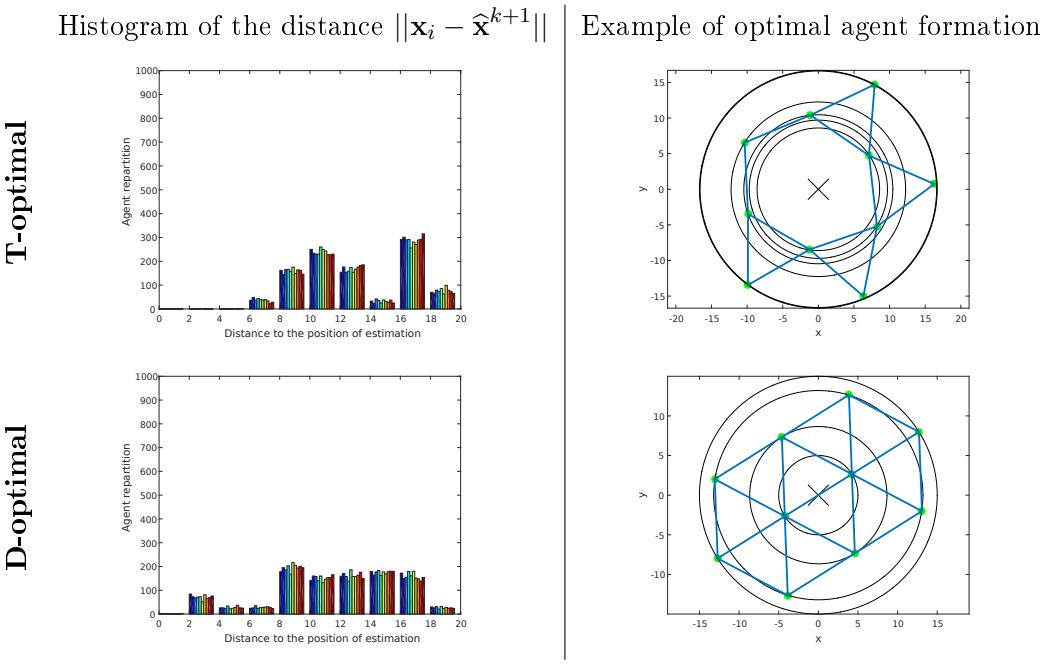

Figure 4.8: Illustration of the optimal positions for 10 healthy sensors

Figures 4.9, 4.10, 4.11, 4.12 and 4.13 show the optimal sensor placement for $N = 4, 5, 7, 8, 10$ sensors with one faulty sensor. One can notice that the non-faulty sensors are located closer to the position of estimation than the faulty sensor.

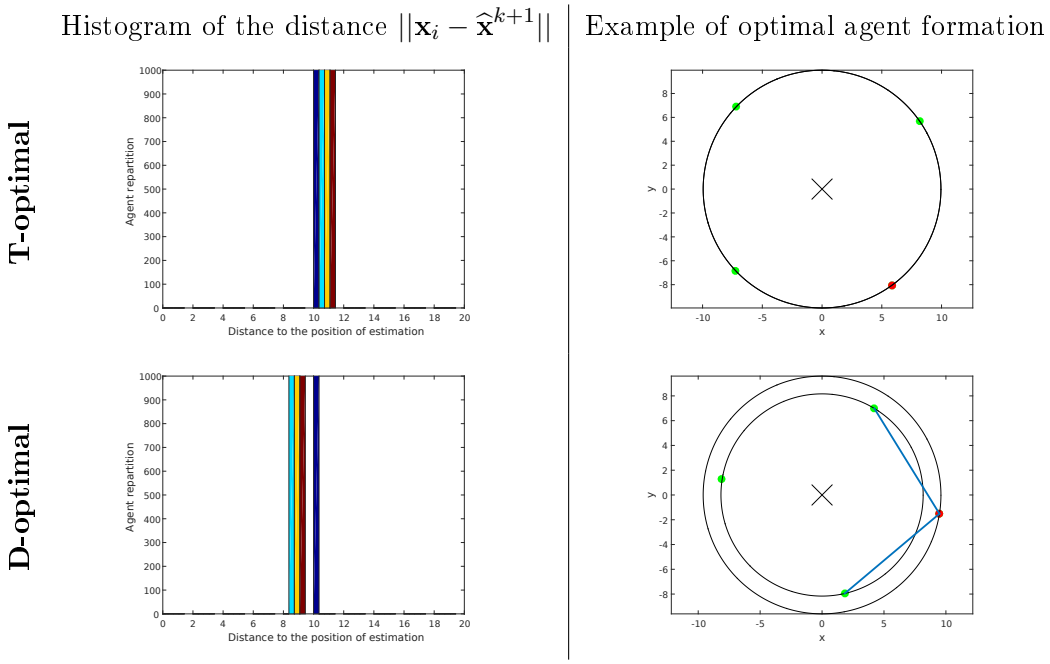

Figure 4.9: Illustration of the optimal positions for 4 sensors, 3 healthy and 1 faulty

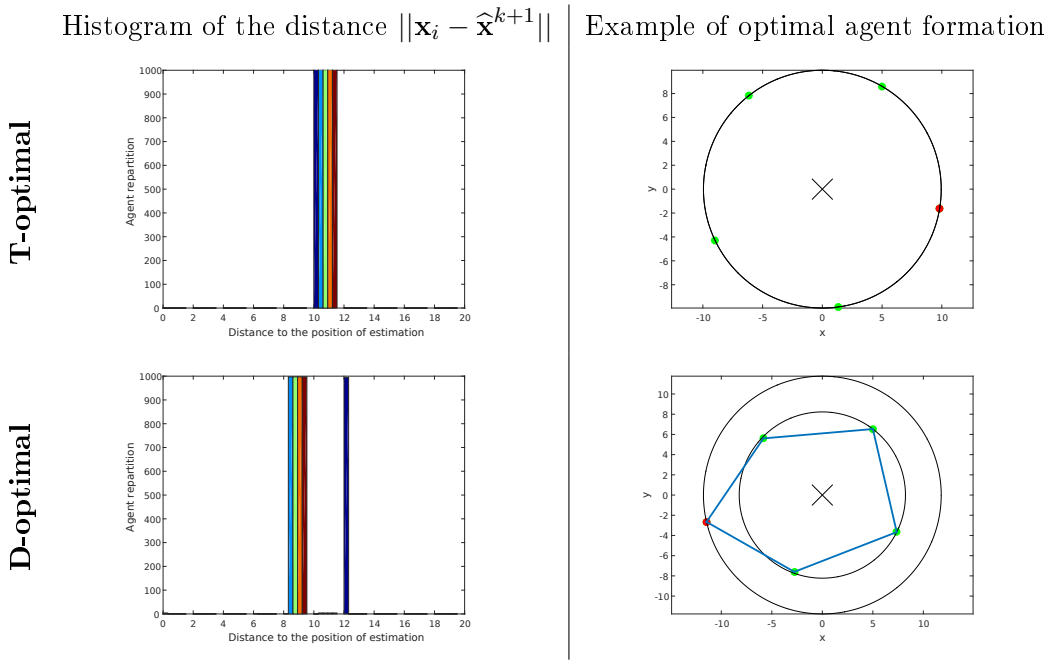

Figure 4.10: Illustration of the optimal positions for 5 sensors, 4 healthy and 1 faulty

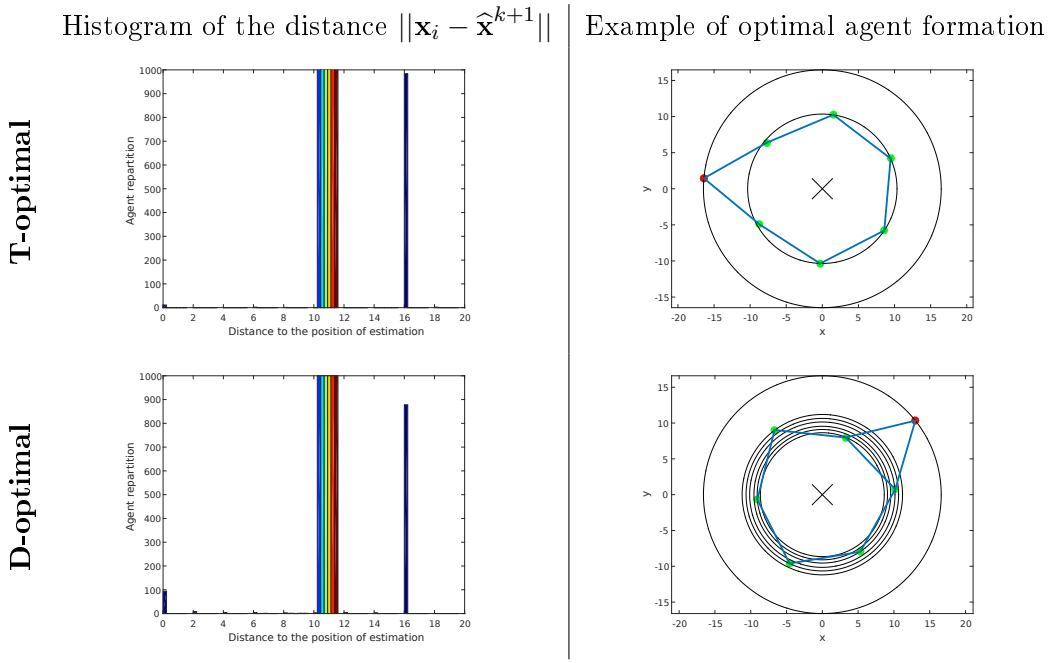

Figure 4.11: Illustration of the optimal positions for 7 sensors, 6 healthy and 1 faulty

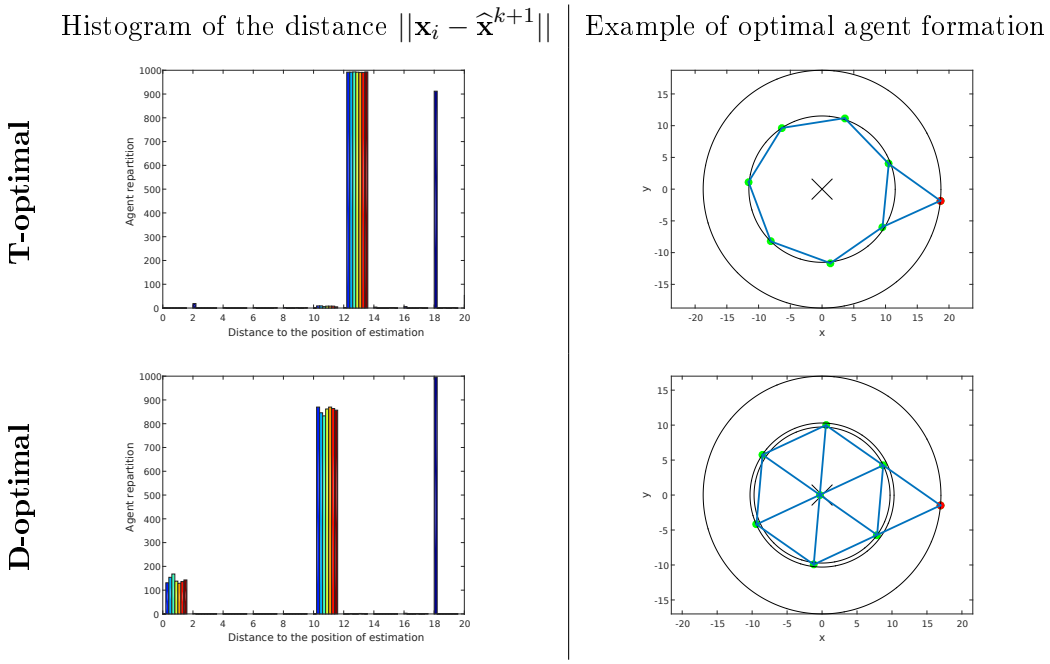

Figure 4.12: Illustration of the optimal positions for 8 sensors, 7 healthy and 1 faulty

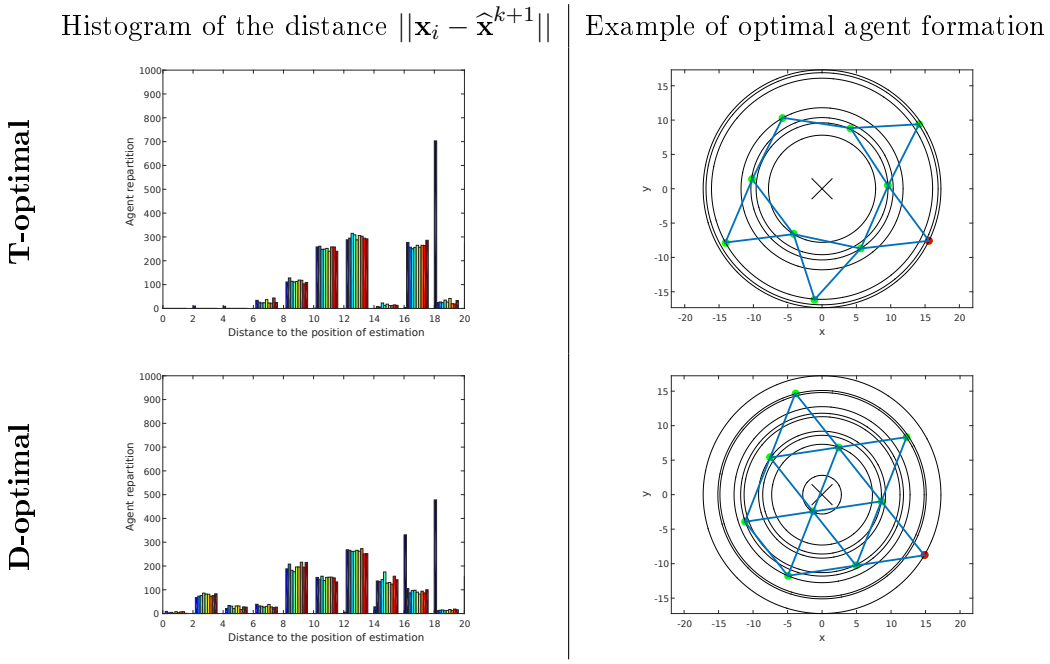

Figure 4.13: Illustration of the optimal positions for 10 sensors, 9 healthy and 1 faulty

A compact formation is defined as a formation where all the agents are at distance R_{safety} from each other. This kind of formation can take the shape of a regular polyhedron with the appropriate number of agents.

From the previous simulations one may deduce the following properties an optimal agent formation should satisfy:

- In a formation with non-faulty sensors, the sensors have to be positioned in a circle or a compact shaped formation satisfying the collision avoidance constraint. The formation should be centred on the position of estimation.

- In a formation with faulty sensors, the faulty sensors have to be positioned on the boundary of the formation, at a higher distance to the position of estimation than healthy sensors.

4.3.2 Minimisation of the modelling error

As previously noted, the sensors must be located at a position that fulfils two conditions:

- collecting measurements to estimate accurately the gradient of ϕ
- avoiding collision between agents.

The local gradient is estimated at time t_k at position $\widehat{\mathbf{x}}_i(t_k)$ and used by agent i to determine the next estimate of the location of the maximum of the field. The second criterion selected to optimise the agent position is the minimisation of the modelling error (4.9). By minimising this error, the spatial disturbance on the estimate resulting of the approximation by the Taylor expansion is reduced. The previous criterion aims to attenuate the effect of faulty agents on the estimation. In this section, when a sensor is considered as faulty, its measurements are removed from the set used for the estimation.

Effect of the modelling error on the estimation

The estimate of $\boldsymbol{\alpha}_i^k$ is obtained by (4.13). The modelling error is one of the components of $\mathbf{y}_{i,k}$. From (4.7) and (4.13), one can express the part of the estimate $\widehat{\boldsymbol{\alpha}}_i^k$ depending on the modelling error $\mathbf{e}_{i,k}$

$$\widehat{\boldsymbol{\alpha}}_i^k = \left(\bar{\mathbf{R}}_{i,k}^{\mathrm{T}} \mathbf{W}_{i,k} \bar{\mathbf{R}}_{i,k}\right)^{-1} \bar{\mathbf{R}}_{i,k}^{\mathrm{T}} \mathbf{W}_{i,k} \left(\bar{\mathbf{R}}_{i,k} \boldsymbol{\alpha}_i^k + \mathbf{n}_{i,k} + \mathbf{e}_{i,k}\right) \tag{4.32}$$

$$\widehat{\boldsymbol{\alpha}}_i^k = \boldsymbol{\alpha}_i^k + \left(\bar{\mathbf{R}}_{i,k}^{\mathrm{T}} \mathbf{W}_{i,k} \bar{\mathbf{R}}_{i,k}\right)^{-1} \bar{\mathbf{R}}_{i,k}^{\mathrm{T}} \mathbf{W}_{i,k} \left(\mathbf{n}_{i,k} + \mathbf{e}_{i,k}\right) \tag{4.33}$$

The expected value of $\widehat{\boldsymbol{\alpha}}_i^k$ is

$$E\left[\widehat{\boldsymbol{\alpha}}_i^k\right] = E\left[\boldsymbol{\alpha}_i^k + \left(\bar{\mathbf{R}}_{i,k}^{\mathrm{T}} \mathbf{W}_{i,k} \bar{\mathbf{R}}_{i,k}\right)^{-1} \bar{\mathbf{R}}_{i,k}^{\mathrm{T}} \mathbf{W}_{i,k} \left(\mathbf{n}_{i,k} + \mathbf{e}_{i,k}\right)\right] \tag{4.34}$$

$$E\left[\widehat{\boldsymbol{\alpha}}_i^k\right] = E\left[\boldsymbol{\alpha}_i^k\right] + \left(\bar{\mathbf{R}}_{i,k}^{\mathrm{T}} \mathbf{W}_{i,k} \bar{\mathbf{R}}_{i,k}\right)^{-1} \bar{\mathbf{R}}_{i,k}^{\mathrm{T}} \mathbf{W}_{i,k} E\left[\left(\mathbf{n}_{i,k} + \mathbf{e}_{i,k}\right)\right] \tag{4.35}$$

The measurement error $\mathbf{n}_{i,k}$ is assumed to be composed of independently distributed zero-mean Gaussian variables. Thus, the bias on the estimate of $\boldsymbol{\alpha}_i^k$ is:

$$E\left[\widehat{\boldsymbol{\alpha}}_i^k\right] - \boldsymbol{\alpha}_i^k = \left(\bar{\mathbf{R}}_{i,k}^{\mathrm{T}} \mathbf{W}_{i,k} \bar{\mathbf{R}}_{i,k}\right)^{-1} \bar{\mathbf{R}}_{i,k}^{\mathrm{T}} \mathbf{W}_{i,k} \mathbf{e}_{i,k} \tag{4.36}$$

The minimisation of the modelling error $\mathbf{e}_{i,k}$ results in minimising the norm of the bias on the estimator of $\boldsymbol{\alpha}_i^k$.

Sensor position minimising the modelling error

The Taylor expansion is obtained at the position $\widehat{\mathbf{x}}_i^k$ which corresponds to the current estimate of the position of the field maximum. The aim is to find the agent positions $\tilde{\mathbf{x}}_i$ that minimise the modelling error. The modelling error of agent i located in relative position $\tilde{\mathbf{x}}_i$ is $e_i\left(\tilde{\mathbf{x}}_i\right)$, component of $\mathbf{e}_{i,k}$. The goal is to find $\mathbf{x}_i^d$, the desired position of agent i so that $\mathbf{x}_i^d = \arg\min_{\tilde{\mathbf{x}}_i \in D} e_i\left(\tilde{\mathbf{x}}_i\right)$

We know that

$$e_i\left(\tilde{\mathbf{x}}_i\right) = \frac{1}{2}\left(\tilde{\mathbf{x}}_i - \widehat{\mathbf{x}}_i^k\right)^{\mathrm{T}} \nabla^2 \phi(\boldsymbol{\chi}_i) \left(\tilde{\mathbf{x}}_i - \widehat{\mathbf{x}}_i^k\right) \tag{4.37}$$

$$||e_i\left(\tilde{\mathbf{x}}_i\right)|| = ||\frac{1}{2}\left(\tilde{\mathbf{x}}_i - \widehat{\mathbf{x}}_i^k\right)^{\mathrm{T}} \nabla^2 \phi(\boldsymbol{\chi}_i) \left(\tilde{\mathbf{x}}_i - \widehat{\mathbf{x}}_i^k\right)|| \tag{4.38}$$

Using appropriate norms for vectors and matrix,

$$||e_i\left(\tilde{\mathbf{x}}_i\right)|| \leq \frac{1}{2}||\tilde{\mathbf{x}}_i - \widehat{\mathbf{x}}_i^k|| \; ||\nabla^2\phi(\boldsymbol{\chi}_i)|| \; ||\tilde{\mathbf{x}}_i - \widehat{\mathbf{x}}_i^k|| \tag{4.39}$$

Assuming that the gradient is K-Lipschitz, and is differentiable, then the upper bound of $||\nabla^2\phi||$ over the definition domain, is equal to the Lipschitz constant K. One can then write $||\nabla^2\phi|| \leq K$ From this, one obtains

$$||e_i\left(\tilde{\mathbf{x}}_i\right)|| \leq \frac{1}{2}||K|| \; ||\tilde{\mathbf{x}}_i - \widehat{\mathbf{x}}_i^k||^2 \tag{4.40}$$

From (4.3.2), it appears clearly that $||e_i\left(\tilde{\mathbf{x}}_i\right)||$ is bounded by a function that decreases when $\tilde{\mathbf{x}}_i$ tends to $\widehat{\mathbf{x}}_i^k$ and is null when $\tilde{\mathbf{x}}_i = \widehat{\mathbf{x}}_i^k$

Minimising the modelling error requires the sensor position $\mathbf{x}_i(t_k)$ to be the closest possible to $\widehat{\mathbf{x}}_i^k$. However, as said previously, there exists a safety distance constraint between the relative positions of the vehicles. The sensor location problem results from a compromise between two antagonist goals: closeness of the agents surrounding $\widehat{\mathbf{x}}_i^k$ and spacing of the vehicles for collision avoidance.

Numerical solution to this problem placement for $N = 3, 5, 7$ and 8 agents under the collision avoidance constraint $\|\mathbf{x}_i - \mathbf{x}_j\|_2^2 \geqslant R_{\text{safety}}^2, \; j > i$ is illustrated in Figure 4.14. The agent positions are represented in green and the blue line shows when two agents are at the safety distance $R_{\text{safety}} = 10$ from each other. All the agent share the same position of estimation $\widehat{\mathbf{x}}_i^k = \widehat{\mathbf{x}}^k, \forall i$. $\widehat{\mathbf{x}}^k$ is represented by the black cross in [0; 0].

From this analysis, one may notice that the sensors that contribute to the estimation have to be close to the estimate position $\widehat{\mathbf{x}}_i^k$. The shapes obtained from the minimisation of the modelling error are similar to the D-optimal one when the agent cannot fit on the desired circle. Considering that the faulty agents do not contribute to the estimation, the healthy agents should be placed closer to $\widehat{\mathbf{x}}_i^k$ than faulty agents.

A state-of-the-art method can be found in (Ögren et al., 2004) where the same problem is treated. A MAS is required to estimate the gradient of an unknown field using least-squares estimate and a second-order Taylor expansion of the real field. The optimal position of the agents is looked for to minimise the expected value of the estimation error. The unknown Hessian of the field is replaced by a

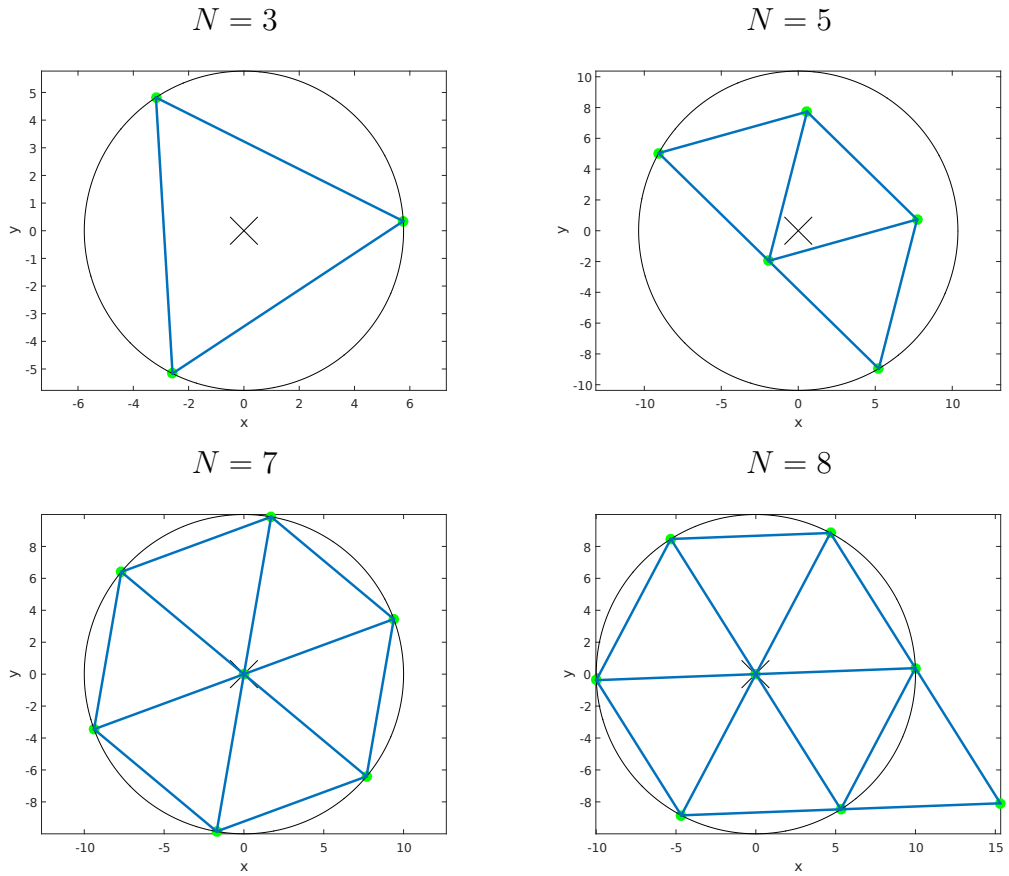

Figure 4.14: Representation of the formation shape for different numbers of agents N obtained by minimising the modelling error

stochastic scalar variable ($\mathcal{N}(0, \sigma_H^2)$) times a rough estimate of the Hessian. The resulting optimisation problem is non convex and non-trivial and no analytical solution is produced but the authors highlight that numerical solutions present a pattern of regular polyhedra around the estimation position.

The formation shape resulting of this state-of-the-art method is similar to the one obtained by minimizing the modelling error of estimation proposed or the D-optimal placement when the agents cannot fit on the optimal circle.

The optimal sensor location methods shown in this thesis provide several results regarding to the positions of healthy sensors. The faulty agents are either excluded from the inputs of the estimation or their measurements are still taken into account

but they should be located farther to the position of estimation than the healthy sensors to play a minor role in the resulting estimates.

The minimisation of the modelling error shows that:

- The agent positions should form a compact formation around $\widehat{\mathbf{x}}_i^k$.

The minimisation of the variance of the estimate from T-optimality shows that:

- The agents should be positioned on a circle if the parameters k_{w}, N, R_{safety} and the constraint (4.16) allow it.
- The faulty agent should be placed farther than the healthy ones.

The minimisation of the variance of the estimate from D-optimality shows that:

- The agents should be positioned on a circle if the parameters k_{w}, N, R_{safety} and the constraint (4.24) allow it.
- When the agent cannot fit on a circle, a compact formation with all the agents as close as possible to the position of estimation $\widehat{\mathbf{x}}_i^k$ while respecting (4.24) should be achieved.
- The faulty agents should be placed farther than the healthy ones from the position of estimation.

The control law and the reconfiguration scheme proposed in this thesis aim at fulfilling these goals.

4.4 Fault detection and isolation scheme for MAS

The sensors equipping the agents of the MAS can become defective and generate outliers. An outlier is defined as a measurement that does not fulfill the hypotheses on the measurement noise. These corrupted measurements have to be identified in order either to be removed from the estimation of the gradient or to decrease their influences on this estimate. Two problems have to be distinguished, the detection problem is about detecting when a fault occurs in the system. It does not intend to look for the origin of the fault. On the contrary, the isolation problem is about

determining the origin of the fault in a system when a fault is detected. Both aspects are treated in this thesis.

This section describes the proposed method used for detecting outliers. It is similar to the direct statistical test presented in (Gertler, 1988) but an adaptive threshold is proposed based on a disturbance analysis for the problem treated in this thesis. This type of methods presents the advantage to be easy to compute, but the results are particularly sensitive to the threshold selection. The method consists in detecting an outlier when a residual r_{FDI} is greater than a given threshold obtained as the product of a constant positive gain k_{FDI} and the assumed noise standard deviation σ_{FDI}, so that an outlier is detected when $r_{\text{FDI}} \geq k_{\text{FDI}}\sigma_{\text{FDI}}$. (Chaloner and Brant, 1988) detailed the impact of the choice of these parameters on the quality of the outlier detection process.

Model-based fault detection and identification (Ding, 2008) uses a model to predict the expected system output, which can then be compared to the actual measurement to generate a residual. This residual should be close to zero or remain within a priori bounds when there is no fault and become large to highlight the occurrence of an outlier.

The problem of detecting accurately an outlier involves being able to operate the distinction between the influence of the modelling error and the noise induced by the sensor malfunction. The modelling error, as said previously, integrates the neglected second-order term in (4.1) that depends on the unknown Hessian matrix. This neglected term has to be evaluated in order to compare it with the variations of the residuals.

Modelling error representation

The modelling error defined in (4.4) depends on the unknown Hessian of the field. A potential representation of the Hessian is to define $\nabla^2\phi$ as a random variable. There, the entries of the Hessian are thus described by three independent Gaussian variables $\tilde{\nabla}^2\phi_i = [A_{11}, A_{21}; A_{21}, A_{22}]$.The error vector $\mathbf{e}_{i,k}$ can be approximated omitting the time dependence by $\tilde{\mathbf{e}}_i$ whose jth row is given by

$$\tilde{\mathbf{e}}_{ij} = \frac{1}{2}(\mathbf{x}_j - \mathbf{x}_i)^T\tilde{\nabla}^2\phi_i(\mathbf{x}_j - \mathbf{x}_i) \tag{4.41}$$

Without further prior information on the Hessian, the mean μ_k can be considered equal to 0. In order to define a suitable value for its variance, σ_k, we assume the gradient field $\nabla\phi$ over D to be K-Lipschitz which results in $||\nabla^2\phi|| \leq K$. Selecting a standard deviation $\sigma_k = \frac{K}{6}$ ensures that in 99% of the cases, the value of A_{mn} will verify $|A_{mn}| < K/2$.

4.4.1 Outlier detection and identification

The residual used in this thesis is designed as the difference between the estimated value of the field obtained by the i-th sensor and its measured value. Each term has to be considered at the same time instant. For convenience, the time dependency is omitted. In our application, the residual is $r_i = \hat{\phi}_i(\mathbf{x}_i) - y_i$. It can be rewritten as

$$r_i = [1\ 0\ 0]\boldsymbol{\alpha}_i - \phi(\mathbf{x}_i) - n_i \tag{4.42}$$

and using (4.2), one gets

$$\begin{aligned} r_i &= [1\ 0\ 0]\left(\mathbf{R}_{i,k}^{\mathrm{T}}\mathbf{W}_{i,k}\mathbf{R}_{i,k}\right)^{-1}\mathbf{R}_{i,k}^{\mathrm{T}}\mathbf{W}_{i,k}(\mathbf{n}_i + \mathbf{e}_i) + n_i \\ &= \mathbf{h}_i\mathbf{n}_i + \mathbf{h}_i\mathbf{e}_i + n_i \end{aligned} \tag{4.43}$$

where $\mathbf{h}_i = [1\ 0\ 0]\left(\mathbf{R}_{i,k}^{\mathrm{T}}\mathbf{W}_{i,k}\mathbf{R}_{i,k}\right)^{-1}\mathbf{R}_{i,k}^{\mathrm{T}}\mathbf{W}_{i,k}$ is a vector of dimension card$(\mathcal{N}_i)$, the number of neighbours of agent i.

With the assumptions on the measurement noise vector $\mathbf{n}_i$ and the modelling error vector $\mathbf{e}_i$, it is possible to check whether this residual is compliant with the expected distribution. Assuming that a faulty sensor introduces an error d_j on the j-th measurement: $y_j = \phi(\mathbf{x}_j) + n_j + d_j$. this error can be a bias or the expression of a higher noise variance ($\sigma_1^2 > \sigma_0^2$). The residual r_i becomes, for $i \neq j$

$$r_i(d_j) = \mathbf{h}_i\mathbf{n}_i + \mathbf{h}_i\mathbf{e}_i - n_i + \mathbf{h}_{ij}d_j, \tag{4.44}$$

where $\mathbf{h}_{ij}$ is the j^{th} entry of $\mathbf{h}_i$. From (4.44), one deduces that the fault d_j is affected by $\mathbf{h}_i$ as well as the measurement noise $\mathbf{n}_i$ and the model error $\mathbf{e}_i$, so that it is impossible to decouple it from these sources of uncertainty. Also note that in

the particular case of a fault acting on the i^{th} sensor, the residual is equal to

$$r_i(d_i) = \mathbf{h}_i\mathbf{n}_i + \mathbf{h}_i\mathbf{e}_i - n_i - d_i, \tag{4.45}$$

which means that the residual r_i is always impacted by outliers on the i^{th} measurement. However, for faults affecting the other sensors, a bank of filters can be built such that the residual r_{ij} becomes insensitive to a fault on the j-th sensor, making it possible to identify the faulty sensor (see Section 4.4.2).

To determine whether the measurement is an outlier or not, the characteristics of the residual are first defined in terms of mean and standard deviation when all the sensors are assumed healthy: $\sigma^2_{\eta,j} = \sigma^2_0,\ j = 1, \ldots, N$

Mean and variance of the residual

The expected value of the residual r_i is

$$E[r_i] = E[\hat{\phi}_i(\mathbf{x}_i) - y_i] \tag{4.46}$$

This yields

$$E[r_i] = E[\phi(\mathbf{x}_i) + \mathbf{h}_i\mathbf{n}_i + \mathbf{h}_i\mathbf{e}_i - \phi(\mathbf{x}_i) - n_i] \tag{4.47}$$

thus,

$$E[r_i] = \mathbf{h}_i E[\mathbf{n}_i] - E[n_i] + E[\mathbf{h}_i\mathbf{e}_i] \tag{4.48}$$

As by hypothesis, in nominal condition, $E[n_i] = 0$, and $E[\mathbf{e}_i] = 0$ since $\mathbf{e}_i \sim \mathcal{N}(0, \sigma^2_k)$, one gets

$$E[r_i] = 0 \tag{4.49}$$

The associated variance is

$$\begin{aligned} E\left[(r_i - E[r_i])^2\right] &= E\left[(\hat{\phi}_i(\mathbf{x}_i) - y_i)^2\right] \\ &= E\left[(\phi(\mathbf{x}_i) + \mathbf{h}_i\mathbf{n}_i + \mathbf{h}_i\mathbf{e}_i - \phi(\mathbf{x}_i) - n_i)^2\right] \\ &= E\left[(\mathbf{h}_i\mathbf{n}_i + \mathbf{h}_i\mathbf{e}_i - n_i)^2\right] \end{aligned} \tag{4.50}$$

The measurement noise $\mathbf{n}_i$ and the modelling error $\mathbf{e}_i$ are independent and with zero mean, leading to

$$E\left[(r_i - E[r_i])^2\right] = E\left[(\mathbf{h}_i\mathbf{n}_i)^2 - 2\mathbf{h}_i\mathbf{n}_i n_i + (\mathbf{h}_i\mathbf{e}_i)^2 + n_i^2\right] \tag{4.51}$$

This leads to the final variance expression

$$E\left[(r_i - E[r_i])^2\right] = \sigma_0^2\left(1 + \mathbf{h}_i^T\mathbf{h}_i - 2\mathbf{h}_i[i]\right) + \mathbf{h}_i^T\mathbf{U}_i\mathbf{h}_i \tag{4.52}$$

where $\mathbf{U}_i$ is a diagonal matrix with j-th term:

$$\frac{\sigma_k^2}{2}\left((\mathbf{x}_j(1) - \mathbf{x}_i(1))^4 + (\mathbf{x}_j(2) - \mathbf{x}_i(2))^4 + 2(\mathbf{x}_j(1) - \mathbf{x}_i(1))^2(\mathbf{x}_j(2) - \mathbf{x}_i(2))^2\right) \tag{4.53}$$

Detection of outlier using adaptive threshold

As the residual is assumed to follow a normal distribution with mean and variance given by (4.49) and (4.52), the detection of outliers can be obtained using a test comparing the residual to an adaptive threshold depending on the previously computed characteristics of the residual and a parameter k_{FDI}. It is usual to consider that a fault has occurred if this threshold is such that the distance between the residual and its mean is above three times its standard deviation (Chaloner and Brant, 1988). Then, if

$$|r_i - \mathbf{h}_i\mathbf{e}_i| < k_{\text{FDI}}\sqrt{\sigma_0^2\left(1 + \mathbf{h}_i\mathbf{h}_i^T - 2\mathbf{h}_i[i]\right) + \mathbf{h}_i^T\mathbf{U}_i\mathbf{h}_i} \tag{4.54}$$

with $k_{\text{FDI}} = 3$, the residual respects the characteristics of the nominal noise distribution with $99,7\%$ confidence. This technique allows to limit the false detection rate. The threshold is adaptive in the sense that its characteristics change for every sensor i and depends on the location of each sensor.

4.4.2 Bank of residuals for FDI

A bank of filters is used to identify which sensor provides a faulty measurement (if any). For the i^{th} sensor, N residuals r_{ij} are built by excluding the j-th mea-

surement from the estimation (4.13), for $j = 1, ..., N$.

$$r_{ij} = \mathbf{h}_i \left[y_1, ..., y_{j-1}, 0, y_{j+1}, ..., y_N\right]^T - y_i \tag{4.55}$$

The sensitivity of these residuals of agent i to faults of agent j is highlighted by equations (4.44) and (4.45). By design, r_{ij} is sensitive to faults on all sensors, except the one affecting the j^{th} sensor (this is usually named as a *generalized filter scheme*). For r_{ii}, since it contains y_i, it remains sensitive to a fault on the i^{th} sensor and is therefore sensitive to all faults. It can be used as a detection signal only, and the $N-1$ other residuals can be used only when r_{ii} raises an alarm to limit the computational load of the method. At every time step, each sensor has a list of sensors that are considered as faulty. A consensus on the potentially faulty sensor is then obtained on the fleet as described in Algorithm 2.

Algorithm 2 Isolation majority vote algorithm

```
Every agent starts with a vote v_i = 0
if One fault is detected in the MAS, see (4.54) then
    for Each agent i that detects a fault do
        for Each j ⊂ N_i do
            N_i^test = N_i \ j
            Compute a new estimate α_{i\j} using (4.13) with N_i^test
            and the corresponding residual r_{i\j} (4.42)
            if test (4.54) on r_{i\j} is healthy then
                v_j = v_j + 1
            end if
        end for
    end for
    The agent with the maximum of votes is identified as the faulty agent.
end if
```

Each sensor broadcasts the list of sensors that it has found to be faulty using its bank of filters. The one that has been identified as such most often is declared faulty.

Note that, since the modelling error grows with the distance between sensors, this vote can be weighted by the term w_{ij} defined by (4.12) to give higher confidence to the sensors that are closer to the faulty one.

4.4.3 FDI results

Some simulations were performed to evaluate the FDI scheme proposed. A two dimensional function ϕ_{FDI} is defined on a space $D = [0,\ 50]^2$.

$$\phi_{\text{FDI}}(x_1, x_2) = 10 \exp\left(-\frac{(x_1 - 10)^2 + (x_2 - 35)^2}{2000}\right) \tag{4.56}$$

A set of N sensors is randomly initialised in D with all sensors located at a minimum relative distance of 10m from the others and at a maximum distance of 15m from at least one other sensor. Each sensor i provides a measurement corrupted by a measurement noise n_i that follows a normal distribution $\mathcal{N}(0, \sigma_0^2)$, $\sigma_0^2 = 0.01$. The variance of the Hessian model is taken as $\sigma_k^2 = \frac{2\sigma_0^2}{6}$. Among the N sensors, one sensor is randomly selected as faulty. The faulty sensor has an additional noise term d:

$$y_i = \phi_{\text{FDI}}(\mathbf{x}_i) + n_i + d. \tag{4.57}$$

d can reflect a bias error or the result of a defective measurement noise variance. Simulations are performed with several values of N and d. Each set of values is tested with 500 runs. Half of the runs simulate scenarios with one faulty sensor and the remaining half simulate scenarios without faulty sensors. The weight matrix used for the estimation of each agent i is defined as:

$$\mathbf{W}_i = \text{diag}\left(\exp\left(\frac{-||\mathbf{x}_1 - \mathbf{x}_i||_2^2}{100}\right), \ldots,\ \exp\left(\frac{-||\mathbf{x}_N - \mathbf{x}_i||_2^2}{100}\right)\right). \tag{4.58}$$

If one sensor detects an error, the output of the detection scheme for the entire network is an error detection. If the output of the network detects a fault when one sensor was indeed defective, this is a true detection. If the output of the network detects a fault when no sensor was defective, this is a false detection.

Receiver Operating Characteristic (ROC) curves, are used to present the characteristics of the FDI schemes for the different parameters. The number of sensors N, as well as the threshold k_{FDI} and the value of the disturbance d are the parameters evaluated in this section.

The results are presented as follow, for $N = 7, 10, 15$ sensors, a constant bias of value $d = 1, 2, 3$ and 5 was introduced. The ROC curve is obtained each time by changing the value of the threshold k_{FDI} between 0.1 to 10 with a 0.1 increment.

For $N = 7$ sensors: Figure 4.15 shows the ROC curves obtained for the detection of an error in a network of 7 sensors. An optimal threshold parameter is a parameter with the best trade-off between the true detection rate and the false detection rate. For a small disturbance $d = 1$, the curve is located near the diagonal axis with an optimal threshold parameter between 3 and 4. When the fault magnitude increases to $d = 2$ and $d = 3$, the ROC curve changes and gets closer to the optimal point $[0, 1]$ that define 0% of false detection rate for 100% of true detection rate. For faults higher than $d = 5$, the ROC curve reaches the optimal point for some value of k_{FDI} around 3 and 4.

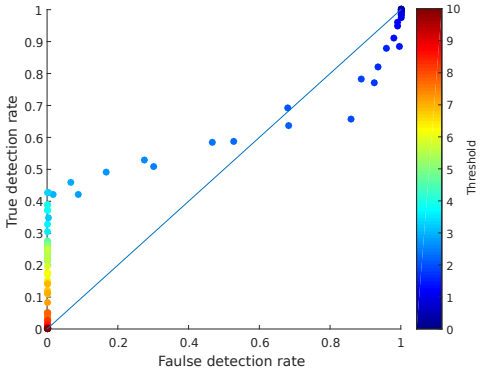

ROC curve for $N = 7$ and $d = 1$

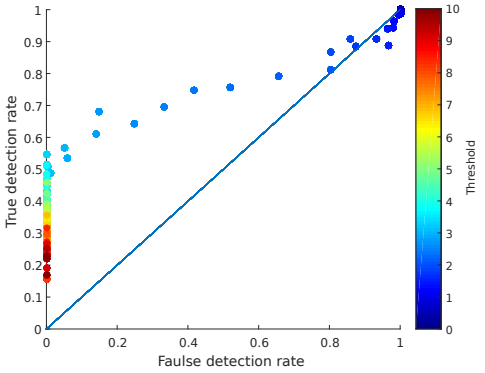

ROC curve for $N = 7$ and $d = 2$

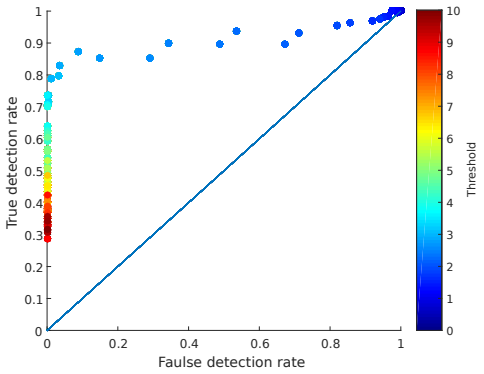

ROC curve for $N = 7$ and $d = 3$

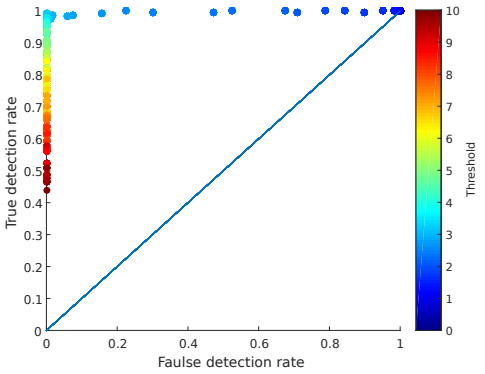

ROC curve for $N = 7$ and $d = 5$

Figure 4.15: ROC curves for 7 sensors

For $N = 10$ sensors: The Figure 4.16 shows the ROC curves obtained for the detection of an error in a network of 10 sensors. As previously, for a small fault magnitude $d = 1$, the curve is located near the diagonal axis with an optimal threshold parameter between 3 and 4. When the fault magnitude increases to $d = 2$ and $d = 3$, the ROC curve changes and gets closer to the optimal point $[0, 1]$, meaning a better trade-off exist between true and false detection for some parameters values. For fault magnitude higher than $d = 5$, the ROC curve shows that the best trade-off between true detection and false detection is reached for some value of k_{FDI} around 3.5 and 4.

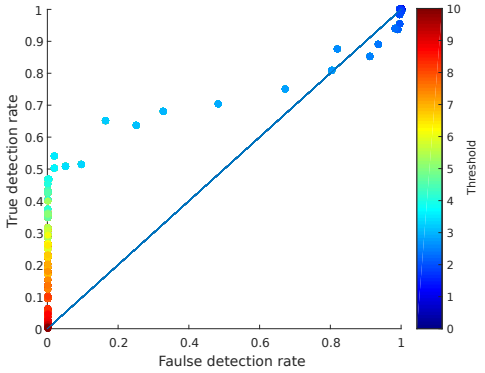

ROC curve for $N = 10$ and $d = 1$

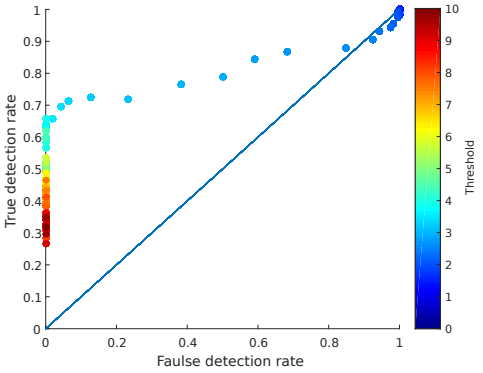

ROC curve for $N = 10$ and $d = 2$

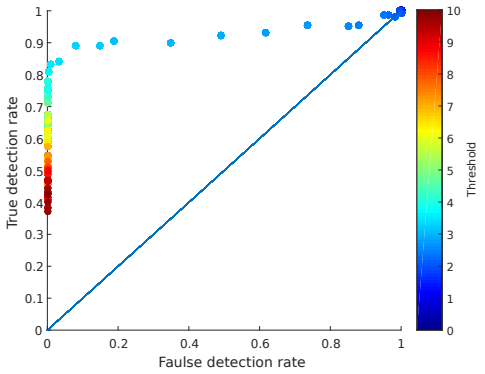

ROC curve for $N = 10$ and $d = 3$

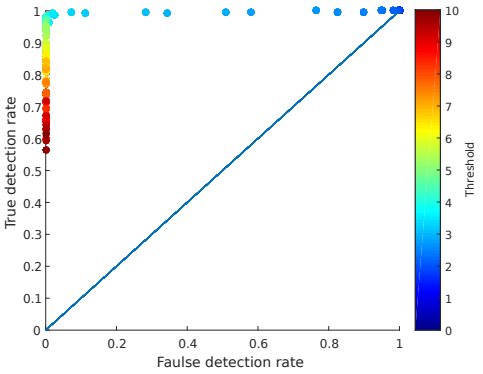

ROC curve for $N = 10$ and $d = 5$

Figure 4.16: ROC curves for 10 sensors

For $N = 15$ sensors: The Figure 4.17 shows the ROC curves obtained for the detection of an error in a network of 15 sensors. For a small fault magnitude $d = 1$, the curve is located near the diagonal axis with an optimal threshold parameter between 3 and 4. When the fault magnitude increases to $d = 2$ and $d = 3$, the ROC curve changes and gets closer to the optimal point $[0, 1]$. For fault magnitude higher than $d = 5$, the ROC curve shows that the optimal point is obtained for some value of k_{FDI} around 4.

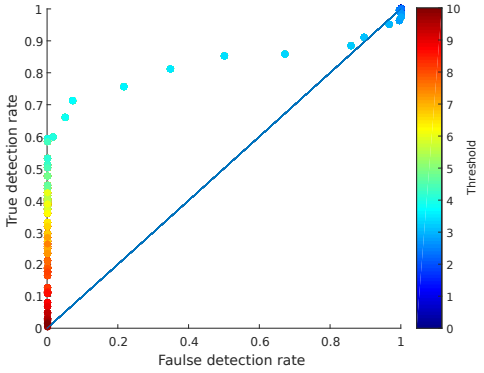

ROC curve for $N = 15$ and $d = 1$

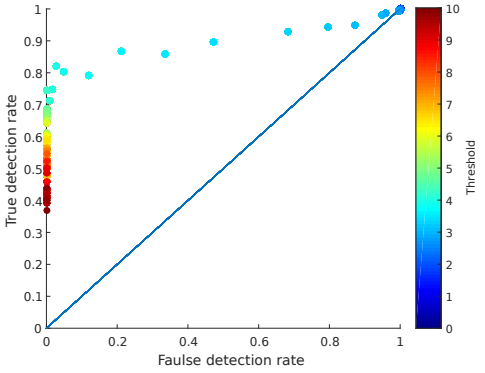

ROC curve for $N = 15$ and $d = 2$

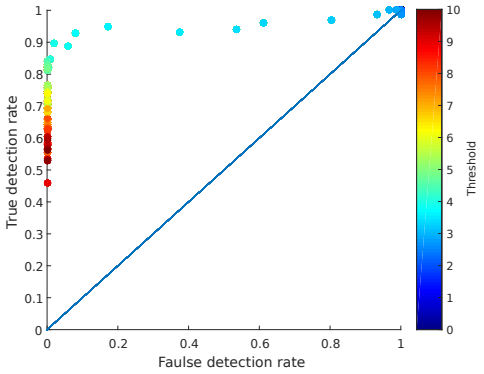

ROC curve for $N = 15$ and $d = 3$

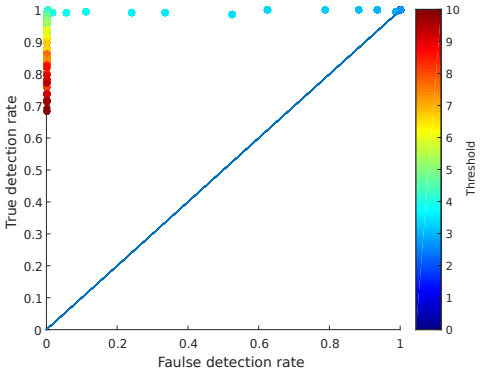

ROC curve for $N = 15$ and $d = 5$

Figure 4.17: ROC curves for 15 sensors

The results presented show that:

- A higher fault d can be detected more easily than a small one as could be expected.

- The optimal threshold parameter k_{FDI} is the one with the best trade-off between true detection and false detection rates. It depends on the number of sensors as, when the number of sensors increase, the optimal value of k_{FDI} also increases.

This second result may come from the proposed adaptive threshold. More sensors may lead the threshold to be smaller. If the threshold decreases, an increase of the threshold parameter k_{FDI} is needed to keep the test performance identical.

When detection of outliers has been realised, it is thus required to be able to detect which sensor is faulty. To do so, a bank of filters is computed for each sensor as described in Section 4.4.2. A vote among all sensors decides in case of fault which one is faulty, the sensor with the majority of votes from the others against him is the one identified as faulty.

The isolation scheme has been tested for different values of $N = 7, 10, 15$, of the threshold parameter $k_{\text{FDI}} = 1, 3, 4, 7, 10$ and of the bias $d = 1, 2, 3, 4, 5, 7$. The simulations have been performed on 1000 runs, with the same experimental procedure as previously. For each run, one agent is randomly selected as faulty and has its measurement corrupted by the fault d. The result are displayed on Figure 4.18 and different conclusions can be drawn.

- The isolation rate increases as the fault increases for all the number of agents N and all the parameter k_{FDI}.
  This result could have been expected as an higher fault is easier to identify.

- For a high parameter k_{FDI}, upper than 4, the isolation rate is near 0 for small faults. Once again, this result could have been expected as an high k_{FDI} means that the threshold for detection is high and would not detect small fault.

- The isolation rate depends on the number of agents and on the parameter k_{FDI}. It appears that the best detection rates are obtained for smaller value of k_{FDI} when N is small ($k_{\text{FDI}} = 3$ for $N = 7$) and larger values of k_{FDI} when N is large ($k_{\text{FDI}} = 4$ for $N = 15$). This result can be linked to the ROC curves illustrated previoulsy. A better trade-off between false detection

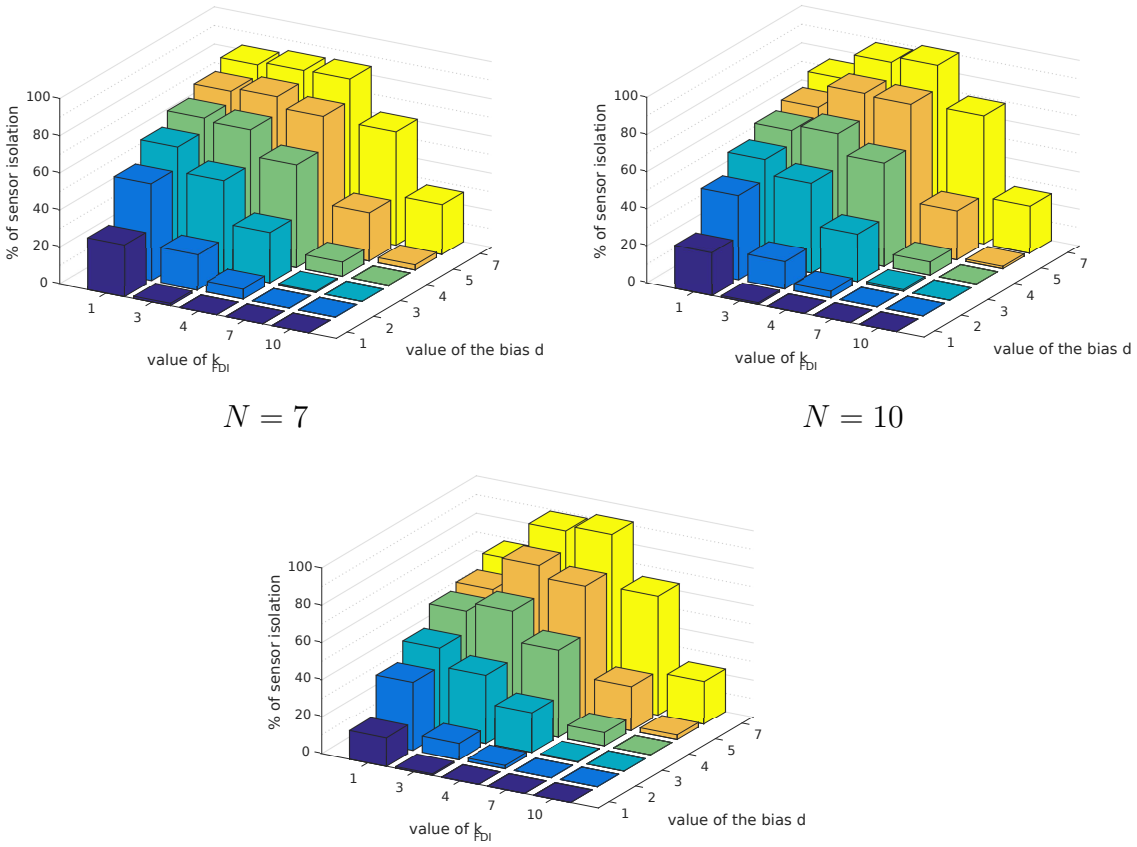

Figure 4.18: Good isolation rate of the faulty sensor

and true detection is obtained for smaller values of k_{FDI} for $N = 7$ than for $N = 15$.

4.5 Conclusion

This chapter has presented the solution proposed to fulfil the maximum seeking mission by relying on a gradient climbing approach.

Firstly, a cooperative estimation scheme by weighted least-squares is proposed to obtain an estimate of the value and gradient of the field model.

Secondly, optimal agent placement for estimation is analysed. Three criteria

are proposed to find the desired positions of the sensors. Analytical and numerical solutions are presented to illustrate the desired formation for the sensors.

Comparison with a state-of-the-art method shows similar results. The main difference is that the proposed method in this thesis takes into account agents with healthy and defective sensors. Optimal sensor placement for defective sensors are proposed to limit the perturbation on the estimate.

Thirdly, to lessen the influence of outlier measurements in case of defective sensors, a fault detection and identification scheme is proposed. The detection part of this scheme is based on an evaluation of the noise measurement in the estimation to find an adaptive threshold for fault detection.

The isolation part of the scheme is carry out using a bank of residuals and a majority vote among the agents to identify the faulty sensor. Simulations show the efficiency of the proposed scheme.

Summary

In this chapter, the contributions were:

- A novel study of optimal sensor placement with three criteria.
- An adaptive fault detection scheme for outlier detection and isolation in a sensor network.

The next chapter presents the control law developed to take into account the sensor position requirements to perform an accurate estimation and move the agents to the local maximum. The FDI scheme will be used to reconfigure the positions of the agents with defective sensors.
Part of the work on optimal sensor placement has been presented in (Kahn et al., 2015a).

Chapter 5

A reconfigurable control law for local maximum seeking by a AMS

Chapter goals

In this chapter, a cooperative control law is presented. It has to fulfil different goals:

- Move the agents in a desired formation.
- Avoid collisions between the agents.
- Move the formation toward the local maximum of the field.

For that purpose, the following subjects are detailed:

- Design of the control law: the different terms that compose the control law and their utility.
- Reconfiguration: the actions taken when the fleet detects that an agent sensor has become faulty.

The previous chapter has presented the estimation tools to estimate the local gradient of the field. It also proposed different formation shapes to optimise the estimation from several criteria and last, it has presented a fault detection and isolation scheme to detect faulty sensors.

In this chapter, a control law is designed to move the agent in the desired formation shape and drive the formation toward the estimated gradient direction. Section 5.1 details the control law proposed and presents a stability analysis of this control law using Lyapunov theory.

After the control law presentation, a reconfiguration scheme is proposed in Section 5.2 to take into account the possibility of a fault on the sensor of an agent and reallocate the agents position among the formation.

Simulations to illustrate the proposed approach are shown in Section 5.3 before a conclusion of the first part of the thesis.

5.1 Design of the control law: a two-layer approach

The control law has to fulfil different objectives.

- The agents have to localise the position of the local maximum of the field (global maximum for uni-modal field). The estimation of the gradient of the field is carried out to this end. The fleet should move toward the maximum along the direction of the gradient.
- The agents have to be positioned in a desired formation. The previous chapter has provided clues regarding optimal sensor positions to measure the field. The control law must place the agents as suggested in Section 4.3.
- As the agents are gathered in a formation, the collisions between agents have to be avoided. This objective is highly important as the safety of the fleet depends on it.

The control law is required to be decentralised. Each agent has to be able to compute its own control law from its own information and information provided by its neighbourhood (Section 3.2).

The global control law is divided in two layers. The low layer will control the agents' movement. It ensures the second and third objectives of the control law: bring the agents in the desired formation and avoid collisions. The high layer takes on the first objective: move the formation along the gradient direction.

5.1.1 High layer: control of the formation

The high layer aims at moving the position of estimation toward the maximum. The position of estimation depends on the measurements performed in discrete time and will be denoted $\widehat{\mathbf{x}}_i^k$. For this reason, the high layer control to move this position is performed in discrete time.

To evaluate a new estimate $\widehat{\mathbf{x}}_i^{k+1}$ of the location of the field maximum from $\widehat{\mathbf{x}}_i^k$ and $\widehat{\boldsymbol{\alpha}}_i^k$, one has first to evaluate whether $\widehat{\mathbf{x}}_i^k$ actually corresponds to an increase of ϕ compared to the value that has been obtained for $\widehat{\mathbf{x}}_i^{k-1}$. Using gradient ascent, one then gets

$$\widehat{\mathbf{x}}_i^{k+1} = \widehat{\mathbf{x}}_i^k + \lambda_i^k \widehat{\nabla\phi}\left(\widehat{\mathbf{x}}_i^k\right) \,/\, \left\| \widehat{\nabla\phi}\left(\widehat{\mathbf{x}}_i^k\right) \right\|_2 . \tag{5.1}$$

Let λ_i^k be the gradient step size at time t_k. One updates λ_i^k as follows

$$\lambda_i^k = \begin{cases} \min\left\{\lambda_{\max}, 2\lambda_i^{k-1}\right\} & \text{if } \widehat{\phi}\left(\widehat{\mathbf{x}}_i^k\right) > \widehat{\phi}\left(\widehat{\mathbf{x}}_i^{k-1}\right), \\ \lambda_i^{k-1}/4 & \text{else,} \end{cases} \tag{5.2}$$

where $\lambda_{\max}$ is a fraction of the maximum displacement an agent can perform during a time slot. The classical step-size adaptation scheme (5.2), see, e.g. (Walter, 2014), enables the agents to slow down when reaching the maximum of the field ϕ. Using this control law, one can prove that the position $\widehat{\mathbf{x}}_i^k$ updated by (5.1) will converge asymptotically to the maximum of any concave field, see, e.g. (Marzat et al., 2014).

5.1.2 Low layer: control of the agents

This layer computes the control input $\mathbf{u}_i(t)$ of agent i that will move the agents using the dynamical model presented in (3.1):

$$M\ddot{\mathbf{x}}_i(t) + C\left(\mathbf{x}_i(t), \dot{\mathbf{x}}_i(t)\right)\dot{\mathbf{x}}_i(t) = \mathbf{u}_i(t) \tag{5.3}$$

This control law is inspired from (Cheah et al., 2009) where the authors designed a control law to bring a MAS in a formation of some particular shape.

The method proposed in this thesis does not define a geometric formation pattern but the formation shape is obtained from a equilibrium between attractive and repulsive forces. The shape of the formation at the equilibrium is the same as

the tight formation obtained in Section 4.3 for the optimal sensor placement.

The control input for the proposed control law is

$$\begin{aligned}\mathbf{u}_i(t) =& M\ddot{\widehat{\mathbf{x}}}_i(t) + C(\mathbf{x}_i(t), \dot{\mathbf{x}}_i(t))\dot{\mathbf{x}}_i(t) - k_1\left(\dot{\mathbf{x}}_i(t) - \dot{\widehat{\mathbf{x}}}_i(t)\right) \\ &+ 2k_2\sum_{j=1}^{N}(\mathbf{x}_i(t) - \mathbf{x}_j(t))\exp\left(-\frac{(\mathbf{x}_i(t) - \mathbf{x}_j(t))^T(\mathbf{x}_i(t) - \mathbf{x}_j(t))}{q}\right) \\ &- k_3^i(\eta_i, t)(\mathbf{x}_i(t) - \widehat{\mathbf{x}}_i(t)),\end{aligned} \tag{5.4}$$

The notation $g_{ij}(t)$ is introduced

$$g_{ij}(t) = \exp\left(-\boldsymbol{\delta}_{ij}(t)^T\boldsymbol{\delta}_{ij}(t)/q\right), \tag{5.5}$$

with $\boldsymbol{\delta}_{ij}(t) = \mathbf{x}_i(t) - \mathbf{x}_j(t)$, the difference of position between agents i and j, and q a parameter depending on the minimum safety distance between agents.

The first two terms $M\ddot{\widehat{\mathbf{x}}}_i(t)$ and $C(\mathbf{x}_i(t), \dot{\mathbf{x}}_i(t))\dot{\mathbf{x}}_i(t)$ compensate the dynamics of the agent. The term $k_1\left(\dot{\mathbf{x}}_i(t) - \dot{\widehat{\mathbf{x}}}_i(t)\right)$ is used to bring the velocity $\dot{\mathbf{x}}_i(t)$ of the i–th agent to the desired velocity $\dot{\widehat{\mathbf{x}}}_i(t)$. $2k_2\sum_{j=1}^{N}\boldsymbol{\delta}_{ij}(t)g_{ij}(t)$ is used as a repulsive term to avoid collisions between the agents. $k_3^i(\eta_i, t)(\mathbf{x}_i(t) - \widehat{\mathbf{x}}_i(t)$ is used as an attractive term to control the agent position $\mathbf{x}_i(t)$ toward the desired position $\widehat{\mathbf{x}}_i(t)$.

The gain $k_1 > 0$ is used to adapt the speed of each agent to the speed of $\widehat{\mathbf{x}}_i$. The constant $k_2 > 0$ determines the relative importance of the collision avoidance term in (5.4). Finally, $k_3^i(\eta_i) > 0$ determines the attractiveness of $\widehat{\mathbf{x}}_i(t)$ and may depend on the sensor state η_i.

In the case where $\widehat{\mathbf{x}}_i(t)$ is computed and updated by the high-layer control law presented previously, one may take an approximation of the velocity of $\widehat{\mathbf{x}}_i^k$ as $\dot{\widehat{\mathbf{x}}}_i(t) = \frac{\lambda_i^k\widehat{\nabla}\phi(\widehat{\mathbf{x}}_i^k)}{\|\widehat{\nabla}\phi(\widehat{\mathbf{x}}_i^k)\|_2 T}$ where T is the sampling period and $\ddot{\widehat{\mathbf{x}}}_i(t) = 0$. Nevertheless, stability analysis for general case with $\dot{\widehat{\mathbf{x}}}_i(t) \neq 0$ and $\ddot{\widehat{\mathbf{x}}}_i(t) \neq 0$ are presented in the next section.

5.1.3 Stability analysis by Lyapunov theory

In this part, the gain $k_3(\eta_i, t)$ is assumed to be constant and all the agents share the same target position, velocity and acceleration: $\widehat{\mathbf{x}}_i(t) = \widehat{\mathbf{x}}(t)$, $\dot{\widehat{\mathbf{x}}}_i(t) = \dot{\widehat{\mathbf{x}}}(t)$

and $\ddot{\hat{\mathbf{x}}}_i(t) = \ddot{\hat{\mathbf{x}}}(t)\ \forall i$. Consider the control law proposed in (5.4) and the positive function V:

$$V(\mathbf{x}(t)) = \frac{1}{2}\sum_{i=1}^{N}\Bigg[(\dot{\mathbf{x}}_i(t) - \dot{\hat{\mathbf{x}}}(t))^T M(\dot{\mathbf{x}}_i(t) - \dot{\hat{\mathbf{x}}}(t)) + (\mathbf{x}_i(t) - \hat{\mathbf{x}}(t))^T k_3^i(\mathbf{x}_i(t) - \hat{\mathbf{x}}(t)) + k_2\sum_{j=1}^{N}\exp\left(-\frac{(\mathbf{x}_i(t) - \mathbf{x}_j(t))^T(\mathbf{x}_i(t) - \mathbf{x}_j(t)}{q}\right)\Bigg] \tag{5.6}$$

where V is positive definite.

One can show, as in (Cheah et al., 2009) that the low-layer control law proposed in (5.4) brings the agents to a stable formation when $t \to \infty$. At equilibrium, V converges asymptotically toward a minimal value depending on the repulsion term. The first part $(\dot{\mathbf{x}}_i(t) - \dot{\hat{\mathbf{x}}}(t))^T M(\dot{\mathbf{x}}_i(t) - \dot{\hat{\mathbf{x}}}(t))$ leads the velocity of the agent to converge toward the desired velocity, the second one $(\mathbf{x}_i(t) - \hat{\mathbf{x}}(t))^T k_3^i(\mathbf{x}_i(t) - \hat{\mathbf{x}}(t))$ leads the agents to converge toward the desired position and the last one $k_2\sum_{j=1}^{N}\exp\left(-\frac{(\mathbf{x}_i(t) - \mathbf{x}_j(t))^T(\mathbf{x}_i(t) - \mathbf{x}_j(t))}{q}\right)$ leads at an equilibrium without collision between the agents. In the following, the time dependency (t) will be omitted for readability.

The time derivative of V is

$$\dot{V}(\mathbf{x}) = \sum_{i=1}^{N}\left[(\dot{\mathbf{x}}_i - \dot{\hat{\mathbf{x}}})^T M(\ddot{\mathbf{x}}_i - \ddot{\hat{\mathbf{x}}}) \quad + (\dot{\mathbf{x}}_i - \dot{\hat{\mathbf{x}}})^T k_3^i(\mathbf{x}_i - \hat{\mathbf{x}}) - k_2\sum_{j=1}^{N}\dot{\boldsymbol{\delta}}_{ij}^T\boldsymbol{\delta}_{ij}\frac{g_{ij}}{q}\right] \tag{5.7}$$

where the last term can be rewritten as:

$$\begin{aligned}\sum_{i=1}^{N}\sum_{j=1}^{N}\dot{\boldsymbol{\delta}}_{ij}^{T}\boldsymbol{\delta}_{ij}\frac{g_{ij}}{q} &= \sum_{i=1}^{N}\sum_{j=1}^{N}(\dot{\mathbf{x}}_i-\dot{\mathbf{x}}_j)^T(\mathbf{x}_i-\mathbf{x}_j)\frac{g_{ij}}{q}\\ &= \sum_{i=1}^{N}\sum_{j=1}^{N}(\dot{\mathbf{x}}_i)^T(\mathbf{x}_i-\mathbf{x}_j)\frac{g_{ij}}{q}-\sum_{i=1}^{N}\sum_{j=1}^{N}(\dot{\mathbf{x}}_j)^T(\mathbf{x}_i-\mathbf{x}_j)\frac{g_{ij}}{q}\\ &= \sum_{i=1}^{N}\sum_{j=1}^{N}(\dot{\mathbf{x}}_i)^T(\mathbf{x}_i-\mathbf{x}_j)\frac{g_{ij}}{q}+\sum_{i=1}^{N}\sum_{j=1}^{N}(\dot{\mathbf{x}}_i)^T(\mathbf{x}_i-\mathbf{x}_j)\frac{g_{ij}}{q}\\ &= 2\sum_{i=1}^{N}\sum_{j=1}^{N}(\dot{\mathbf{x}}_i)^T(\mathbf{x}_i-\mathbf{x}_j)\frac{g_{ij}}{q}\end{aligned} \tag{5.8}$$

From the previous equations, $\dot{V}$ can be expressed as

$$\begin{aligned}\dot{V} =&\sum_{i=1}^{N}\Bigg[(\dot{\mathbf{x}}_i-\dot{\widehat{\mathbf{x}}})^T(\mathbf{u}_i-C(\mathbf{x}_i,\dot{\mathbf{x}}_i)\dot{\mathbf{x}}_i-M\ddot{\widehat{\mathbf{x}}})+(\dot{\mathbf{x}}_i-\dot{\widehat{\mathbf{x}}})^Tk_3^i(\mathbf{x}_i-\widehat{\mathbf{x}})\\ &-2k_2\sum_{j=1}^{N}(\dot{\mathbf{x}}_i)^T(\mathbf{x}_i-\mathbf{x}_j)\frac{g_{ij}}{q}\Bigg]\end{aligned} \tag{5.9}$$

$$\begin{aligned}\dot{V} =&\sum_{i=1}^{N}\Bigg[(\dot{\mathbf{x}}_i)^T\left(\mathbf{u}_i-C(\mathbf{x}_i,\dot{\mathbf{x}}_i)\dot{\mathbf{x}}_i-M\ddot{\widehat{\mathbf{x}}}+k_3^i(\mathbf{x}_i-\widehat{\mathbf{x}})-2k_2\sum_{j=1}^{N}(\mathbf{x}_i-\mathbf{x}_j)\frac{g_{ij}}{q}\right)\\ &-(\dot{\widehat{\mathbf{x}}})^T(u_i-C(\mathbf{x}_i,\dot{\mathbf{x}}_i)\dot{\mathbf{x}}_i-M\ddot{\widehat{\mathbf{x}}}+k_3^i(\mathbf{x}_i-\widehat{\mathbf{x}}))\Bigg]\end{aligned} \tag{5.10}$$

Using the expression of $\mathbf{u}_i$ given in (5.4), (5.10) becomes:

$$\dot{V} \;=\; \sum_{i=1}^{N}\left[(\dot{\mathbf{x}}_i)^T(-k_1\dot{\mathbf{x}}_i+k_1\dot{\widehat{\mathbf{x}}})-(\dot{\widehat{\mathbf{x}}})^T2k_2\sum_{j=1}^{N}(\mathbf{x}_i-\mathbf{x}_j)\frac{g_{ij}}{q}-k_1\dot{\mathbf{x}}_i+k_1\dot{\widehat{\mathbf{x}}}\right] \tag{5.11}$$

The last term of (5.11) can be rewritten as

$$\begin{aligned}\dot{V} = & \sum_{i=1}^{N}\left[-k_1\dot{\mathbf{x}}_i^T\dot{\mathbf{x}}_i + k_1(\dot{\mathbf{x}}_i)^T\dot{\widehat{\mathbf{x}}} + k_1(\dot{\widehat{\mathbf{x}}})^T\dot{\mathbf{x}}_i - k_1(\dot{\widehat{\mathbf{x}}})^T\dot{\widehat{\mathbf{x}}}\right] \\ & -2k_2\sum_{i=1}^{N}\sum_{j=1}^{N}(\dot{\widehat{\mathbf{x}}})^T\mathbf{x}_i\frac{2g_{ij}}{q} + 2k_2\sum_{i=1}^{N}\sum_{j=1}^{N}(\dot{\widehat{\mathbf{x}}})^T\mathbf{x}_j\frac{2g_{ij}}{q} \qquad (5.12) \\ = & \sum_{i=1}^{N}\left[-k_1\dot{\mathbf{x}}_i^T\dot{\mathbf{x}}_i + 2k_1(\dot{\mathbf{x}}_i)^T\dot{\widehat{\mathbf{x}}} - k_1(\dot{\widehat{\mathbf{x}}})^T\dot{\widehat{\mathbf{x}}}\right]\end{aligned}$$

The final expression of $\dot{V}$ is

$$\dot{V} = -\sum_{i=1}^{N}\left[k_1(\dot{\mathbf{x}}_i - \dot{\widehat{\mathbf{x}}})^T(\dot{\mathbf{x}}_i - \dot{\widehat{\mathbf{x}}})\right] \leq 0 \qquad (5.13)$$

The derivative $\dot{V}$ is negative semi-definite for the designed control law, V is thus a Lyapunov function. Thus, this guarantees that the states of the agents converge locally to equilibrium. Since $(\dot{\mathbf{x}}_i - \dot{\widehat{\mathbf{x}}})$ is bounded, applying the Barbalat lemma as in (Cheah et al., 2009) guarantees the asymptotical global stability. This means that the speed of each platform will match the reference speed $\dot{\widehat{\mathbf{x}}}$, and all the vehicles will move closer to $\widehat{\mathbf{x}}$. This leads to an equilibrium in the formation as the attraction term and the repulsion term compensate each other.

5.1.4 Experiment with a robotic platform

To illustrate the results obtained on a real system, an experiment has been performed on Lego Mindstorms NTX robotic platform. This experiment aims at highlighting the effectiveness of the proposed estimation and gradient climbing formation control on a small basic platform. The robot is built as a two motorised wheels differential vehicle and its computational abilities are low as it only embeds an ARM7 processor. Figure 5.1 shows the robot (identified as "Markov") and its kinematic representation. The low-layer control law proposed in (5.4) cannot be directly used for this non-holonomic robot. Only the decentralised estimation and the high-layer gradient climbing strategy have been tested.

For the i-th robot, practical control of linear and angular velocities via the

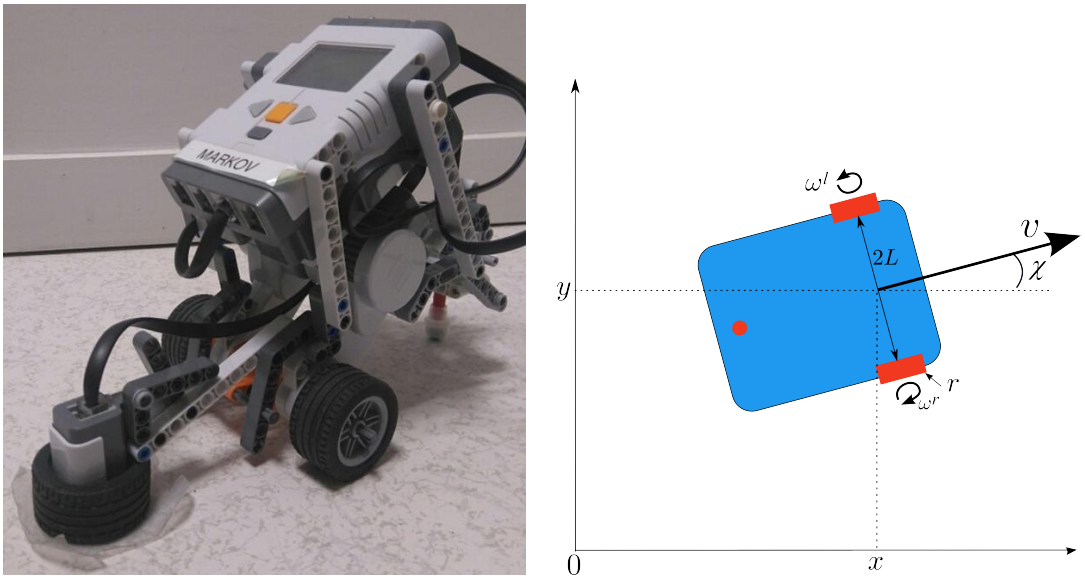

Markov robot Kinematic model of the robot

Figure 5.1: Robotic platform and kinematic representation

controllable rotation speeds of the wheels ω_i^l and ω_i^r is achieved by

$$\begin{cases} v_i = \frac{(\omega_i^l + \omega_i^r)}{2} r \\ u_i^\omega = \frac{(\omega_i^r - \omega_i^l)}{2L} r \end{cases} \tag{5.14}$$

where r is the wheel radius and L the half-axis length. The velocity v_i is set to a constant value for simplicity, the only control input is thus $\mathbf{u}_i = u_i^\omega$, which is constrained between $\pm\Delta\omega_{max}$.

The state of the agent is $\underline{\mathbf{x}}_i^T(t_k) = [x_{1,i}(t_k), x_{2,i}(t_k), \tau_i(t_k)]$ and its discrete time dynamical model is

$$\begin{cases} x_{1,i}(t_{k+1}) = x_{1,i}(t_k) + T v_i(t_k) \cos(\tau_i(t_k)) \\ x_{2,i}(t_{k+1}) = x_{2,i}(t_k) + T v_i(t_k) \sin(\tau_i(t_k)) \\ \tau_i(t_{k+1}) = \tau_i(t_k) + T u_i^\omega(t_k) \end{cases} \tag{5.15}$$

where T is the sampling time step.

Localization of the robot is provided by odometry using this model (embedded

wheel sensors have an accuracy of 1 degree). Since the test missions are limited in duration, this localization method was deemed sufficient for estimating the position of the robots in spite of the error accumulated by odometry.

An uni-modal field presented in Figure 5.2 is used for the simulation. The grey level field is printed on a 2×2m surface and the agents move on it. The grey level field is defined such that its maximum value is taken by the darkest area. A single maximum can be found in the field, which thus respects the conditions for convergence by gradient climbing.

A fleet of $N = 3$ agents is considered. Each agent is equipped with a sensor that measures the field ϕ in front of it. The measurements of all agents of the fleet are shared with the other agents to perform cooperative estimation as presented in Section 4.2. The communication is performed via Bluetooth. The agents are positioned at the lower left angle of the map in the lighter part at the beginning of the experiment. The goal is to move the fleet to the position of the maximum of ϕ.

The cooperative estimation is performed autonomously by each agent (embedded NXC code) and the direction of the estimated gradient is used to give the direction of the movement. Figure 5.3 shows the estimated gradient along the trajectory of one of the robots.

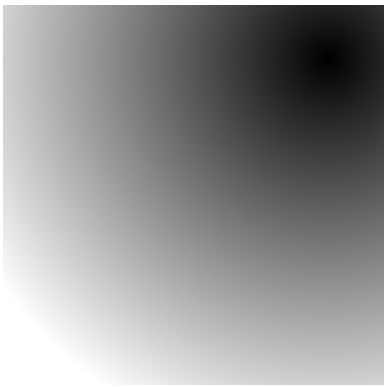

Figure 5.2: Spatial field ϕ represented by grey level

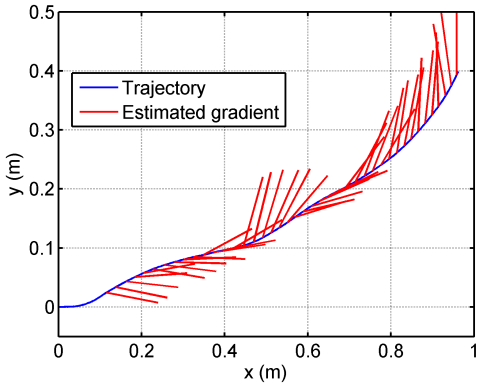

Figure 5.3: Trajectory and gradient direction estimate

The trajectories and the sensor measurements of the fleet are presented on Figure 5.5. The x_1-axis and x_2-axis represent the space coordinates while the

x_3-axis represents the grey level measured by the sensors at each position. One can notice that the agents reach the position of the maximum on the right upper corner of the map. Figure 5.4 shows the fleet of agents performing the mission. This experimentation shows a mission fulfilled using cooperative estimation for gradient climbing.

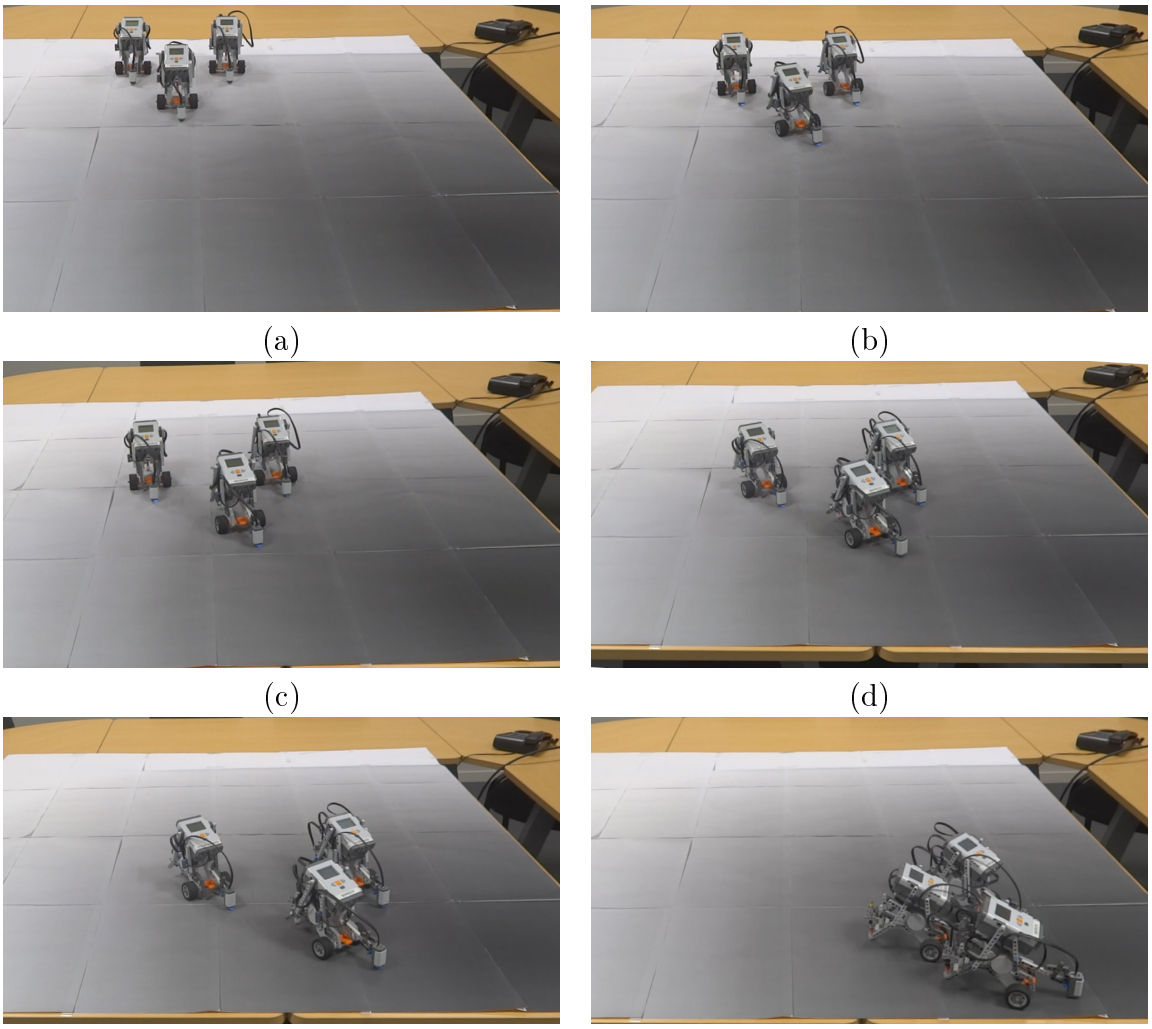

(a) (b) (c) (d) (e) (f)

Figure 5.4: Illustration of the gradient climbing mission with 3 robots

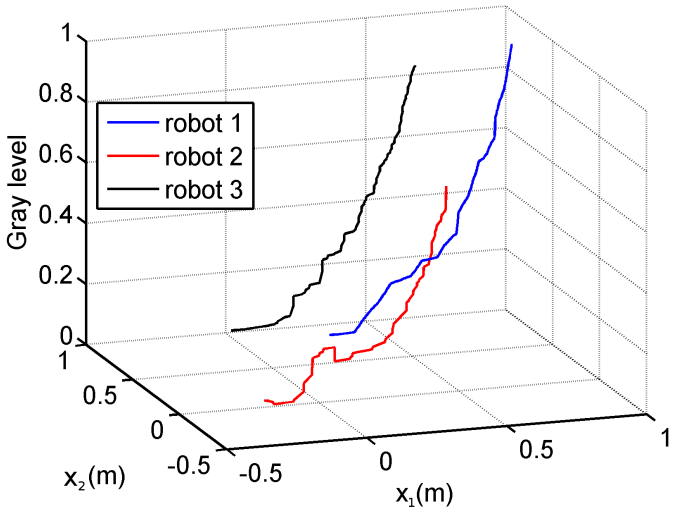

Figure 5.5: Fleet trajectories and measurements

5.2 Fleet reconfiguration with a faulty-sensor

The sensor placement analysis in Section 4.3 shows that the optimal agent locations when the collision avoidance constraint does not allow them to fit on a circle is a compact formation the closest possible to the position of estimation. All the agents try to reach the position of estimation while doing a trade-off with the security distance between agents to avoid collision.

5.2.1 Control law modification

To perform the agent placement in presence of an agent equipped with a faulty sensor, the control law proposed in Section 5.1.2 is adapted.

As indicated in Section 4.3, agents with faulty sensors should be driven farther away from $\widehat{\mathbf{x}}_i(t)$ than agents with healthy sensors. Such a behaviour is obtained by modifying the value of gain $k_3^i\left(\eta_i(t_k)\right)$ in (5.4). Assume that an agent undergoing faulty state cannot recover (e.g. $p_{10} = 0$), the gain $k_3^i\left(\eta_i(t_k)\right)$ can only be modified once by agents. The number of agents is constant, so a finite number of modifications of gains is possible. These modifications do not affect the stability analysis

of the MAS using the Lyapunov approach as long as the gains remain positive.

To analyse the effect of a change of $k_3^i(\eta_i(t_k))$ on the position of agent i relative to the position of $\widehat{\mathbf{x}}$, consider first the fleet at equilibrium, with all sensors in healthy state. At equilibrium, (3.1), combined with (5.4) make each command $\mathbf{u}_i$ asymptotically equal to 0 for the i-th agent

$$\mathbf{u}_i = \sum_{i=1}^{N} \left[-k_3^i(\eta_i(t_k))(\mathbf{x}_i - \widehat{\mathbf{x}}) + 2k_2 \sum_{j \neq i} (\mathbf{x}_i - \mathbf{x}_j) \frac{g_{ij}}{q} \right] = 0 \tag{5.16}$$

$$\sum_{i=1}^{N} \left[-k_3^i(\eta_i(t_k))\mathbf{x}_i + k_3^i(\eta_i(t_k))\widehat{\mathbf{x}} + \sum_{j \neq i} 2k_2 \frac{g_{ij}}{q} \mathbf{x}_i - \sum_{j \neq i} 2k_2 \frac{g_{ij}}{q} \mathbf{x}_j \right] = 0 \tag{5.17}$$

$$\sum_{i=1}^{N} \left[\mathbf{x}_i \left(-k_3^i(\eta_i(t_k)) + \sum_{j \neq i} 2k_2 \frac{g_{ij}}{q} \right) + k_3^i(\eta_i(t_k))\widehat{\mathbf{x}} - \sum_{j \neq i} 2k_2 \frac{g_{ij}}{q} \mathbf{x}_j \right] = 0 \tag{5.18}$$

$$\sum_{i=1}^{N} \left[\mathbf{x}_i \left(-k_3^i(\eta_i(t_k)) + \sum_{j \neq i} 2k_2 \frac{g_{ij}}{q} \right) + k_3^i(\eta_i(t_k))\widehat{\mathbf{x}} \right] = \sum_{i=1}^{N} \left[\sum_{j \neq i} 2k_2 \frac{g_{ij}}{q} \mathbf{x}_j \right] \tag{5.19}$$

$$\begin{aligned} &\sum_{i=1}^{N} \left[\mathbf{x}_i \left(-k_3^i(\eta_i(t_k)) + \sum_{j \neq i} 2k_2 \frac{g_{ij}}{q} \right) + \widehat{\mathbf{x}} \left(k_3^i(\eta_i(t_k)) - \sum_{j \neq i} 2k_2 \frac{g_{ij}}{q} \right) \right] \\ &= \sum_{i=1}^{N} \left[\sum_{j \neq i} 2k_2 \frac{g_{ij}}{q} (\mathbf{x}_j - \widehat{\mathbf{x}}) \right] \end{aligned} \tag{5.20}$$

$$= \sum_{i=1}^{N} \left[(\mathbf{x}_i - \widehat{\mathbf{x}}) \left(-k_3^i(\eta_i(t_k)) + \sum_{j \neq i} 2k_2 \frac{g_{ij}}{q} \right) \right] = \sum_{i=1}^{N} \left[\sum_{j \neq i} 2k_2 \frac{g_{ij}}{q} (\mathbf{x}_j - \widehat{\mathbf{x}}) \right] \tag{5.21}$$

One may get

$$\sum_{i=1}^{N}[\mathbf{x}_i - \widehat{\mathbf{x}}] = \sum_{i=1}^{N}\left[\frac{2k_2}{2k_2\sum_{j\neq i}\frac{g_{ij}}{q} - k_3^i(\eta_i)}\sum_{j\neq i}(\mathbf{x}_j - \widehat{\mathbf{x}})\frac{g_{ij}}{q}\right]. \tag{5.22}$$

Now, assume that at a given time instant, the i-th sensor becomes defective and has been identified as such. Assuming that the positions of the other agents are not significantly affected by the modification of η_i, $\sum_{j\neq i}(\mathbf{x}_j - \widehat{\mathbf{x}})\frac{g_{ij}}{q}$ is approximately constant. To drive the i-th sensor away from $\widehat{\mathbf{x}}_i$, one has to ensure that the absolute value of

$$\gamma^i(\eta_i) = \sum_{i=1}^{N}\frac{2k_2}{2k_2\sum_{j\neq i}\frac{g_{ij}}{q} - k_3^i(\eta_i)} \tag{5.23}$$

when $\eta_i = 1$ is larger than its absolute value when $\eta_i = 0$. This is performed by appropriately modifying the value of $k_3^i(\eta_i)$. By taking a value of $k_3^i(\eta_i = 0) > k_3^i(\eta_i = 1)$, the agents with defective sensors will be placed farther of the position of estimation than agents with normal sensors.

5.3 Simulations of the proposed methods

To illustrate the results obtained in this chapter and in the previous one, simulations on `Matlab` have been performed. The experiment of the previous section on robotic platformS has shown the validity of the high layer approach on a real system. The simulations are performed to highlight the two-layer control law and the reconfiguration scheme.

Figure 5.6 illustrates the reconfiguration scheme. The experimental field is a two dimensional uni-modal Gaussian function centred in [10 35] with covariance $10^3\mathbf{I}_2$ with $\mathbf{I}_2$ the identity matrix of dimension 2. The agents are initialised randomly in the area.

Agents with defective sensors are represented by red dots while agents with healthy sensors are represented with green dots. At time t_1 the formation reaches an equilibrium around the target position indicated by the black star. At t_2 an agent in the center of the formation, near the estimation position is detected to have a defective sensor. The control gain k_3 of this agent is then modified. Times t_3 and t_4 show the movement of the faulty agent to reach the boundary of the

formation.

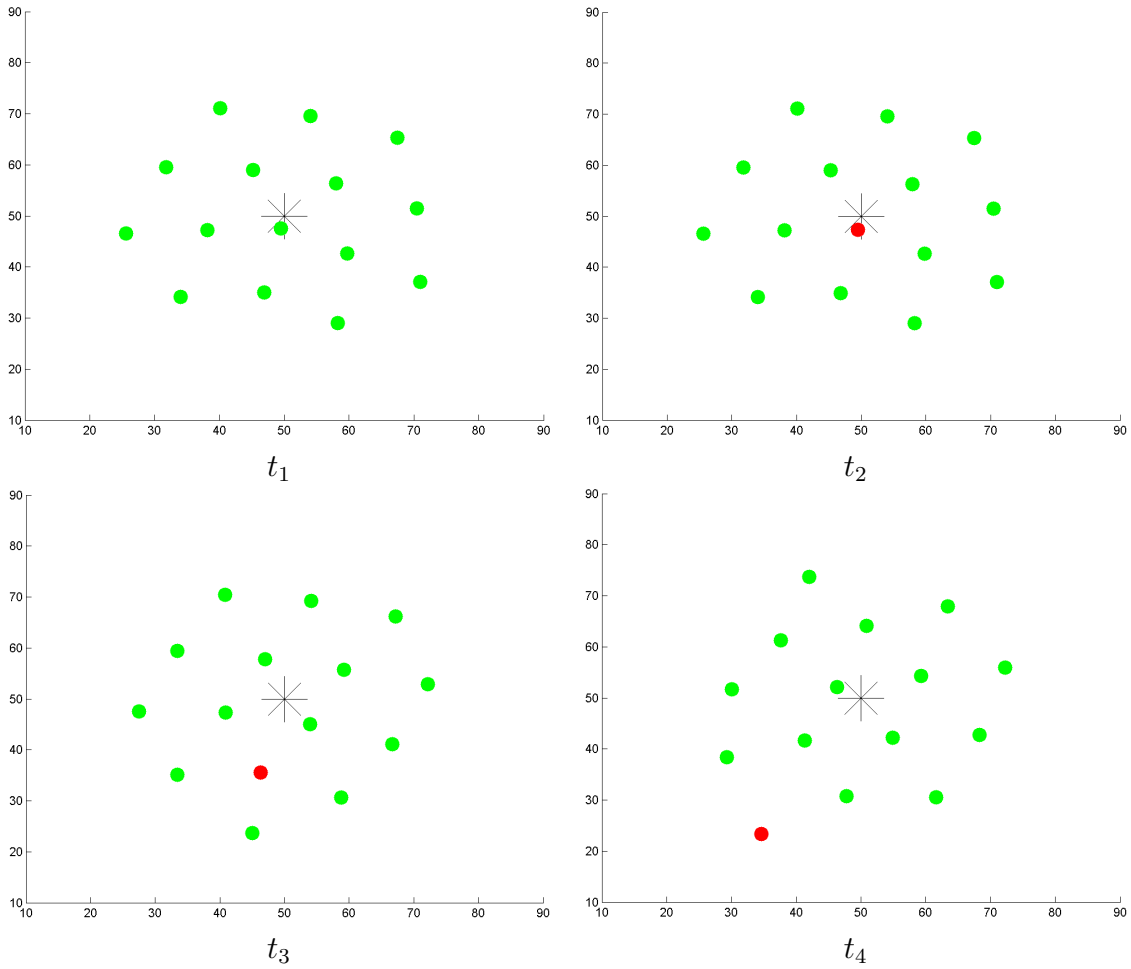

Figure 5.6: Illustration of the reconfiguration technique

Under the assumption of complete communication graph, all the agents share the same information. The estimate $\widehat{\boldsymbol{\alpha}}_i^k$ and position $\widehat{\mathbf{x}}_i^k$ are the same for all agents of the fleet.

Simulation of the control law with reconfiguration

A full simulation has been performed with gradient estimation, fault detection identification and reconfiguration. The parameters are those of Section 5.2.1, except for k_3, which is now a function $k_3(\eta_i)$of the sensor state. $k_3(0) = 1600$ for an

agent with normal sensor and $k_3(1) = 10$ for an agent with defective sensor. Each agent has a probability $p_{01} = 0.005$ to turn defective at each time step.

A fleet of $N = 15$ agents is initialised around position $\widehat{\mathbf{x}}_i^0 = [40,\ 7]$. Figure 5.7 shows at t_1 the fleet near the starting position in formation. Green dots represent agents with normal sensors while black dots represent agents with defective sensors. At time t_2, the fleet progresses toward the maximum of the field when a defective agent is detected. The reconfiguration scheme is used to adapt the gain k_3 for the defective agent. At time t_3 the agents continue the mission despite the faulty agent. The fleet carry on toward the maximum while the defective agent starts to move inside the fleet to reach the boundary of the formation. At time t_4, the fleet gathers around the position of the field maximum. The faulty agent has moved to the border of the fleet by the reconfiguration scheme to limit its influence.

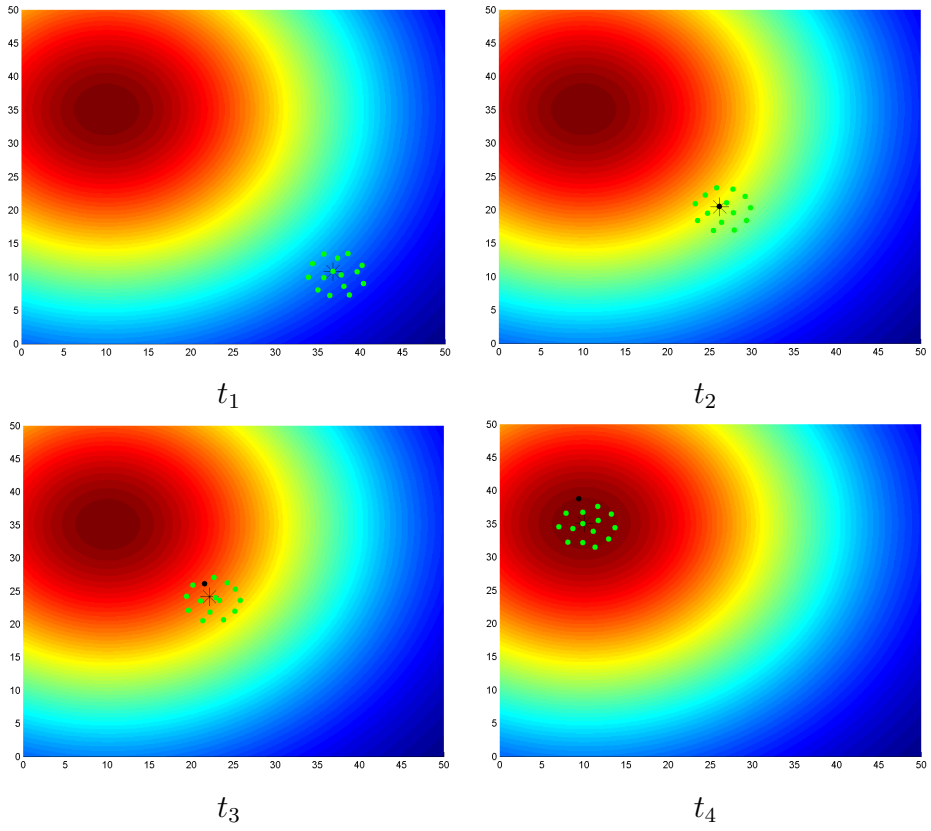

Figure 5.7: Illustration of gradient climbing with FDI and formation reconfiguration

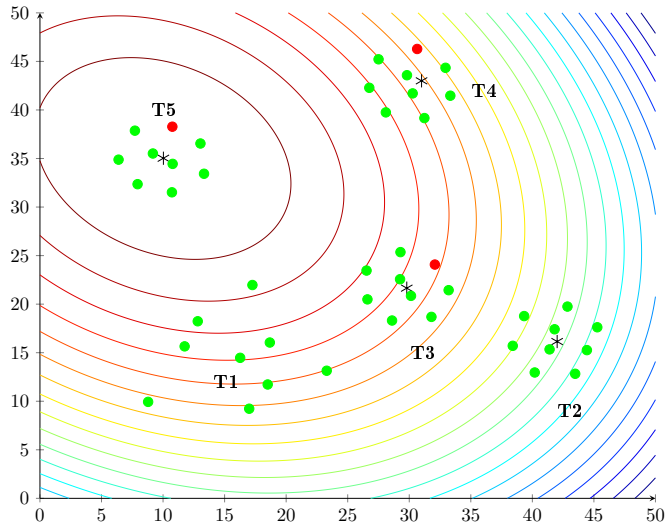

Figure 5.8: Illustration of gradient climbing with a faulty agent

Figure 5.8 shows a gradient climbing with a faulty agent and a reconfiguration action. At $T1$ the agents are initialised. At $T2$ the agents are gathered around the position of estimation. At $T3$ an agent becomes faulty. At $T4$ the fleet is lead toward a wrong direction by the faulty agent because the reconfiguration scheme was not applied. At time $T5$, the reconfiguration scheme has been successful and the fleet reached the maximum of the field.

5.4 Conclusion of Part II

5.4.1 Proposed solution

The first part of our work presents a local approach to search for the maximum of a field with a fleet of autonomous agents. The proposed solution relies on a cooperative estimation by the fleet of the gradient of the field. This estimation is carried out using a weighted least-square estimation considering measurements and positions of the agents at one single time step. The computations required can be effortlessly performed as demonstrated by the experimentation on low computational power platforms such as the LEGO Mindstorms.

An analysis of the sensor placement for the estimation with three different

criteria leads to the definition of optimal locations. A control law is then defined to move the agents to such positions while avoiding collision. Stability of the guidance law has been demonstrated using Lyapunov theory.

The measurements of the agents are used to drive the fleet toward the maximum of the unknown field. A defective sensor sending abnormal measurements to the whole fleet can lead the agents to move toward a wrong direction and never fulfil the mission. A fault detection and identification scheme is used to detect outliers in the measurements and isolate the defective agents.

The designed control law takes into account the faulty sensor and performs a reconfiguration of the agent position inside the fleet. Several simulations and experiment have been presented to illustrate the effectiveness of the proposed approach.

5.4.2 Limitations of the local approach and perspectives

Several limitations of the proposed approach have to be taken into account. The reliability of a gradient estimation from noisy measurement is dependent on the model chosen (modelling error) and the amount of the noise (measurement error). The least-square estimation is sensitive to the level of the disturbances of the measurements. The proposed approach is suited for situations with prior knowledge on the noise of the system.

The agents have to stay gathered in a formation (circular or compact) to perform the estimation of the gradient as shown in Section 4.3. This may lead to a loss of efficiency of the use of a MAS. The agents cannot divide the exploration task between them to achieve it in parallel. Moreover, the local estimation of the gradient can lead the fleet to a dead-end when it reaches an area where the field remains constant (i.e. with null gradient).

The last limitation of the local approach concerns the application field. The local approach will stop at the first maximum encounter. Only uni-modal fields are thus good candidates for using the local approach to the global maximum.

The next part of this thesis is devoted to methods to overcome these limitations.

Summary

In this chapter, the contributions have been:

- Design of a novel double layer control law to:
  - Bring the agents in the desired formation.
  - Lead the formation to the maximum of the field by gradient climbing.
  - Reconfigure the formation shape in case of a fault on an agent sensor.
- Proof of stabitity of the proposed control law using Lyapunov theory

The next chapter will introduce the second part of this thesis and try to overcome the issues of the local approach by proposing a global search strategy.

The control law proposed in this chapter has been presented in (Kahn et al., 2015a), and the experiment has been presented in (Marzat et al., 2014)

Part III

Global approach

Chapter 6

Global maximisation of an unknown field with MAS using Kriging

Chapter goals

In this chapter, in order to overcome the issues of local search, a global model of the field is sought for. The characteristics of the global model are obtained using Gaussian process regression, or Kriging. Kriging has been proved to be the best unbiased linear estimator derived from a finite set of measurements and considering the covariance of the modelled field. Two aspects of the global model are addressed:

- Definition and construction of the Kriging model.
- Use of the Kriging model for optimisation.

The previous control law is adapted to the global search and simulations are performed to illustrate the proposed approach. A comparison with a state-of-the-art method is presented.

In the first part of the thesis, we introduced a maximum seeking scheme based on a local model of an unknown field and its gradient. The agents of a MAS have to gather near the same position to perform a local estimation of the gradient of

the field. The MAS is driven to a maximum following the gradient direction and stops at the first maximum encountered. The local approach has some issues that should be fixed with a global search.

Compared to the local search that uses limited spatial information of the field to perform the optimisation, the global search uses information from the entire field. We propose to use a Kriging model of the field updated using the collected measurements. As the model provides a mean value and covariance of the estimated field, it is possible to use this information to select future sampling points in order to drive the MAS towards the global maximum.

The method consists in :

- Updating the Kriging model of the field using the measurements provided by the agents.
- Deriving from the updated model potential locations of the field maximum.
- Sending the MAS to explore these locations while avoiding unnecessary measurements.
- Collecting the new measurements obtained.

The associated control law aims at:

- Leading the agents to their desired position to perform a measurement
- Avoiding collisions

6.1 Elements of Kriging

Kriging (or Gaussian process regression) is an interpolation method used to design a model of a field from punctual samples and assumptions on the covariance function (Sasena, 2002, Schonlau, 1997). The unknown function is approximated by a Gaussian process. Kriging provides the best unbiased linear estimate of a function between the sampling positions.

Consider the field f:

$$f : \mathbf{p} \in D \subset \mathbb{R}^2 \rightarrow f(\mathbf{p}) \in \mathbb{R} \tag{6.1}$$

f is modelled by Y:

$$Y(\mathbf{p}) = \mathbf{r}(\mathbf{p})^T \boldsymbol{\beta} + Z(\mathbf{p}) \tag{6.2}$$

where $\mathbf{r}$ is a regression vector, $\boldsymbol{\beta}$ a parameter vector and Z a Gaussian process with zero mean and covariance function C.

$$C(Z(\mathbf{p}_1), Z(\mathbf{p}_2)) = \sigma_z^2 \xi(\mathbf{p}_1, \mathbf{p}_2) \tag{6.3}$$

where ξ is some correlation function, σ_z^2 is the nominal variance of the Gaussian process, $\mathbf{p}_1$ and $\mathbf{p}_2$ are two positions. ξ is usually selected (Schonlau, 1997) under the form

$$\xi(\mathbf{p}_1, \mathbf{p}_2) = \exp\left[-\frac{||\mathbf{p}_1 - \mathbf{p}_2||^2}{\theta^2}\right] \tag{6.4}$$

θ is a parameter reflecting the range of the spatial covariance of the Gaussian process. The nominal variance of the Gaussian process and the covariance function form are known a priori or estimated from the sampled data. Considering n sampling points $[\mathbf{p}_1, ..., \mathbf{p}_n]$, one can write

$$\mathbf{Y} = \begin{bmatrix} Y(\mathbf{p}_1) \\ ... \\ Y(\mathbf{p}_n) \end{bmatrix} = \underbrace{\begin{bmatrix} \mathbf{r}^T(\mathbf{p}_1) \\ ... \\ \mathbf{r}^T(\mathbf{p}_n) \end{bmatrix}}_{\mathbf{R}} \boldsymbol{\beta} + \underbrace{\begin{bmatrix} Z(\mathbf{p}_1) \\ ... \\ Z(\mathbf{p}_n) \end{bmatrix}}_{\mathbf{Z}} \tag{6.5}$$

$$\mathbf{k}_p = [\xi(\mathbf{p}, \mathbf{p}_1), ..., \xi(\mathbf{p}, \mathbf{p}_n)]^T; \quad \mathbf{K}_{ij} = \xi(\mathbf{p}_i, \mathbf{p}_j) \tag{6.6}$$

A linear estimator of f is $\hat{Y}(\mathbf{p}) = \mathbf{a}_p^T \mathbf{Y}$. The bias of this estimator is

$$E[Y(\mathbf{p}) - \mathbf{a}_p^T \mathbf{Y}] = E[Y(\mathbf{p})] - E[\mathbf{a}_p^T \mathbf{Y}] = \mathbf{r}(\mathbf{p})^T \boldsymbol{\beta} - \mathbf{a}_p^T \mathbf{R} \boldsymbol{\beta} \tag{6.7}$$

And its variance is:

$$\begin{aligned} E[(Y(\mathbf{p}) - \mathbf{a}_p^T \mathbf{Y})^2] &= E[Y(\mathbf{p})^2 - 2\mathbf{a}_p^T \mathbf{Y} Y(\mathbf{p}) + \mathbf{a}_p^T \mathbf{Y}\mathbf{Y}^T \mathbf{a}_p] \\ &= E[(\mathbf{r}(\mathbf{p})^T \boldsymbol{\beta} + Z(\mathbf{p}))^2 \\ &\quad - 2\mathbf{a}_p^T (\mathbf{R}\boldsymbol{\beta} + \mathbf{Z})(\mathbf{r}(\mathbf{p})^T \boldsymbol{\beta} + Z(\mathbf{p})) \\ &\quad + \mathbf{a}_p^T (\mathbf{R}\boldsymbol{\beta} + \mathbf{Z})(\mathbf{R}\boldsymbol{\beta} + \mathbf{Z})^T \mathbf{a}_p] \\ &= (\mathbf{a}_p \mathbf{R}\boldsymbol{\beta} - \mathbf{r}(\mathbf{p})^T \boldsymbol{\beta}) + \mathbf{a}_p^T \sigma_z^2 \mathbf{K} \mathbf{a}_p + \sigma_z^2 - 2\mathbf{a}_p^T \sigma_z^2 \mathbf{k}_p \end{aligned} \tag{6.8}$$

A zero bias is desired for the estimator. This imposes

$$(a_p\mathbf{R} - \mathbf{r}(\mathbf{p})^T)\boldsymbol{\beta} = 0 \tag{6.9}$$

The minimal variance is found using a Lagrange multiplicator $\boldsymbol{\lambda}$, as

$$\mathcal{L}(\mathbf{a}_p, \boldsymbol{\lambda}) = \mathbf{a}_p\sigma_z^2\mathbf{K}\mathbf{a}_p^T + \sigma_z^2 - 2\mathbf{a}_p\sigma_z^2\mathbf{k}_p - 2\boldsymbol{\lambda}(\mathbf{r}(\mathbf{p})^T - \mathbf{a}_p^T\mathbf{R}) \tag{6.10}$$

$$\frac{\partial\mathcal{L}(\mathbf{a}_p, \boldsymbol{\lambda})}{\partial\mathbf{a}_p} = \sigma_z^2\mathbf{K}\mathbf{a}_p - \sigma_z^2\mathbf{k}_p - \boldsymbol{\lambda}\mathbf{R}^T \tag{6.11}$$

The optimal values of $\mathbf{a}_p$ and $\boldsymbol{\lambda}$ are the solution of the system of equations

$$\left\{\begin{array}{rcl} \sigma_z^2\mathbf{K}\mathbf{a}_p - \boldsymbol{\lambda}\mathbf{R}^T &=& \sigma_z^2\mathbf{k}_p \\ \mathbf{R}\mathbf{a}_p &=& \mathbf{r}(\mathbf{p}) \end{array}\right. \tag{6.12}$$

$$\begin{pmatrix} -\boldsymbol{\lambda}\frac{1}{\sigma_z^2} \\ \mathbf{a}_p \end{pmatrix} = \begin{pmatrix} 0 & \mathbf{R}^T \\ \mathbf{R} & \mathbf{K} \end{pmatrix}^{-1} \begin{pmatrix} \mathbf{r}(\mathbf{p}) \\ \mathbf{k}_p \end{pmatrix} \tag{6.13}$$

$$\begin{aligned} \hat{Y}(\mathbf{p}) &= \mathbf{a}_p^T\mathbf{Y} \\ &= \begin{pmatrix} \mathbf{r}(\mathbf{p})^T & \mathbf{k}_p^T \end{pmatrix} \begin{pmatrix} 0 & \mathbf{R}^T \\ \mathbf{R} & \mathbf{K} \end{pmatrix}^{-1} \begin{pmatrix} 0 \\ \mathbf{Y} \end{pmatrix} \end{aligned} \tag{6.14}$$

The Schur complement formula gives:

$$\begin{aligned} \begin{pmatrix} 0 & \mathbf{R}^T \\ \mathbf{R} & \mathbf{K} \end{pmatrix}^{-1} &= \begin{pmatrix} \mathbf{I} & 0 \\ -\mathbf{K}^{-1}\mathbf{R} & \mathbf{I} \end{pmatrix} \begin{pmatrix} (-\mathbf{R}^T\mathbf{K}\mathbf{R})^{-1} & 0 \\ 0 & \mathbf{K}^{-1} \end{pmatrix} \begin{pmatrix} \mathbf{I} & -\mathbf{R}^T\mathbf{K}^{-1} \\ 0 & \mathbf{I} \end{pmatrix} \\ &= \begin{pmatrix} (\mathbf{R}^T\mathbf{K}\mathbf{R})^{-1} & (\mathbf{R}^T\mathbf{K}\mathbf{R})^{-1}\mathbf{R}^T\mathbf{K}^{-1} \\ \mathbf{K}^{-1}\mathbf{R}^T(\mathbf{R}^T\mathbf{K}\mathbf{R})^{-1} & -\mathbf{K}^{-1}\mathbf{R}(\mathbf{R}^T\mathbf{K}\mathbf{R})^{-1}\mathbf{R}^T\mathbf{K}^{-1} + \mathbf{K}^{-1} \end{pmatrix} \end{aligned} \tag{6.15}$$

The least square estimate of $\boldsymbol{\beta}$ is considered: $\widehat{\boldsymbol{\beta}} = (\mathbf{R}^T\mathbf{K}\mathbf{R})^{-1}\mathbf{R}^T\mathbf{K}^{-1}\mathbf{Y}$

$$\begin{aligned} \widehat{Y}(\mathbf{p}) &= \begin{pmatrix} \mathbf{r}(\mathbf{p})^T & \mathbf{k}_p^T \end{pmatrix} \begin{pmatrix} (\mathbf{R}^T\mathbf{K}\mathbf{R})^{-1}\mathbf{R}^T\mathbf{K}^{-1}\mathbf{Y} \\ -\mathbf{K}^{-1}\mathbf{R}(\mathbf{R}^T\mathbf{K}\mathbf{R})^{-1}\mathbf{R}^T\mathbf{K}^{-1}\mathbf{Y} + \mathbf{K}^{-1}\mathbf{Y} \end{pmatrix} \\ &= \begin{pmatrix} \mathbf{r}(\mathbf{p})^T & \mathbf{k}_p^T \end{pmatrix} \begin{pmatrix} \widehat{\boldsymbol{\beta}} \\ -\mathbf{K}^{-1}\mathbf{R}\widehat{\boldsymbol{\beta}} + \mathbf{K}^{-1}\mathbf{Y} \end{pmatrix} \end{aligned} \tag{6.16}$$

$$\widehat{Y}(\mathbf{p}) = \mathbf{r}(\mathbf{p})^T\widehat{\boldsymbol{\beta}} + \mathbf{k}_p^T\mathbf{K}^{-1}(\mathbf{Y} - \mathbf{R}\widehat{\boldsymbol{\beta}}) \tag{6.17}$$

The mean of the Kriging estimator is given by (6.17) if we consider $\boldsymbol{\beta}$ instead of its estimate:

$$\mu(\mathbf{p}) = \mathbf{r}(\mathbf{p})^T\boldsymbol{\beta} + \mathbf{k}_p^T\mathbf{K}^{-1}(\mathbf{Y} - \mathbf{R}\boldsymbol{\beta}) \tag{6.18}$$

The variance of the prediction error then has the form

$$\sigma^2(\mathbf{p}) = E[(\hat{Y}(\mathbf{p}) - \mathbf{a}_p\mathbf{Y})^2] = \sigma_z^2(1 - \mathbf{k}_p^T\mathbf{K}^{-1}\mathbf{k}_p)) \tag{6.19}$$

where σ_z^2 is the variance of the field.

In the case of noisy measurements presented in equation (3.4), the variance of the Gaussian measurement noise can be taken into account in the Kriging model (Picheny et al., 2013) as a modification of the correlation matrix $\mathbf{K}$:

$$\tilde{\mathbf{K}} = \mathbf{K} + \sigma_0^2\mathbf{I}_n \tag{6.20}$$

with $\tilde{\mathbf{K}}$ the new covariance matrix used to compute the variance of the Kriging model, σ_0^2 the variance of the measurements for healthy sensors and $\mathbf{I}_n$ an identity matrix of size n.

At every point $\mathbf{x}$, a model of the function f can be computed. The mean value of the Kriging model of $f(\mathbf{x})$ is $\mu(\mathbf{x})$ and the variance at $\mathbf{x}$ is $\sigma^2(\mathbf{x})$.

Figure 6.1 illustrates the evolution of the Kriging model with a new sampling point. The real 1-D function $y(x) = \cos(x) + \cos(0.7x)$ is plotted in blue and the mean of the model in red. The black dashed line represents the confidence area of one standard deviation, where the true function is supposed to be with a probability of 0.68. The parameters are $\theta = 5$ and $\sigma_z = 2$. In Figure 6.1 (a), the confidence area is larger for $\mathbf{x} \in [2, 6]$. The mean of the model is also quite far from the real function. Figure 6.1 (b) has an extra sampling point at $\mathbf{x} = 4$ compared to Figure 6.1 (a). The confidence region shrinks around the new sampling point and the mean of the model is getting closer to the real function.

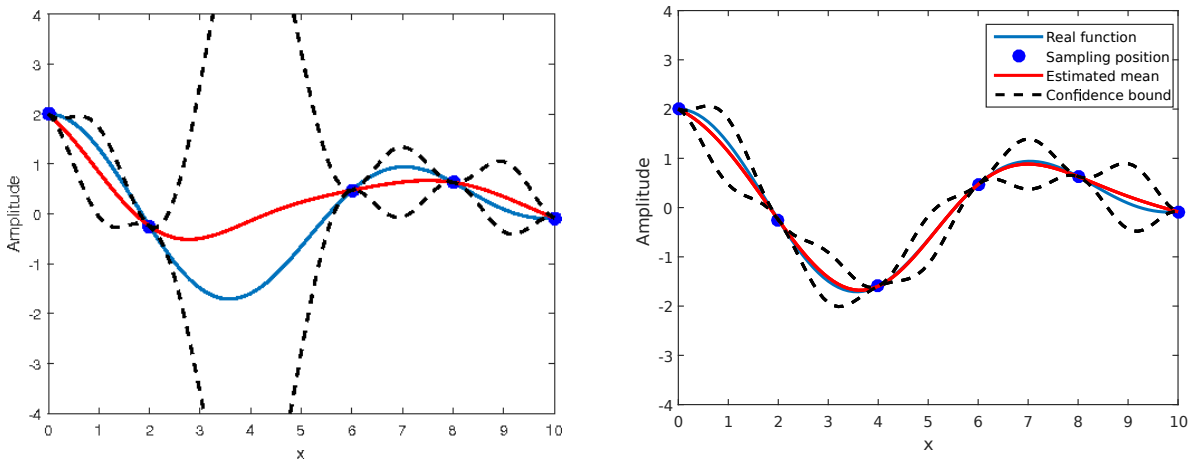

(a) 5 sampling points (b) 6 sampling points

Figure 6.1: Kriging illustration

6.2 Kriging model construction

The Kriging model of the field is updated from the data collected by the agents. The set of positions and measurements $S_i(t_k)$ presented in Section 3.2 represents the data available for agent i at time t_k to compute the Kriging model. The estimated field $\widehat{\phi}_{i,k}$ is obtained as the mean of the Kriging model obtained from $S_i(t_k)$.

$$S_i(t_k) = \bigcup_{\ell=0}^{k} \{[y_j(t_\ell), \mathbf{x}_j(t_\ell)] \mid j \in \mathcal{N}_i(t_\ell) \cap \mathcal{M}(t_\ell)\}\,. \tag{6.21}$$

where $\mathcal{M}(t_k)$ is the set of agents that collect a measurement at time t_k, $\mathcal{N}_i(t_k)$ the set of neighbours of agent i at time t_k.

Each agent i estimates the parameters of the Kriging model from $S_i(t_k)$ and updates them each time some data point is added to $S_i(t_k)$ (i.e. $S_i(t_k-1) \neq S_i(t_k)$). Each agent i possesses its own model of the field composed by the mean $\widehat{\phi}_{i,k}(\mathbf{x})$ and the variance $\sigma_i^2(\mathbf{x})$ for all positions $\mathbf{x} \in D$.

The deterministic mean model of the field $\mathbf{r}^T\boldsymbol{\beta}$ is taken as a first-order polynomial, as in the local method. The regression matrix $\mathbf{R}_i(t_k)$ of agent i is thus built as follows

$$\mathbf{R}_i(t_k) = \begin{bmatrix} 1 \ (\mathbf{x}_{i,1} - \mathbf{x}_i(t_k))^T \\ ... \\ 1 \ (\mathbf{x}_{i,m} - \mathbf{x}_i(t_k))^T \end{bmatrix} \tag{6.22}$$

with $[\mathbf{x}_{i,1}, ..., \mathbf{x}_{i,m}]$ the points of $S_i(t_k)$. The parameter vector $\boldsymbol{\beta}_i$ is composed of $[\phi_i(\mathbf{x}_m) \quad \nabla_{x_1}\phi_i(\mathbf{x}_m) \quad \nabla_{x_2}\phi_i(\mathbf{x}_m)]$.

The vector $\mathbf{k}_\mathbf{x}$ is computed from the points $[\mathbf{x}_{i,1}, ..., \mathbf{x}_{i,m}]$ in $S_i(t_k)$ and $\mathbf{x} \in D$:

$$\mathbf{k}_\mathbf{x} = [\xi(\mathbf{x}, \mathbf{x}_{i,1}), ..., \xi(\mathbf{x}, \mathbf{x}_{i,m})]. \tag{6.23}$$

Depending on the communication range R and the exchange scheme between the agents, the model of the field may be different from one agent to another. If R is large enough to cover the entire area D then all the agents share the same information and $S_i(t_k) = S_j(t_k) \ \forall i, j$.

6.3 Design of sampling policy

Sampling criterion for Kriging

The mission consists in finding the position of the global maximum of the field. The Kriging model is obtained at time t_k from the n sampling points available in $S_i(t_k)$. A sampling criterion is needed to find the best positions to perform a new measurement while searching for the field maximum.

Several methods exist to choose the next sampling point for updating the Kriging model in order to find the maximum of the field, regardless of the agent dynamics constraints.

Kushner's criterion (Kushner, 1962) uses the Gaussian cumulative distribution function to maximize the probability of improving the best value yet obtained. This criterion (6.24) promotes local extrema over exploration.

$$\mathcal{C}_{\text{Kushner}}(\mathbf{x}) = P(\mu(\mathbf{x}) > f_{\max} + \epsilon) \tag{6.24}$$

where $f_{\max}$ is the maximum of the function over all the sampling points, $\mu(\mathbf{x})$ is the Kriging estimate of the function f at position $\mathbf{x}$, ϵ is a tuning parameter.

The *Expected Improvement* (EI) (Schonlau et al., 1996) used by the *Efficient Global Optimisation* (EGO) algorithm (Jones et al., 1998) is similar to the Kushner's criterion but achieves a trade-off between exploration and search of the maximum (6.25). It involves the probability density function of the Kriging model to consider exploration as well as local improvement.

$$\mathcal{C}_{\mathrm{EI}}(\mathbf{x}) = (f_{\max} + \mu(\mathbf{x}))\Psi(z) + \hat{\sigma}(\mathbf{x})\psi(z) \tag{6.25}$$

where $z = \dfrac{f_{\max} + \hat{f}(\mathbf{x})}{\hat{\sigma}(\mathbf{x})}$, Ψ and ψ the cumulative density and probability density functions of the normal distribution $\mathcal{N}(0,1)$. The convergence to the global optimum of the field for such system under validation of the assumption on the covariance has been proven in (Bull, 2011, Vazquez and Bect, 2010). These results show the efficiency of using Kriging modelling for global optimisation problems.

The lower confidence bounding (LCB) function has been proposed in (Cox and John, 1997).

$$\mathcal{C}_{\mathrm{lcb}}(\mathbf{x}) = \mu(\mathbf{x}) + b_{\mathrm{lcb}}\hat{\sigma}(\mathbf{x}) \tag{6.26}$$

where b_{lcb} is a tuning parameter for the exploration. It is useful to find positions where either the function can reach an extremum, or the uncertainty is high.

These methods cannot be directly applied in the case considered as the choice of the location of the next sampling point should be constrained by the dynamics of the vehicles embedding the sensors. The following methods are more adapted to exploration and search with dynamics constraints.

Choi's criterion introduced in (Choi et al., 2008), provides a general framework of navigation criterion using combinations of the Kriging model characteristics.

$$\mathcal{C}_{\mathrm{Choi}}(\mathbf{X}(t)) = \frac{\sum_{p=1}^{4} \lambda_p(t)\Xi_p(\mathbf{X}(t), t)}{\sum_{p=1}^{4} \lambda_p(t)} \tag{6.27}$$

with $\mathbf{X}(t)$ a vector with the positions of the N agents at time t. The functions $\Xi_p(\mathbf{X}(t), t)$ for $p = 1$ to 4 consist in

$$\Xi_1(\mathbf{X}(t), t) = \mu(\mathbf{X}(t))$$

$$\Xi_2(\mathbf{X}(t), t) = -\mu(\mathbf{X}(t))$$

$$\Xi_3(\mathbf{X}(t), t) = \sigma^2(\mathbf{X}(t))$$

and

$$\Xi_4(\mathbf{X}(t), t) = \frac{1}{2}\ln(2\pi\sigma^2(\mathbf{X}(t)))$$

The resulting navigation criterion is obtained by selecting the values of weights $\lambda_p(t)$ during the different phases of the exploration. A high weight value $\lambda_1(t)$ leads the fleet toward the maximum of the Kriging model, while on the contrary a high value of $\lambda_2(t)$ leads the fleet away from this maximum. The third and fourth weight values are dedicated to emphasize the exploration of the area either by minimising the variance of the model or by minimising its entropy.

Using time-varying values for the $\lambda_p(t)$ during the mission makes it possible to switch from a strategy of exploration aiming at reducing the uncertainty on the estimated field to a strategy tracking the estimated maximum.

Xu's criterion proposed in (Xu et al., 2011) is derived from Choi's initial criterion. It consists in the sum of the variances of the Kriging model obtained for a set $\mathcal{J}$ of points of interest.

$$\mathcal{C}_{\mathrm{Xu}}(\mathbf{X}(t)) = \frac{1}{|\mathcal{J}|}\sum_{j\in\mathcal{J}}\sigma^2_{z_j}(\mathbf{X}(t)) \tag{6.28}$$

where $\mathbf{X}(t)$ is a vector with the positions of the N agents at time t, $|\mathcal{J}|$ is the cardinality of $\mathcal{J}$ and $\sigma^2_{z_j}$ is the variance of the Kriging model at the target point j. This criterion helps to determine the sampling positions of all the sensors that reduce the average of the variance over the targeted points that are a priori selected to cover the area of interest.

Both Choi and Xu methods provide iteratively the position of the next sampling points. Once they are reached, new measurements are provided and added to the

set of sampling points (see Algorithm 3).

Algorithm 3 Iterative Kriging-based optimization

1: Perform Kriging estimation of the field from the current sampling points
2: Choose the position of the next sampling point(s) using a criterion among the ones described in (6.24), (6.25), (6.26) or (6.28)
3: Obtain measurement(s) at the position(s) found at the previous step
4: Add the measurement(s) and the position(s) to the current sampling point
5: Go back to Step 1 until budget of evaluations is exhausted or maximum found

6.4 Proposed Kriging-based criterion for maximum seeking with a MAS

Kushner's criterion, the *Expected Improvement* and the *LCB* criterion make it possible to select in the search domain the point which is the best candidate to improve the estimate of to the optimum of the function. Using these criteria may result in sampling points remotely located in the domain. Choi's and Xu's criteria can be tuned to either promote exploration improving the accuracy of the estimation over the domain or location of the maximum. They are well-suited for problems where the distance between two successive sampling points has to be taken into account in the computation budget.

The criterion presented in this thesis aims at defining iteratively new measurement locations that the agents should reach in order to find the maximum of the field over the search domain using a Kriging model. Inspired by the *LCB* criterion, it has been thus designed to perform a trade-off between exploring currently unknown areas and improving the current value of the extremum.

6.4.1 Proposed Kriging-based criterion

Finding the global maximum is the mission the MAS must fulfill. In order to limit the search effort, the criterion to be designed should make it possible to discard areas where the probability of finding the maximum is low. This probability can be derived using the characteristics of the Kriging model. The areas where the values of the mean plus two or three times the corresponding standard deviations remain

below the current estimated maximum can be rejected as having a low probability of containing the effective maximum. As the search must be performed by mobile agents, the criterion must also include terms prompting each agent to search in areas that are closest to its current location.

The criterion should thus be designed to provide the agents with new locations so that

- the fleet finally locates the position of the maximum,
- the search is limited to *areas of interest*,
- the next point allocated to each agent is close to its current position.

Assume that the estimate of the maximum of ϕ available to agent i at time t_k is

$$f^i_{\max}(t_k) = \max_{\mathbf{x}\in S_i(t_k)} \{\hat{\phi}_{i,k}(\mathbf{x})\}. \tag{6.29}$$

Let the cost of the proposed criterion $J_i^{(k)}(\mathbf{x})$ be defined as

$$J_i^{(k)}(\mathbf{x}) = \|\mathbf{x}_i(t_k) - \mathbf{x}\|^2 - \sum_{j\in\mathcal{N}_i(t_k)} \alpha\|\mathbf{x}_j(t_k) - \mathbf{x}\|^2, \tag{6.30}$$

The next sampling point for agent i is defined as

$$\mathbf{x}_i^d(t_k) = \arg\min_{\mathbf{x}\in D} \left\{ J_i^{(k)}(\mathbf{x}) \right\} \tag{6.31a}$$

$$\text{s.t. } \hat{\phi}_{i,k}(\mathbf{x}) + b\sigma_{\phi,i,k}(\mathbf{x}) > f^i_{\max}(t_k) \tag{6.31b}$$

where α and b are two positive tuning parameters.

The criterion translates the fact that the displacement should be limited while the constraint (6.31b), derived from (6.26), enables to reject regions with low probability of containing the maximum. The first term of $J_i^{(k)}(\mathbf{x})$ limits the displacement by looking to the closest point to $\mathbf{x}_i(t_k)$ that verifies the constraint. The second term of $J_i^{(k)}(\mathbf{x})$ is used to spread the agents by selecting a target point far from the neighbours of agent i. The value α should keep the repulsive term in the same order of magnitude as the attractive term. A value of $\alpha = \frac{1}{N_i}$ respects this constraint.

The constraint (6.31b) defines the subset of D that potentially contains the global maximum (the *areas of interest*). These areas consist of the positions where the mean of the model $\hat{\phi}_{i,k}(\mathbf{x})$ plus $b\sigma_{\phi,i,k}(\mathbf{x})$ are higher than the maximum sampled value $f^i_{\max}(t_k)$.

The areas of interest have a probability of containing a maximum that depends on the parameter b. By restricting the search to the areas that respect (6.31b), the search space tends to decrease. Using (6.30), agent i searches in this subset for a sampling point close to the current agent location $\mathbf{x}_i(t_k)$ and far enough from the other agent locations $\mathbf{x}_j(t_k)$, $j \in \mathcal{N}_i(t_k)$, so that the agents spread in the area.

6.4.2 Proposed criterion illustration

The criterion proposed in (6.31) is illustrated using a toy example. The function $f(x) = \cos(x)+\cos(0.7x)$ is studied on the interval $[0;\ 10]$. Two agents are initially at $x = 4$ and $x = 9.5$. Several steps of the algorithm are illustrated in Figure 6.2. The blue curve represents f. The red curve represents the mean μ of the model and the black dashed line represents the confidence bound for $b\sigma$ with $b = 3$ (i.e., 99.7% confidence at each point that the true function value is within the bounds). The value of $f_{\max}$ is represented by a green dashed line. As the constraint (6.31b) requires $\hat{\phi}_{i,k}(\mathbf{x}) + b\sigma_{\phi,i,k}(\mathbf{x}) > f^i_{\max}(t_k)$, a value $\varepsilon > 0$ is chosen to select the next sampling position such as $\hat{\phi}_{i,k}(\mathbf{x})+b\sigma_{\phi,i,k}(\mathbf{x}) \geq f^i_{\max}(t_k)+\varepsilon$. The value $f^i_{\max}(t_k)+\varepsilon$ is represented by the solid green line (for $\varepsilon = 0.4$, the value is take large to be visible on the figures). the areas of interest that verify the constraint are represented by a grey line.

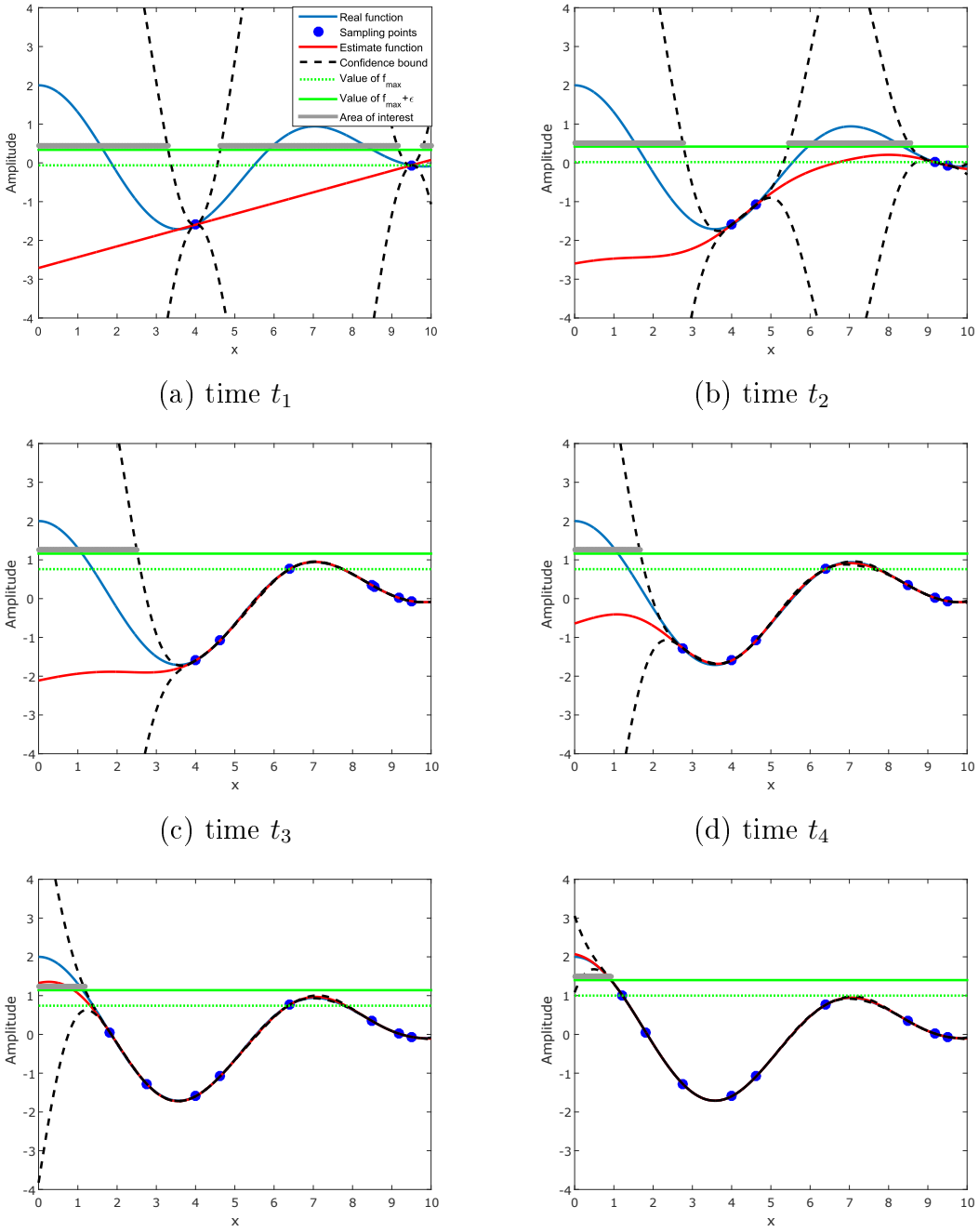

(a) time t_1 (b) time t_2

(c) time t_3 (d) time t_4

(d) time t_5 (e) time t_6

Figure 6.2: Illustration of the sampling criterion (6.31)

At time t_1, one observes the model with measurements taken at the two initial positions. The next sampling point will be selected in the area defined by the dashed black line representing the uncertainty and the green solid line representing the best value found. The cost (6.30) implies that the sampling points of each agent should be as close as possible to the agent position. This leads to the next sampling points to be selected at $x = 4.63$ and $x = 9.18$. The model with the two added measurements is represented in Figure 6.2 (b).

Figure 6.2(c) to (e) represent the evolution of the model with new sampling points selected by the proposed criteria. The maximum seeking does not end at t_6 but continues by selecting new measurement points in the left part of the space.

With the addition of new sampling points, the areas of interest defined as the areas that fulfil the constraint tend to decrease. This scheme reduces the search space for a new sampling point.

6.5 Optimisation solver

The criteria in Sections 6.3 and 6.4 need auxiliary maximisation algorithms to find the sampling positions. The solver used by (Xu et al., 2011) and that used during this thesis are presented in what follows.

6.5.1 Gradient-based method

The search for the optimum of the criterion (6.28) proposed in (Xu et al., 2011) is performed using a gradient descent algorithm. Let $\mathbf{X}(t)$ be a vector with the positions of the N agents at time t, and $\mathbf{X}(t_{k+1})$ be a vector with the desired positions of the N agents at time t_{k+1}. The optimisation problem can be written as:

$$\mathbf{X}(t_{k+1}) = \arg\min_{\mathbf{X}\in D} \mathcal{C}_{\mathrm{Xu}}(\mathbf{X}) \tag{6.32}$$

Let $\nabla_{\mathbf{X}}\mathcal{C}_{\mathrm{Xu}}(\mathbf{X}(t_k))$ denotes the gradient vector of $\mathcal{C}_{\mathrm{Xu}}(\mathbf{X}(t_k))$ at the positions $\mathbf{X}(t_k)$. The desired position vector $\mathbf{X}(t_{k+1})$ is obtained as

$$\mathbf{X}(t_{k+1}) = \mathbf{X}(t_k) - K_{Xu}\nabla_{\mathbf{X}}\mathcal{C}_{\mathrm{Xu}}(\mathbf{X}(t_k)) \tag{6.33}$$

where K_{Xu} is a movement step.

Using the gradient limits the computation complexity as it does not require to re-evaluate the criterion $\mathcal{C}_{\mathrm{Xu}}(\mathbf{X})$ at new points of the search domain. However, the gradient search cannot be guaranteed to converge to the global extremum. As pointed out by the authors, other optimisation techniques could be used, but should increase the computation cost.

6.5.2 DIRECT solver

The optimal solution of criterion (6.31) cannot be sought for using gradient descent algorithm as the gradient at the agent positions is not defined because they are not located in the areas of interest. To perform efficient optimisation, global and local searches must be performed. The DIRECT (DIviding RECTangles) algorithm has been used to solve our optimisation problem because of its efficiency compared to other methods (Jones et al., 1993). This solver performs local and global search simultaneously, while other algorithms most often perform one step after the other.

This algorithm was developed for unconstrained problems but a non-linear constrained version has been proposed (Finkel, 2003). DIRECT algorithm proceeds as follows:

1. Evaluation of the criterion at the center of the search space
2. Select a set of candidate rectangles for division in the potentially optimal space. Testing whether the candidate rectangle is feasible is performed by evaluating the constraint functions on each vertex and comparing the results with their objective values.
3. Split the candidate rectangle in three and evaluate the center of new rectangles Update of the potentially optimal space with new optimal found.
4. Check the stopping condition of the algorithm.

The stopping condition of the algorithm is given by evaluating the number of calls to the cost function, the number of iterations or the number of non-evolutions of the best estimate of the optimum found. When a large part of the design space does not fulfil the constraint, the algorithm is not always able to find an optimal

solution. This situation can occur with our criterion when most of the area D is explored and only few small areas fulfil the constraint.

Other global solvers taking constraints into account may have been used to solve the proposed criterion such as the ones described in Section 2.5.2.

6.6 Control law: from local search to global search

The control law of the agents for the global search is similar to the one for the local search. The low layer used to control the agent is the only one reused, as the high one was designed to perform gradient climbing and is thus not applicable anymore. In the local approach case, all the agents gathered around the same position to perform the gradient estimation by least-square estimation. In the present case, each agent i has to reach its desired position $\mathbf{x}_i^d(t)$ determined by the solution of (6.31). Therefore, using this approach, the agents spread in the search space to collect measurements that are incorporated in the Kriging model.

The new control input is similar to the one of Section 5.1.2 equation (5.4) with $\mathbf{x}_i^{\mathrm{d}}(t)$ instead of $\widehat{\mathbf{x}}_i(t)$. As $\mathbf{x}_i^{\mathrm{d}}$ is a fixed position until the criterion finds a new sampling position, its velocity $\dot{\mathbf{x}}_i^{\mathrm{d}}(t)$ and acceleration $\ddot{\mathbf{x}}_i^{\mathrm{d}}(t)$ are chosen null. When an agent reaches its desired position, a new measurement is performed and a new desired position is computed. The new control input is

$$\begin{aligned}\mathbf{u}_i(t) =& C(\mathbf{x}_i(t), \dot{\mathbf{x}}_i(t))\dot{\mathbf{x}}_i(t) - k_1\dot{\mathbf{x}}_i(t) - k_3^i(\theta_i, t)\mathbf{x}_i(t) \\ &+ 2k_2\sum_{j=1}^{N}(\mathbf{x}_i(t) - \mathbf{x}_j(t))\exp\left(-\frac{(\mathbf{x}_i(t) - \mathbf{x}_j(t))^T(\mathbf{x}_i(t) - \mathbf{x}_j(t))}{q}\right) \end{aligned} \quad (6.34)$$

where $k_1 > 0$ is used to adapt the speed of each agent to the speed of $\mathbf{x}_i^{\mathrm{d}} = 0$. The constant $k_2 > 0$ determines the relative importance of the collision avoidance term. Finally, $k_3^i(\theta_i) > 0$ determines the attractiveness of $\mathbf{x}_i^{\mathrm{d}}$.

The same result of stability analysis of the control law by Lyapunov theory (Section 5.1.3) demonstrates that each agent i converges asymptotically to equilibrium toward the position $\mathbf{x}_i^{\mathrm{d}}$ while avoiding collision with the other vehicles.

6.7 Simulation results

6.7.1 Global search method for MAS

Simulations were carried out to illustrate the proposed global optimisation scheme for MAS. A the first time step, all the agents perform measurements near their initial positions to compute a Kriging model from the initial values in $S_i(t_k)$. Depending on the communication graph $\mathcal{G}$, the agents may exchange their data with the entire fleet and have the same knowledge ($S_i(t_k) = S_j(t_k)$ for all i and j), or only exchange with their neighbours. In the case treated, the communication graph is assumed to be complete, delay and loss of communications are not considered. From the proposed sampling criterion (6.31), each agent determines a target position in the area of interest that may contain the maximum. The control law moves the agent to the desired position. When the agent arrives at a distance less than $\delta > 0$ of the target location, $||\mathbf{x}_i(t_k) - \mathbf{x}_i^{\mathrm{d}}(t_k)|| < \delta$, a new measurement is performed. After the sampling by an agent, the set S of the agents and those of its neighbours is updated as well as the Kriging model. The criterion is then used to find new desired positions for all the agents that have updated their Kriging model. The search stops when no point satisfies (6.31b) anymore.

Algorithm 4 summarizes the steps performed for maximum seeking.

6.7.2 Simulation of the proposed method

Simulation conditions

To test the efficiency of the global search, we consider a 2D multi-modal function ϕ_{test} shown in Figure 6.3, with one global maximum and two local ones. The function is defined on $D = [0,\ 50] \times [0,\ 50]$ and has been generated as the sum of three two-dimension Gaussian functions with maxima equal to 1.2, 1, and 1, located at (15, 15), (40, 35), and (10, 35). The global maximum is located at (14.9407, 16.1450) with a value of 1.2509.

$$\begin{aligned}\phi_{test}(x,y) =& 1\ \exp(-(0.005(x-10)^2 + 0.005(y-40)^2)) \\ &+ 1\ \exp(-(0.005(x-40)^2 + 0.005(y-35)^2)) \\ &+ 1.2\ \exp(-(0.005(x-15)^2 + 0.005(y-15)^2)),\end{aligned} \tag{6.35}$$

Algorithm 4 Maximum seeking Algorithm

```
for every time t_k do
    for each agent i do
        if ||x_i(t_k) − x_i^d(t_k)|| < δ then
            Acquire measurement y_i at x_i(t_k) as shown in (3.4)
        end if
        Exchange information with agents in N_i(t_k)
        Update S_i(t_k)
        if S_i(t_k) ≠ S_i(t_{k−1}) then
            Update the Kriging model (6.18) and (6.19)
            Solve (6.31) to find x_i^d(t_{k+1})
        end if
        Compute the control input u_i(t_k) (6.34) so as to:
        - Move the agent to x_i^d(t_k)
        - Avoid collision with the other agents
    end for
end for
```

We consider a MAS with $N = 5$ agents. The initial positions of the agents are uniformly randomly generated in the area D. The communication range R of the agents is larger than the size of the map, giving a complete communication graph $\mathcal{G}$ among the fleet. This means that all the agents will get the same set of sampling points $S_i, \forall i$ and so the same Kriging model ($\hat{\phi}_{i,k}(\mathbf{x}) = \hat{\phi}_{j,k}(\mathbf{x}) = \hat{\phi}_k(\mathbf{x})$, $\sigma_{\phi,i,k}(\mathbf{x}) = \sigma_{\phi,j,k}(\mathbf{x}) = \sigma_{\phi,k}(\mathbf{x})$ and $f^i_{\max}(t_k) = f^j_{\max}(t_k) = f_{\max}(t_k)\ \forall i, j$). The sensors are healthy and have a measurement noise as stated in (3.4) with variance $\sigma_0^2 = 0.01$.

The parameters of the control law are $q = 0.1$, $k_1 = 47$, $k_2 = 50$, $k_3 = 1600$, $M = 1$ kg, and $C = 0.001$ kg/s. The sampling period is $T = 0.01$s. The criterion parameter are $b = 3$ and $\alpha = \frac{1}{N} = \frac{1}{3}$. The Kriging parameters are $\theta = 50$ and $\sigma_z^2 = 0.5$.

As highlighted in Section 6.4.2, it is not easy to satisfy a strict constraint such as $\hat{\phi}_k(\mathbf{x}) + b\sigma_{\phi,k}(\mathbf{x}) > f_{\max}(t_k)$. The parameter $\varepsilon > 0$ is introduced to modify the constraint into $\hat{\phi}_k(\mathbf{x}) + b\sigma_{\phi,k}(\mathbf{x}) \geq f_{\max}(t_k) + \varepsilon$, with $\varepsilon = 0.01$. This leads the sampling point to be selected inside the area of interest and not on its boundary.

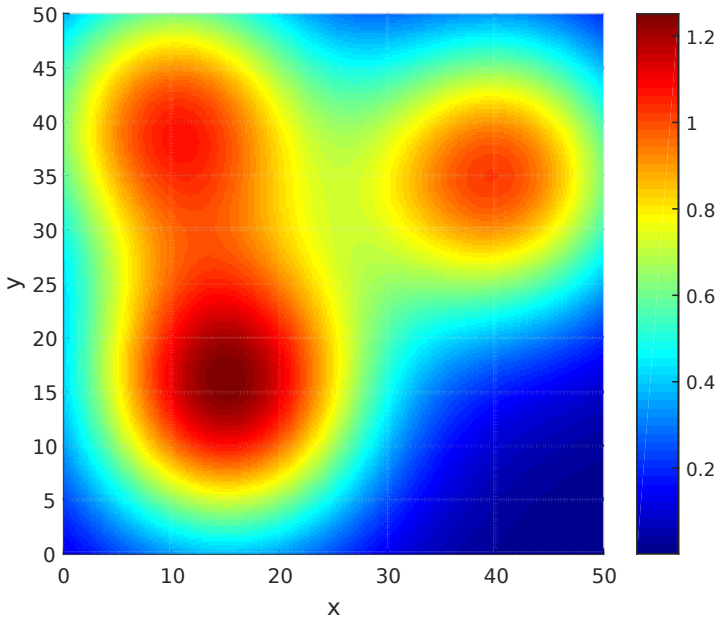

Figure 6.3: Test function ϕ_{test}

Remark Conflict between agents may happen when the desired positions of more than one agent are too close to each other. In this configuration, the agents can stay blocked. They are too far from their desired positions to perform a measurement and cannot come closer because of the collision avoidance repulsive terms. Different methods are possible to avoid these conflicts. A distance to the desired position to perform measurement (δ) larger than the repulsive radius is a solution, as well as a modification of the control law gain similar to the mechanism introduced for reconfiguration in Section 5.2 in case of conflict.

Simulation 1: maximum seeking with our criterion

Figures 6.4 and 6.5 illustrate the search for the maximum performed by the agents on ϕ_{test}. The field represented is the one defined in the constraint of our criterion (6.31b): $\phi_{\text{upper}} = \widehat{\phi}_k(\mathbf{x}) + b\sigma_{\phi,k}(\mathbf{x})$ that represents the field plus the uncertainty. Blue parts represent low values while red ones represent high values (the color map scale changes in each image). The black spots represent the agent positions while the red ones represent the sampling positions. $f_{\max}$ is the maximum value

of the model on the sampling points. When a measurement is performed, the uncertainty around this position decreases. The spatial correlation function (6.3) defined in the Kriging model is the main element that controls the performance of the Kriging-based criterion. By design, assuming that the correlation function is well chosen (or known a priori), the function ϕ_{upper} is an upper bound of ϕ_{test} at any point of D with a probability depending on parameter b.

Our criterion aims at finding the position of the maximum of ϕ_{test} by exploring the space in the areas where ϕ_{upper} is higher than the current maximum found $f_{\max}$. At time t_1 the agents are randomly placed on the map and perform 5 first measurements. With these first measurements, a Kriging model is computed and used to find the position of the next sampling point for each agent. At time t_2 the agents start to move toward their desired positions. At time t_{100}, the agents have started to spread on the map while performing measurements. The uncertainty decreases in the visited areas. At time t_{200}, the agents continue to spread in the area. The distance between the measurements depends on the model and the constraint values. When the new sampling point increases the value of $f_{\max}$, then the next sampling points are close to each other as it can be seen near position (20, 20). On the contrary, when sampling is performed in an area without update of $f_{\max}$, the next sampling positions are far from each other as can be seen in the right down corner of the map. Between time t_{300} and t_{400}, the agents continue to explore the area. The agents near the real position of the maximum perform sampling close to each other until there is no more improvement, then the sampling distance becomes higher. At time t_{600}, only a small area of high uncertainty remains. At time t_{660} the value of ϕ_{upper} in the last zone of uncertainty decreases, meaning that the upper bound of possible value of ϕ_{test} decreases as well. At time t_{760}, the agents perform sampling in the last area of D with potential presence of the maximum. No more point that fulfils the constraint (6.31b) can be found in the area. The maximum seeking mission finishes, since the system should have found the position of the maximum.

As can be noticed by comparing the map of ϕ_{upper} at time t_{760} in Figure 6.5 and the real function ϕ_{test} in Figure 6.3, the real map does not correspond exactly to the one on the simulation. This is because the sampling criterion mission was to locate the maximum by only exploring areas of interest. Some areas remain with high uncertainty but with low probability of presence of the maximum.

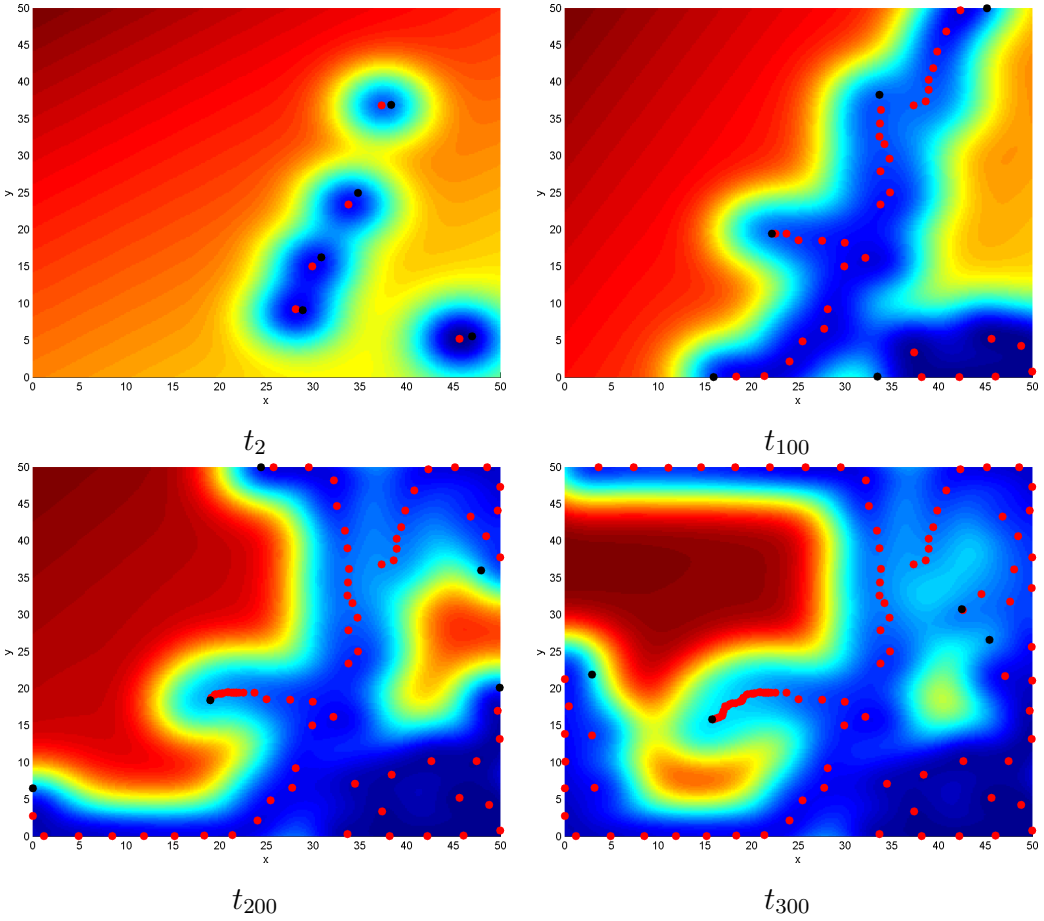

Figure 6.4: Illustration of the search of maximum of ϕ_{test} by 5 agents

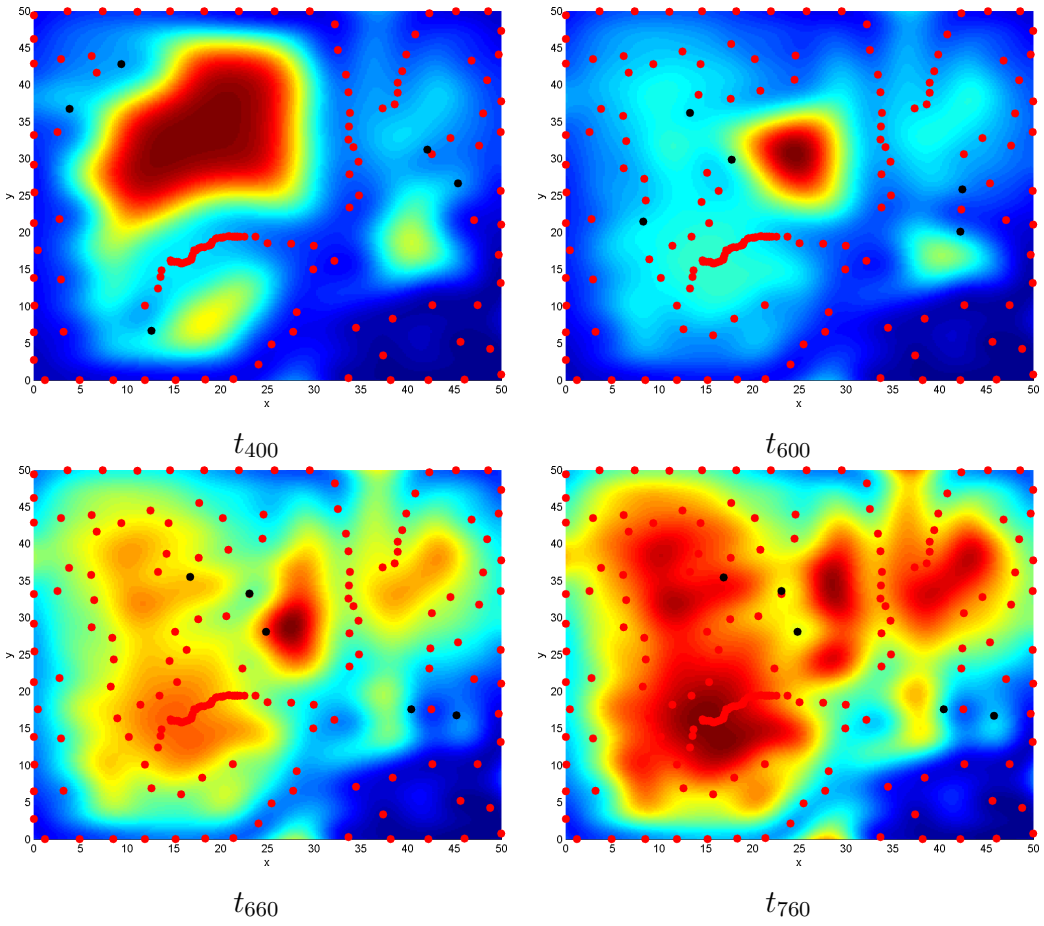

Figure 6.5: Illustration of the search of maximum of ϕ_{test} by 5 agents

Figure 6.6 presents an analysis of the search shown in Figure 6.4 and Figure 6.5. Figure 6.6 (a) and (b) represent respectively the evolution of the value of $f_{\max}$ and the error between the estimated position of the maximum and the real one. Both evolutions are mainly due to the agent shown near position [20 20] in Figure 6.4. As Figure 6.5. Figure 6.6 (a) shows, the detection of the real maximum is performed between iterations number 150 and 300. Figure 6.6 (c) displays the integral of the area that fulfils the constraint (6.31b). As the number of performed sampling increases, the integral of the area of potential position of the maximum decreases. The search does not stop when the positions of the real maximum is found (near iteration 310) but continues until there are no more areas of interest to explore. The search stops near iteration 750, when no more points can be found

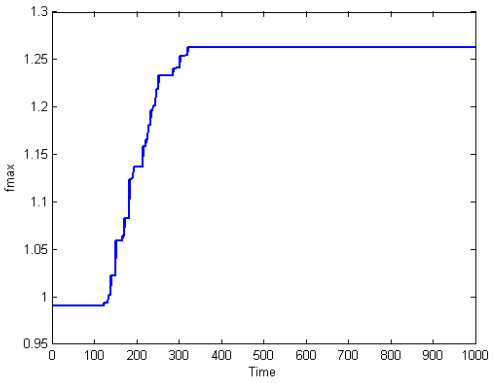

(a) Evolution of the value of $f_{\max}$

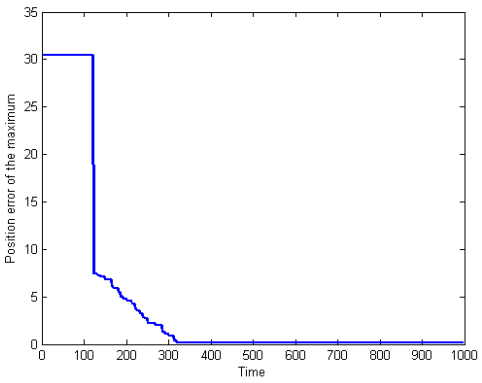

(b) Error between $f_{\max}$ position and the real maximum

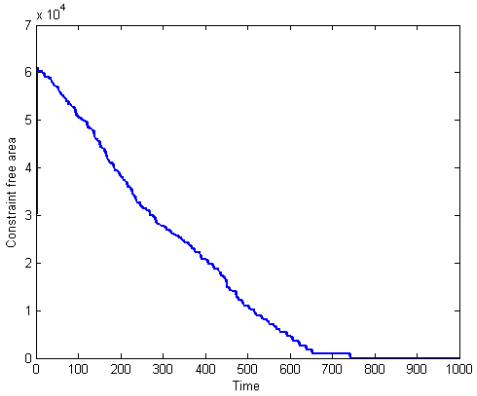

(c) Evolution of the size of the area where the constraint is satisfied

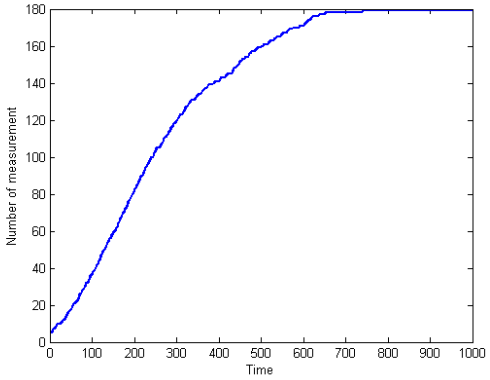

(d) Number of measurements for all the MAS for all the agents of the MAS

Figure 6.6: Convergence to the maximum with the proposed criterion

that fulfil the constraint (6.31b). Figure 6.6 (d) shows the number of measurements performed during the search. In a first time, the number of measurements increases rapidly until iteration 400. Between iterations 400 and 700, the number of new measurements reduces until becoming null. This is due to the exploration already performed by the agents, making the exploration area reduce. When the areas of interest are small, the agents need more time to go from one area to the other. Less measurements are needed to explore small areas.

6.7.3 Simulation: comparison with a state-of-the-art method

A comparison is done between two techniques, one using the proposed criterion (6.31) and one using the criterion (6.28) introduced by (Xu et al., 2011). As stated before, the same solver cannot be used for both criteria (see Section 6.5). We used DIRECT to maximise our criterion while a gradient descent method is used for (6.28). The method proposed by Xu moves the agent following the gradient direction during a sampling period τ before performing a measurement. Two different values of this period have been tested: $\tau_1 = 5T$ and $\tau_2 = 20T$. For both criteria, a fleet of $N = 3$ agents perform the search mission. The field to explore is ϕ_{test} presented in equation (6.35) defined on $D = [0;\ 50]^2$. For both criteria, the communication graph is assumed complete with a communication range $R > 50\sqrt{2}$. The measurements are assumed to be noise free. 100 target points $\mathcal{J}$ of the criterion (6.28) are uniformly distributed on a grid to cover D.

The parameters of the control law are still $q = 0.1$, $k_1 = 47$, $k_2 = 50$, $k_3 = 1600$, $M = 1$ kg, and $C = 0.001$ kg/s. The sampling period of the simulation is $T = 0.01$s. The criterion parameters are $b = 3$ and $\alpha = \frac{1}{N} = \frac{1}{3}$. As the control law brings asymptotically the agents to the desired position $\mathbf{x}_i^{\mathrm{d}}(t_k)$ with a null desired velocity $\dot{\mathbf{x}}_i^{\mathrm{d}}(t_k) = 0$, it has been chosen to sample a measurement when $||\mathbf{x}_i(t_k) - \mathbf{x}_i^{\mathrm{d}}(t_k)|| < 0.01$ m. The Kriging parameters were $\theta = 50$ and $\sigma_k^2 = 0.5$.

The following results are obtained from an average over several random initial locations of the agents in D for each criteria. Each simulation lasts 1000 time steps. The blue curves represent the proposed criterion, while the red and black ones illustrate the criterion of Xu with respectively $\tau_1 = 5T$ and $\tau_2 = 20T$. These sets of parameters are denoted Xu5 and Xu20 for convenience. Solid lines are averaged results while dotted lines correspond to the minimal and maximal values collected over all the runs.

Figure 6.7 illustrates the speed of convergence of the estimated position of $f_{\max}(t_k)$ by comparing the estimated position with the real value. All the methods start with an average distance to the maximum between 20m and 25m as the size of the area D is $[0;\ 50]^2$. The proposed criterion and Xu20 have the fastest decrease, with 300 time steps, the distance error to the maximum falls to 5m. Then the Xu20 criterion stays at the same error distance until the end of the simulation. The proposed criterion continues instead to decrease until step 400

where it stabilises around a distance error of 1. Using the criterion Xu5 one obtains a slower convergence and reaches the distance error only at step 500, but then continues to decrease near the same level than the proposed criterion.

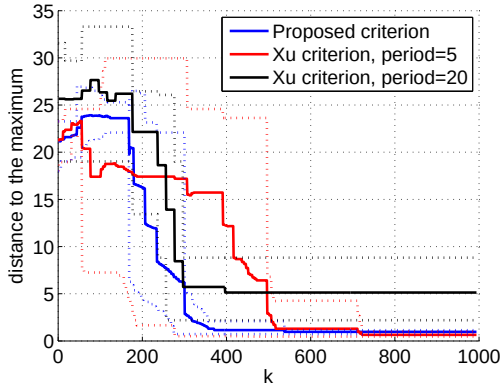

Figure 6.7: Distance to the maximum with respect to the time

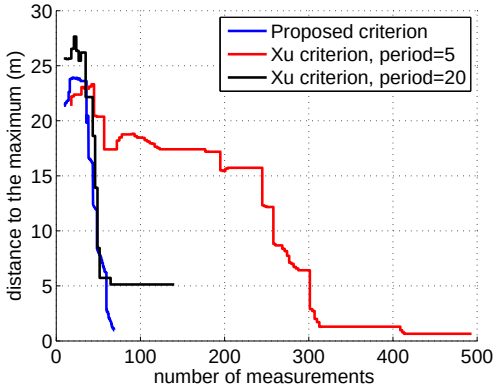

Figure 6.8: Distance to the maximum with respect to the number of measurements

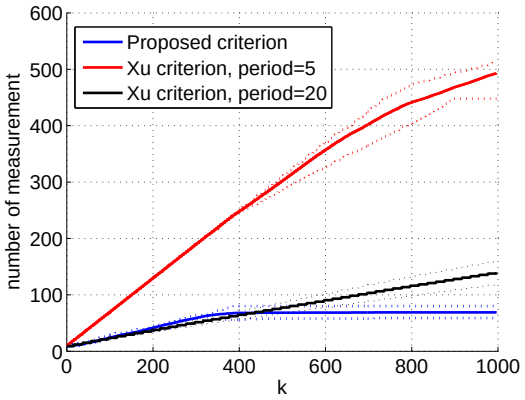

Figure 6.9: Number of measurements as a function of time

Figure 6.8 illustrates the effect stated previously for the number of measurement. With only around 70 measurements, maximisation using Xu20 leads to an error of 5m. The proposed criterion reaches an error of 1m with less than 90 measurements when Xu5 needs more than 300 measurement to reach the same level of error.

Figure 6.9 shows the number of measurements performed considering the three methods. Xu5 has the larger amount of measurements and performed around 500 measurements during the 1000 time steps of simulation. Using Xu20 and the proposed criterion, one has a similar number of measurements until time step 400. Then the proposed criterion stops measuring after the position of the maximum is found. Xu20 instead, continues to perform measurements and finishes the simulation with a bit less than 300 measurements.

All methods present a similar dispersion of results. The reference method (Xu) exhibits different characteristics depending on the choice of the sampling period τ. When τ is small, convergence to the maximum is accurate but slow and the number of measurements is large. When τ is larger, the distance to the maximum decreases quickly but never converges, while few measurements are required. The proposed method does not need a tuning of τ and appears to combine all desired properties: a quick convergence to the maximum is achieved with few measurements.

While the reference method is built for field exploration by minimizing the variance of the Kriging model using displacement of the agents to areas of high uncertainty, the proposed criterion (6.31) allows to focus only on exploring areas where the maximum could be located. These simulation results support the use of the proposed criterion to limit the exploration area for a faster convergence to the maximum with few information.

A deeper analysis of the state-of-the-art method can help to select better parameters $\mathcal{J}$ and τ. But as the authors of (Xu et al., 2011), did not present a suitable way to select the parameters, no clue was found to choose them more efficiently.

6.8 Conclusions and perspectives of Part III

6.8.1 Conclusions

We proposed in this second part a global extremum search method for MAS based on Kriging. This method is designed on a novel criterion that takes into account the limitation of the MAS for sampling and which:

- Limits the movement by selecting sampling points near the current agent positions.

- Constrains the search only in areas of interest, limiting exploration.

The proposed criterion favourably compares to other criteria from the literature with Kriging by MAS.

6.8.2 Perspectives

A main perspective is a fault detection and isolation scheme for the global approach. A faulty sensor can produce outliers that may disturb the model estimation. In the first part of this thesis, the model designed was a local second-order Taylor expansion computed at every time step. The global approach used in this part of the thesis is built on a Kriging model of the field as described in Section 6.1. As previously, an outlier can lead the system to a wrong position of the maximum. An FDI scheme has to be adapted to the new conditions of our system: the agents are spread and not maintained in formation any more. A FDI based on local estimation from neighbours is thus not possible.

Proposed idea

We propose to use the same kind of residual as in Section 4.4.1 but instead of using a local estimate of the field at the sensor position, we use the Kriging estimate. The new residual $r_i^{(2)}$ would then be defined as

$$r_i^{(2)}(t_k) = \widehat{\phi}_{i,k}(\mathbf{x}_i(t_k)) - y_i(t_k) \tag{6.36}$$

In the global search without FDI, the agent perform a measurement only at the desired position stated by the criterion (6.31). The sensor is not used during the movement. Instead, the agent could acquire measurements during the movement to the desired sampling point to detect if the sensor is defective. The measurements collected during the movement would not be incorporated into the Kriging model to keep the model as light as possible and for computational power reason.

The idea is to detect if the sensor is fautly and to remove its measurement from the estimation input before a faulty measurement is added to the model. In what follows, we assume that sensors are not faulty at the beginning of the mission and take a first un-faulty measurement to initialised the model.

A first model can be computed from the initial measurements. As a consequence of Kriging, the model is quite certain near the sampling point and becomes more uncertain as the agents move away from their past sampling points. From the Kriging model, one can also design a threshold on the residual for outlier detection.

$$|r_i^{(2)}(t_k)| > m\sigma_{\phi,i,k}(\mathbf{x}_i(t_k) \tag{6.37}$$

where m is a tuning parameter for the threshold. For instance, by taking $m = 3$ the threshold on the residual will be 3 times the standard deviation of the model at the current position of the sensor. Under correct model covariance hypothesis, this means that $99,7\%$ of the measurements should be less than this bound. If the residual exceeds this value, the probability of the sensor to be faulty is higher than 0.997.

Main issues

The proposed FDI scheme using Kriging has two main issues that compromise its utilisation without countermeasures. The first one is the possible inclusion of faulty measurements in the model and the second is a detection issue.

For the first one, the proposed scheme aims at detecting faulty sensors and remove them from the set of data used by each sensor to perform the Kriging estimate. The scheme is performed from measurements that are not included in the Kriging model. If a faulty sensor is not detected on time or if the sensor turns to be faulty when it performs a measurement at a sampling position, then the model will be faulty.

An outlier in the model can have two effects:

- Create a virtual maximum that will be identified instead of the real one.
- Distort the value of the model and change the areas of interest, modifying the future exploration trajectories.

The second main issue concerns the detection capability. By using the threshold described in equation (6.37), the detection performance comes directly from the value of the covariance of the model at the agent position. At the beginning of the mission, the covariance value is high over most of the area D. Only very high outliers compared to regular measurements will be detected because only them

could overcome the value of $m\sigma_{\phi,i,k}(\mathbf{x}_i(t_k))$. To detect outliers with accuracy, the uncertainty should be low.

In future work, we could continue the research to find a solution for the FDI scheme with Kriging. A possibility would be to define a new sampling criterion that keeps the agents close to the others. This new criterion should be linked with a prior filter that decides of the trustfulness of the measurements. Before adding any measurement to the model, each agent could determine with its neighbours if the measurements are faulty or not.

Another perspective concerns the case where faulty data are integrated in the model. A scheme should provide the possibility for the system to isolate the data from a particular agent. If an agent is detected as faulty, an unknown number of defective data could have been taken in the model. To suppress the faulty data, the healthy agent may have to retrace the trajectory of the faulty one to test if the previous data of the faulty agent are defective or not. This scheme would require a replanning of the mission where some agents stop the maximum seeking to verify the integrity of the model before continuing the mission.

Summary

In this chapter, the main contribution is the presentation of a new sampling criterion for optimisation based on Kriging. This criterion is designed for MAS and takes the dynamics of the agents into account.
The control law proposed in the previous Part of this thesis is adapted to perform extremum seeking of a multi-modal field. Comparison with a state-of-the-art method is also presented.
The next chapter will conclude this thesis and propose perspectives for future works.

The sampling criterion for optimisation based on Kriging with MAS proposed in this chapter has been presented in (Kahn et al., 2015b).

Chapter 7

Conclusion and perspectives

The objectives of this thesis were to propose solutions to the problem of extremum seeking of an unknown spatial field with a MAS. Two search strategies have been considered using two different models of the field and resulting in local and global searches. The local search relies on a description of the field under the form of a first-order spatial expansion while the global approach uses a recursively updated Kriging model of the field. The two approaches result in rather different search policies, the first one leading to a formation fleet and the second one to a strategy of disseminating the agents over the search domain.

Local approach for maximum seeking with a MAS

Contributions The local strategy for finding the maximum of an unknown field is derived from a cooperative estimation of the field and its gradient. The solution proposed in this thesis includes three contributions. The first one deals with the optimal sensor placement for estimation. The second one consists in a fault detection and isolation process adapted to our estimation. The third contribution is the design of a novel control law for our MAS. The proposed solution for maximum seeking uses the optimal sensor placement to allocate positions to the embedded sensors and detects when a sensor become defective using the FDI scheme. The control law is then used to drive the agents to their allocated positions and reconfigure the MAS when a fault occurs and has been efficiently detected.

A sensor state that can take two values, healthy or defective has been associated with each embedded sensor of the MAS. The optimal sensor locations for estimation are determined taking into account this state value. Three different criteria have been proposed for characterizing the location. The first one is the trace of the information matrix (T-optimal). The second one is the determinant of the information matrix (D-optimal) and the third one is the amplitude of the modelling error resulting from the estimation. Analytical solutions for D-optimal and T-optimal criteria show that if the collision avoidance constraints between agents allow it, an optimal solution can be found on a circle centred on the estimate position of the current maximum for both healthy and defective sensors. The radius of this circle varies according to the selected optimality criterion and on the available knowledge of the variations of the unknown field. Numerical solutions have shown that when the constraints do not allow the agents to be located on such a circle, then the defective agents have to be placed farther from the position of estimation than the healthy ones. Results obtained for D-optimal criterion lead us to surmise that compact formations around the position of estimation are optimal. The analytical solution for the modelling error minimisation indicates that the agents performing the estimation have to come close to the position of estimation in a compact formation.

When an agent becomes defective, the resulting estimate may suffer from the faulty measurement it provides to the cooperative estimation. In order to compensate for this effect, one must detect when such a change of sensor state occurs. The fault detection and isolation scheme proposed uses an analysis of the noise effect on the estimate to design an adaptive threshold for outlier detection. Once a fault is detected in the MAS, a bank of filters and a majority vote consensus are used to isolate the faulty agent.

A control law has been designed to move the agents to their desired positions. It consists in two layers. The high layer moves the position of estimation along the direction of the estimated gradient. The low layer proposes a novel decentralised control law for MAS. It brings the agents in a compact formation centred at the position of estimation, satisfying the optimal sensor placement requirements. Moreover, a single tuning parameter on a faulty agent leads the formation to per-

form a reconfiguration by moving the faulty agent at the formation boundary. The stability analysis of the low-layer control law has been obtained using Lyapunov theory.

Perspectives Several mid-term and long-term directions are proposed below. The first perspective of work is the implementation of the developed approaches on autonomous platforms in order to realise experiments to validate the feasibility of embedding the methods. Future works should continue on optimal sensor placement. An analytical solution to the optimal placement problem could be searched for when the constraints on the relative distance between agents make it impossible to locate all agents on the same circle (for T-optimal and D-optimal criteria). Another direction of research is the development of new criteria derived from the design of different forms of estimators.

The fault detection and isolation scheme proposed is based on a statistical model of the Hessian of the unknown field. The parameters of this model are selected using assumptions on the variation of the field. The validation of these assumptions is difficult to perform. Two directions of improvement could be investigated. It consists in either using a test based on other models of detection or defining a scheme for parametric representation of the Hessian matrix.

The proposed control law is decentralised so that each agent computes its own control input but global knowledge of the distributed estimates is required. In practical case, information is limited to a neighbourhood of each agent. Impact of this limitation on the stability and performances of the control law should be investigated.

Global approach for maximum seeking with a MAS

Contributions To overcome the issue of the local search, global search solutions have been investigated. The global strategy proposed relies on a meta-model of the unknown field. Kriging modelling has been selected because it provides simultaneously an estimate of the field and of its variability. These features are exploited to design a search criterion defining locations that the agents should visit to sample new measurements improving the current estimate of the maximum

of the field. This criterion aims at spreading the agents in the search space to update the model while limiting the search space to areas of interest with potential presence of the maximum. The uncertainty of the model obtained by Kriging is used to define these areas of interest, where the maximum is less likely to be found..

The proposed sampling criterion has been compared with state-of-the-art sampling criteria for MAS and has been shown to improve the speed of convergence to the global maximum and decrease the number of sampling points required. The low layer of the control law has been adapted to the global search approach, to make the agents reach the subsequent desired positions instead of staying in formation.

Perspectives As for the local approach, the first perspective of work is the implementation of the developed approaches on autonomous platforms.

Some developments for the FDI scheme are required for the global search approach. The problem relies on how to correct the Kriging model in case of occurrences of faults on the embedded sensors. Solutions to rectify the Kriging model in case of fault data injection still have to be found.

The Kriging model presented in the simulation results of this thesis is a centralised model which requires to dispose of a global communication network. Future work should include decentralization of the model estimation within a neighbourhood and study of consensus on shared information between time-varying neighbours.

The work presented in this thesis did not consider communications issues. Shorter communication ranges should be first considered and potential loss of data during communication exchanges should be taken into account. This should result in adaptations on the cooperative estimation, the search criterion and modification of the FDI scheme. Most of the approaches have been designed in such a way that they can be easily decentralised. The efficient decentralisation of the proposed methods is a highly interesting topic for future practical applicability..

Bibliography

Ali Ahmadzadeh, Gilad Buchman, Peng Cheng, Ali Jadbabaie, Jim Keller, Vijay Kumar, and George Pappas. Cooperative control of UAVs for search and coverage. In *Proceedings of the AUVSI conference on unmanned systems*, volume 2, 2006.

Ian F Akyildiz, Dario Pompili, and Tommaso Melodia. Underwater acoustic sensor networks: research challenges. *Ad hoc networks*, 3(3):257–279, 2005.

Shafiq Alam, Gillian Dobbie, Patricia Riddle, and M Asif Naeem. A swarm intelligence based clustering approach for outlier detection. In *IEEE Congress on Evolutionary Computation (CEC)*, pages 1–7. IEEE, 2010.

Fabrizio Angiulli, Stefano Basta, and Clara Pizzuti. Distance-based detection and prediction of outliers. *IEEE Transactions on Knowledge and Data Engineering*, 18(2):145–160, 2006.

Randal W Beard, JR Lawton, and Fred Y Hadaegh. A feedback architecture for formation control. In *Proceedings of the American Control Conference (ACC)*, volume 6, pages 4087–4091, 2000.

Ronald W Becker and GV Lago. A global optimization algorithm. In *Proceedings of the 8th Allerton Conference on Circuits and Systems Theory*, pages 3–12, 1970.

Adrian N Bishop and Andrey V Savkin. On false-data attacks in robust multi-sensor-based estimation. In *IEEE International Conference on Control and Automation (ICCA)*, pages 10–17. IEEE, 2011.

Emrah Bıyık and Murat Arcak. Gradient climbing in formation via extremum seeking and passivity-based coordination rules. *Asian Journal of Control*, 10(2): 201–211, 2008.

Jovan D Bošković and Raman K Mehra. Multiple model-based adaptive reconfigurable formation flight control design. In *IEEE Conference on Decision and Control*, volume 2, pages 1263–1268. IEEE, 2002.

Adam D Bull. Convergence rates of efficient global optimization algorithms. *The Journal of Machine Learning Research*, 12:2879–2904, 2011.

Stefano Carpin and Lynne E Parker. Cooperative leader following in a distributed multi-robot system. In *IEEE International Conference on Robotics and Automation*, volume 3, pages 2994–3001. IEEE, 2002.

Kathryn Chaloner and Rollin Brant. A bayesian approach to outlier detection and residual analysis. *Biometrika*, 75(4):651–659, 1988.

Abbas Chamseddine, Youmin Zhang, and Camille Alain Rabbath. Trajectory planning and re-planning for fault tolerant formation flight control of quadrotor unmanned aerial vehicles. In *American Control Conference (ACC)*, pages 3291–3296. IEEE, 2012.

Chien Chern Cheah, Saing Paul Hou, and Jean Jacques E Slotine. Region-based shape control for a swarm of robots. *Automatica*, 45(10):2406–2411, 2009.

Qin Chen and JYS Luh. Coordination and control of a group of small mobile robots. In *IEEE International Conference on Robotics and Automation*, pages 2315–2320. IEEE, 1994.

Jae-Young Choi, Sung-Jib Yim, Yoon Jae Huh, and Yoon-Hwa Choi. A distributed adaptive scheme for detecting faults in wireless sensor networks. *WSEAS Transactions on Communications*, 8(2):269–278, 2009a.

Jongeun Choi, Songhwai Oh, and Roberto Horowitz. Cooperatively learning mobile agents for gradient climbing. In *IEEE Conference on Decision and Control (CDC)*, pages 3139–3144. IEEE, 2007.

Jongeun Choi, Joonho Lee, and Songhwai Oh. Swarm intelligence for achieving the global maximum using spatio-temporal Gaussian processes. In *American Control Conference*, pages 135–140. IEEE, 2008.

Jongeun Choi, Songhwai Oh, and Roberto Horowitz. Distributed learning and cooperative control for multi-agent systems. *Automatica*, 45(12):2802–2814, 2009b.

Dennis Cook. Assessment of local influence. *Journal of the Royal Statistical Society. Series B (Methodological)*, pages 133–169, 1986.

Jorge Cortés. Distributed Kriged Kalman filter for spatial estimation. *IEEE Transactions on Automatic Control*, 54(12):2816–2827, 2009.

Jorge Cortés, Sonia Martinez, Timur Karatas, and Francesco Bullo. Coverage control for mobile sensing networks. In *IEEE International Conference on Robotics and Automation*, volume 2, pages 1327–1332. IEEE, 2002.

Dennis D Cox and Susan John. Sdo: A statistical method for global optimization. *Multidisciplinary design optimization: state of the art*, pages 315–329, 1997.

Antoine Cully, Jeff Clune, Danesh Tarapore, and Jean-Baptiste Mouret. Robots that can adapt like animals. *Nature*, 521(7553):503–507, 2015.

Daniel-Ioan Curiac, Madalin Plastoi, Ovidiu Banias, Constantin Volosencu, Roxana Tudoroiu, and Alexa Doboli. Combined malicious node discovery and self-destruction technique for wireless sensor networks. In *IEEE International Conference on Sensor Technologies and Applications*, pages 436–441. IEEE, 2009.

Karthik Dantu and Gaurav S Sukhatme. Detecting and tracking level sets of scalar fields using a robotic sensor network. In *IEEE International Conference on Robotics and Automation*, pages 3665–3672. IEEE, 2007.

Veronique Delouille, Ramesh Neelsh Neelamani, and Richard G Baraniuk. Robust distributed estimation using the embedded subgraphs algorithm. *IEEE Transactions on Signal Processing*, 54(8):2998–3010, 2006.

Steven X Ding. *Model-based fault diagnosis techniques: design schemes, algorithms, and tools*. Springer Science & Business Media, 2008.

Daniel E Finkel. DIRECT optimization algorithm user guide. *Center for Research in Scientific Computation, North Carolina State University*, 2, 2003.

Janos J Gertler. Survey of model-based failure detection and isolation in complex plants. *IEEE Control Systems Magazine*, 8(6):3–11, 1988.

David E Golberg. Genetic algorithms in search, optimization, and machine learning. *Addion wesley*, 1989, 1989.

Rishi Graham and Jorge Cortés. Spatial statistics and distributed estimation by robotic sensor networks. In *American Control Conference (ACC)*, pages 2422–2427. IEEE, 2010.

Andreas O Griewank. Generalized descent for global optimization. *Journal of optimization theory and applications*, 34(1):11–39, 1981.

Dongbing Gu and Huosheng Hu. Spatial Gaussian process regression with mobile sensor networks. *IEEE Transactions on Neural Networks and Learning Systems*, 23(8):1279–1290, 2012.

Eldon Hansen and G William Walster. *Global optimization using interval analysis: revised and expanded*, volume 264. CRC Press, 2003.

Nikolaus Hansen, Sibylle D Müller, and Petros Koumoutsakos. Reducing the time complexity of the derandomized evolution strategy with covariance matrix adaptation (cma-es). *Evolutionary Computation*, 11(1):1–18, 2003.

JE Hurtado, Rush D Robinett III, Clark R Dohrmann, and Steven Y Goldsmith. Decentralized control for a swarm of vehicles performing source localization. *Journal of Intelligent and Robotic Systems*, 41(1):1–18, 2004.

Germán Ibacache-Pulgar, Gilberto A Paula, and Manuel Galea. On influence diagnostics in elliptical multivariate regression models with equicorrelated random errors. *Statistical Methodology*, 16:14–31, 2014.

Tao Jiang, Nader Meskin, Ehsan Sobhani-Tehrani, Khashayar Khorasani, and Camille-Alain Rabbath. Fault tolerant cooperative control for UAV rendezvous problem subject to actuator faults. In *Defense and Security Symposium*, pages 1493–1495. International Society for Optics and Photonics, 2007.

Donald R Jones, Cary D Perttunen, and Bruce E Stuckman. Lipschitzian optimization without the Lipschitz constant. *Journal of Optimization Theory and Applications*, 79(1):157–181, 1993.

Donald R Jones, Matthias Schonlau, and William J Welch. Efficient global optimization of expensive black-box functions. *Journal of Global optimization*, 13 (4):455–492, 1998.

Brian J Julian, Michael Angermann, Mac Schwager, and Daniela Rus. A scalable information theoretic approach to distributed robot coordination. In *IEEE/RSJ International Conference on Intelligent Robots and Systems (IROS)*, pages 5187–5194. IEEE, 2011.

Arthur Kahn, Julien Marzat, Hélene Piet Lahanier, and Michel Kieffer. Cooperative estimation and fleet reconfiguration for multi-agent systems. In *IFAC Workshop on Multi-Vehicule Systems*, pages 11–16. IFAC, 2015a.

Arthur Kahn, Julien Marzat, Hélene Piet-Lahanier, and Michel Kieffer. Global extremum seeking by Kriging with a multi-agent system. In *17th IFAC Symposium on System Identification, SYSID 2015*. IFAC, 2015b.

Harold J Kushner. A versatile stochastic model of a function of unknown and time varying form. *Journal of Mathematical Analysis and Applications*, 5(1):150–167, 1962.

Kenneth L Lange, Roderick JA Little, and Jeremy MG Taylor. Robust statistical modeling using the T distribution. *Journal of the American Statistical Association*, 84(408):881–896, 1989.

Jonathan RT Lawton, Randal W Beard, and Brett J Young. A decentralized approach to formation maneuvers. *IEEE Transactions on Robotics and Automation*, 19(6):933–941, 2003.

Jerome Le Ny and George J Pappas. On trajectory optimization for active sensing in Gaussian process models. In *Proceedings of the 48th IEEE Conference on Decision and Control*, pages 6286–6292. IEEE, 2009.

Naomi Ehrich Leonard and Edward Fiorelli. Virtual leaders, artificial potentials and coordinated control of groups. In *Proceedings of the 40th IEEE Conference on Decision and Control*, volume 3, pages 2968–2973. IEEE, 2001.

Naomi Ehrich Leonard, Derek Paley, Francois Lekien, Rodolphe Sepulchre, David M Fratantoni, Russ E Davis, et al. Collective motion, sensor networks, and ocean sampling. *Proceedings of the IEEE*, 95(1):48–74, 2007.

Li Li and Huajing Fang. Bounded consensus tracking for second-order multi-agent systems with communication delay and sampled information. In *Proceedings of International Conference on Modelling, Identification & Control (ICMIC)*, pages 584–589. IEEE, 2012.

Xiangpeng Li, Dong Sun, Jie Yang, and Shuang Liu. Connectivity constrained multirobot navigation with considering physical size of robots. In *IEEE International Conference on Automation and Logistics (ICAL)*, pages 24–29. IEEE, 2011.

Xingyan Li and Lynne E Parker. Sensor analysis for fault detection in tightly-coupled multi-robot team tasks. In *IEEE International Conference on Robotics and Automation*, pages 3269–3276. IEEE, 2007.

Cheng-Lin Liu and Fei Liu. Consensus problem of second-order multi-agent systems with input delay and communication delay. In *Chinese control conference (CCC)*, pages 4747–4752, 2011.

Fei Liu and Cheng-Lin Liu. Consensus of second-order multi-agent systems under communication delay. In *Chinese Control and Decision Conference (CCDC)*, pages 739–744. IEEE, 2010.

Sauro Longhi, Andrea Monteriu, and Massimo Vaccarini. Cooperative control of underwater glider fleets by fault tolerant decentralized mpc. In *17th IFAC World Congress*, pages 16021–16026, 2008.

Kevin M Lynch, Ira B Schwartz, Peng Yang, Randy Freeman, et al. Decentralized environmental modeling by mobile sensor networks. *IEEE Transactions on Robotics*, 24(3):710–724, 2008.

Julien Marzat, Hélène Piet-Lahanier, Frédéric Damongeot, and Eric Walter. Model-based fault diagnosis for aerospace systems: a survey. *Proceedings of the Institution of Mechanical Engineers, Part G: Journal of Aerospace Engineering*, pages 1329–1360, 2012.

Julien Marzat, Hélène Piet-lahanier, and Arthur Kahn. Cooperative guidance of Lego Mindstorms NXT mobile robots. In *11th International Conference on Informatics in Control, Automation and Robotics*, volume 2, pages 605–610, Vienne, Austria, 2014.

Georges Matheron. *The theory of regionalized variables and its applications*, volume 5. École nationale supérieure des mines, 1971.

Luis Merino, Fernando Caballero, JR Dios, and Aníbal Ollero. Cooperative fire detection using unmanned aerial vehicles. In *Proceedings of the 2005 IEEE International Conference on Robotics and Automation (ICRA)*, pages 1884–1889. IEEE, 2005.

Nader Meskin and Khashayar Khorasani. Actuator fault detection and isolation for a network of unmanned vehicles. *IEEE Transactions on Automatic Control*, 54(4):835–840, 2009.

Nader Meskin and Khashayar Khorasani. *Fault Detection and Isolation: Multi-Vehicle Unmanned Systems*. Springer Science & Business Media, 2011.

Abdul Nurunnabi and Geoff West. Outlier detection in logistic regression: A quest for reliable knowledge from predictive modeling and classification. In *IEEE 12th International Conference on Data Mining Workshops (ICDMW)*, pages 643–652. IEEE, 2012.

Petter Ögren, Edward Fiorelli, and Naomi Ehrich Leonard. Cooperative control of mobile sensor networks: Adaptive gradient climbing in a distributed environment. *IEEE Transactions on Automatic Control*, 49(8):1292–1302, 2004.

Reza Olfati-Saber. Distributed Kalman filter with embedded consensus filters. In *44th IEEE Conference on Decision and Control and European Control Conference (CDC-ECC)*, pages 8179–8184. IEEE, 2005.

Reza Olfati-Saber. Flocking for multi-agent dynamic systems: Algorithms and theory. *IEEE Transactions on Automatic Control*, 51(3):401–420, 2006.

Reza Olfati-Saber. Distributed Kalman filtering for sensor networks. In *46th IEEE Conference on Decision and Control*, pages 5492–5498. IEEE, 2007.

T Panigrahi, B Mulgrew, and Babita Majhi. Robust distributed linear parameter estimation in wireless sensor network. In *International Conference on Energy, Automation, and Signal (ICEAS)*, pages 1–5. IEEE, 2011.

Lynne E Parker. ALLIANCE: An architecture for fault tolerant multirobot cooperation. *IEEE Transactions on Robotics and Automation*, 14(2):220–240, 1998.

Lynne E Parker. Cooperative robotics for multi-target observation. *Intelligent Automation & Soft Computing*, 5(1):5–19, 1999.

Victor Picheny, Tobias Wagner, and David Ginsbourger. A benchmark of Kriging-based infill criteria for noisy optimization. *Structural and Multidisciplinary Optimization*, 48(3):607–626, 2013.

Poonam Poonam and Maitreyee Dutta. Performance analysis of clustering methods for outlier detection. In *IEEE International Conference on Advanced Computing & Communication Technologies (ACCT)*, pages 89–95. IEEE, 2012.

Luc Pronzato and Éric Walter. Robust experiment design via maximin optimization. *Mathematical Biosciences*, 89(2):161–176, 1988.

Wei Ren and Randal Beard. Virtual structure based spacecraft formation control with formation feedback. *AIAA Guidance, Navigation and Control Conference and Exhibit*, 4963, 2002.

Wei Ren and Randal Beard. Decentralized scheme for spacecraft formation flying via the virtual structure approach. *Journal of Guidance, Control, and Dynamics*, 27(1):73–82, 2004.

Wei Ren, Randal W Beard, and Ella M Atkins. A survey of consensus problems in multi-agent coordination. In *Proceedings of the American Control Conference (ACA)*, pages 1859–1864. IEEE, 2005.

Craig W Reynolds. Flocks, herds and schools: A distributed behavioral model. In *ACM Siggraph Computer Graphics*, volume 21, pages 25–34. ACM, 1987.

Yohan Rochefort, Helene Piet-Lahanier, Sylvain Bertrand, Dominique Beauvois, and Didier Dumur. Guidance of flocks of vehicles using virtual signposts. In *Proceedings of the 18th IFAC World Congress, Milan, Italy*, pages 5999–6004, 2011.

Michael James Sasena. *Flexibility and efficiency enhancements for constrained global design optimization with Kriging approximations*. PhD thesis, University of Michigan, 2002.

Matthias Schonlau. *Computer experiments and global optimization*. PhD thesis, University of Waterloo, 1997.

Matthias Schonlau, William J Welch, and DR Jones. Global optimization with nonparametric function fitting. In *Proceedings of the Section on Physical and Engineering Sciences, American Statistical Association*, pages 183–186, 1996.

Mac Schwager, Jean-Jacques Slotine, and Daniela Rus. Decentralized, adaptive control for coverage with networked robots. In *IEEE International Conference on Robotics and Automation (ICRA)*, pages 3289–3294. IEEE, 2007.

Mac Schwager, Jean-Jacques Slotine, and Daniela Rus. Consensus learning for distributed coverage control. In *EEE International Conference on Robotics and Automation (ICRA)*, pages 1042–1048. IEEE, 2008.

Mac Schwager, Brian J Julian, and Daniela Rus. Optimal coverage for multiple hovering robots with downward facing cameras. In *IEEE International Conference on Robotics and Automation (ICRA)*, pages 3515–3522. IEEE, 2009a.

Mac Schwager, James McLurkin, Jean-Jacques E Slotine, and Daniela Rus. From theory to practice: Distributed coverage control experiments with groups of robots. In *Experimental Robotics*, pages 127–136. Springer, 2009b.

Mac Schwager, Daniela Rus, and Jean-Jacques Slotine. Unifying geometric, probabilistic, and potential field approaches to multi-robot deployment. *The International Journal of Robotics Research*, 30(3):371–383, 2011.

Pete Seiler and Raja Sengupta. Analysis of communication losses in vehicle control problems. In *Proceedings of the American Control Conference (ACC)*, volume 2, pages 1491–1496. IEEE, 2001.

Joongbo Seo, Youdan Kim, Seungkeun Kim, and Antonios Tsourdos. Consensus-based reconfigurable controller design for unmanned aerial vehicle formation flight. *Proceedings of the Institution of Mechanical Engineers, Part G: Journal of Aerospace Engineering*, 226(7):817–829, 2012.

Gopinadh Sirigineedi, Antonios Tsourdos, Brian White, Peter Silson, et al. Decentralised cooperative aerial surveillance for harbour security: A formal verification approach. In *IEEE GLOBECOM Workshops (GC Wkshps)*, pages 1831–1835. IEEE, 2010.

Francisco J Solis and Roger J-B Wets. Minimization by random search techniques. *Mathematics of operations research*, 6(1):19–30, 1981.

Haiyu Song, Li Yu, and Dan Zhang. Distributed set-valued estimation in sensor networks with limited communication data rate. *Journal of the Franklin Institute*, 350(5):1264–1283, 2013.

Kazuo Sugihara and Ichiro Suzuki. Distributed motion coordination of multiple mobile robots. In *IEEE International Symposium on Intelligent Control*, pages 138–143. IEEE, 1990.

Kar-Han Tan and M Anthony Lewis. Virtual structures for high-precision cooperative mobile robotic control. In *Proceedings of the 1996 IEEE/RSJ International Conference on Intelligent Robots and Systems' (IROS)*, volume 1, pages 132–139. IEEE, 1996.

Fang Tang and Lynne E Parker. Asymtre: Automated synthesis of multi-robot task solutions through software reconfiguration. In *IEEE International Conference on Robotics and Automation (ICRA)*, pages 1501–1508. IEEE, 2005.

Fang Tang and Lynne E Parker. A complete methodology for generating multi-robot task solutions using asymtre-d and market-based task allocation. In *IEEE International Conference on Robotics and Automation (ICRA)*, pages 3351–3358. IEEE, 2007.

Herbert G Tanner, George J Pappas, and Vijay Kumar. Leader-to-formation stability. *IEEE Transactions on Robotics and Automation*, 20(3):443–455, 2004.

Virginia Torczon. On the convergence of pattern search algorithms. *SIAM Journal on optimization*, 7(1):1–25, 1997.

Aimo Torn and Antanas Zilinskas. *Global optimization*. Springer-Verlag New York, Inc., 1989.

Christophe Tricaud, Maciej Patan, Dariusz Uciński, and YangQuan Chen. D-optimal trajectory design of heterogeneous mobile sensors for parameter estimation of distributed systems. In *American Control Conference (ACA)*, pages 663–668. IEEE, 2008.

Antonios Tsourdos. A formal model approach for the analysis and validation of the cooperative path planning of a UAV team. In *IEEE Seminar on Autonomous Agents in Control*, pages 67–73. IET, 2005.

Dariusz Ucinski and Yang Quan Chen. Time-optimal path planning of moving sensors for parameter estimation of distributed systems. In *IEEE Conference on Decision and Control and European Control Conference (CDC-ECC)*, pages 5257–5262. IEEE, 2005.

Emmanuel Vazquez and Julien Bect. Convergence properties of the expected improvement algorithm with fixed mean and covariance functions. *Journal of Statistical Planning and inference*, 140(11):3088–3095, 2010.

Éric Walter. *Numerical Methods and Optimization*. Springer, 2014.

Éric Walter and Luc Pronzato. Qualitative and quantitative experiment design for phenomenological models—a survey. *Automatica*, 26(2):195–213, 1990.

Paul KC Wang. Navigation strategies for multiple autonomous mobile robots moving in formation. *Journal of Robotic Systems*, 8(2):177–195, 1991.

Tsang-Yi Wang, Li-Yuan Chang, and Pei-Yin Chen. A collaborative sensor-fault detection scheme for robust distributed estimation in sensor networks. *IEEE Transactions on Communications*, 57(10):3045–3058, 2009.

Xiaohua Wang, Vivek Yadav, and SN Balakrishnan. Cooperative UAV formation flying with obstacle/collision avoidance. *IEEE Transactions on Control Systems Technology*, 15(4):672–679, 2007.

Ryan K Williams and Gaurav S Sukhatme. Probabilistic spatial mapping and curve tracking in distributed multi-agent systems. In *IEEE International Conference on Robotics and Automation (ICRA)*, pages 1125–1130. IEEE, 2012.

Yunfei Xu, Jongeun Choi, and Songhwai Oh. Mobile sensor network navigation using Gaussian processes with truncated observations. *IEEE Transactions on Robotics*, 27(6):1118–1131, 2011.

Xiao Yan, Jian Chen, and Dong Sun. Multilevel based topology design and formation control of robot swarms. In *IEEE International Conference on Robotics and Biomimetics (ROBIO)*, pages 174–179. IEEE, 2011.

Xiao Yan, Jian Chen, and Dong Sun. Multilevel-based topology design and shape control of robot swarms. *Automatica*, 48(12):3122–3127, 2012.

Jingyi Yao, Raul Ordonez, and Veysel Gazi. Swarm tracking using artificial potentials and sliding mode control. *Journal of Dynamic Systems, Measurement, and Control*, 129(5):749–754, 2007.

Michael M Zavlanos and George J Pappas. Distributed formation control with permutation symmetries. In *Decision and Control, 2007 46th IEEE Conference on*, pages 2894–2899. IEEE, 2007.

Fumin Zhang and Naomi Ehrich Leonard. Cooperative filters and control for cooperative exploration. *IEEE Transactions on Automatic Control*, 55(3):650–663, 2010.

Fumin Zhang, Edward Fiorelli, and Naomi Ehrich Leonard. Exploring scalar fields using multiple sensor platforms: Tracking level curves. In *IEEE Conference on Decision and Control*, pages 3579–3584. IEEE, 2007.

Xiaodong Zhang, Thomas Parisini, and Marios M Polycarpou. Adaptive fault-tolerant control of nonlinear uncertain systems: an information-based diagnostic approach. *IEEE Transactions on Automatic Control*, 49(8):1259–1274, 2004.

Xiaodong Zhang, Marios M Polycarpou, and Thomas Parisini. Fault diagnosis of a class of nonlinear uncertain systems with Lipschitz nonlinearities using adaptive estimation. *Automatica*, 46(2):290–299, 2010a.

Yang Zhang, Nirvana Meratnia, and Paul Havinga. Outlier detection techniques for wireless sensor networks: A survey. *IEEE Communications Surveys & Tutorials*, 12(2):159–170, 2010b.

Yu Zhang and Lynne E Parker. Iq-asymtre: Synthesizing coalition formation and execution for tightly-coupled multirobot tasks. In *IEEE/RSJ International Conference on Intelligent Robots and Systems (IROS)*, pages 5595–5602. IEEE, 2010.

Cen Zhaohui and Hassan Noura. A composite fault tolerant control based on fault estimation for quadrotor UAVs. In *IEEE Conference on Industrial Electronics and Applications (ICIEA)*, pages 236–241. IEEE, 2013.

Shanshan Zheng, Tao Jiang, and John S Baras. Robust state estimation under false data injection in distributed sensor networks. In *IEEE Global Telecommunications Conference (GLOBECOM)*, pages 1–5. IEEE, 2010.

Commande coopérative reconfigurable pour la recherche d'extremum

Résumé Le problème traité dans cette thèse concerne la recherche coopérative de la position du maximum d'un champ spatial initialement inconnu dans une zone prédéfinie avec un système multi-agent composé de véhicules autonomes. Ce problème se décompose en deux parties, la première s'intéresse aux méthodes d'estimation du champ utilisé pour l'optimisation, et la seconde concerne la conception de lois de commande pour le déplacement de la flotte d'agents.
Deux solutions ont été proposées en ce qui concerne les méthodes d'estimation. La première approche s'appuie sur une stratégie de recherche locale qui cherche à estimer le gradient du champ inconnu dans le but de déplacer les agents selon cette direction. La problématique du placement optimal des agents a été abordée et trois critères ont été proposés afin de déterminer les formations qui fournissent la meilleure qualité d'estimation du champ. Une méthode coopérative de détection et d'identification de défauts de mesure utilisant un seuil adaptatif a également été proposée. La deuxième solution d'estimation s'appuie sur une stratégie de recherche globale du maximum. Le champ est modélisé par krigeage et la recherche est effectuée en utilisant les propriétés statistiques de ce méta-modèle. Un nouveau critère d'échantillonnage a été développé pour permettre au système multi-agent de localiser la position du maximum global tout en limitant le nombre de mesures et en tenant compte des contraintes dynamiques des véhicules.
Les deux méthodes d'estimation fournissent les positions où effectuer les mesures du champ. Une loi de commande distribuée a donc été conçue pour permettre aux agents d'atteindre leurs positions désirées. Cette loi permet de reconfigurer la formation tel que recommandé par l'analyse de placement optimal lorsqu'un capteur est détecté comme défaillant dans le cas de l'estimation locale. La même loi de commande a été adaptée pour rallier les positions désignées itérativement par la stratégie de recherche globale.
Mots clés: Commande coopérative - Détection et identification de défaut - Optimisation à base de krigeage - Placement optimal de capteurs - Système multi-agent

Reconfigurable cooperative control for extremum seeking

Abstract This thesis addresses the localisation of the maximum of an unknown spatial field in a delimited area. The search is performed by a multi-agent system composed of autonomous vehicles. The mission can be divided in two parts, the first one focuses on the estimation methods for optimisation, and the second one concerns the control law to move the fleet of agents.
Two solutions have been proposed for the estimation part. The first one relies on a local search strategy that estimates the gradient of the unknown field and moves the agents along the gradient direction. The optimal sensor placement of the agents has been investigated and three criteria have been proposed to find the formation shape required for efficient estimation. Moreover, a sensor fault detection and isolation scheme using an adaptive threshold has been presented. The second estimation solution is a global search strategy based on a Kriging model of the field. A new sampling criterion is defined for the multi-agent system to locate the position of the global maximum while limiting the number of measurements and taking into account the agent dynamics.
Both solutions provide a set of desired sampling positions to the agents. A distributed control law has been designed to guide the agents toward these locations. This control law is also used in the local approach to gather the agents in a desired formation and reconfigure it when a fault has been detected, following the optimal sensor placement analysis. The same control law has been adapted to reach the positions specified iteratively by the Kriging-based global search strategy.
Keywords: Cooperative control - Fault detection and isolation - Kriging-based optimisation - Multi-agent system - Optimal sensor placement